JRC Scientific and Technical Reports

Multi-Year Analysis of Standard Ocean Colour Products for the European Seas

Chlorophyll *a* Concentration and Diffuse Attenuation Coefficient

F. Mélin & V. Vantrepotte

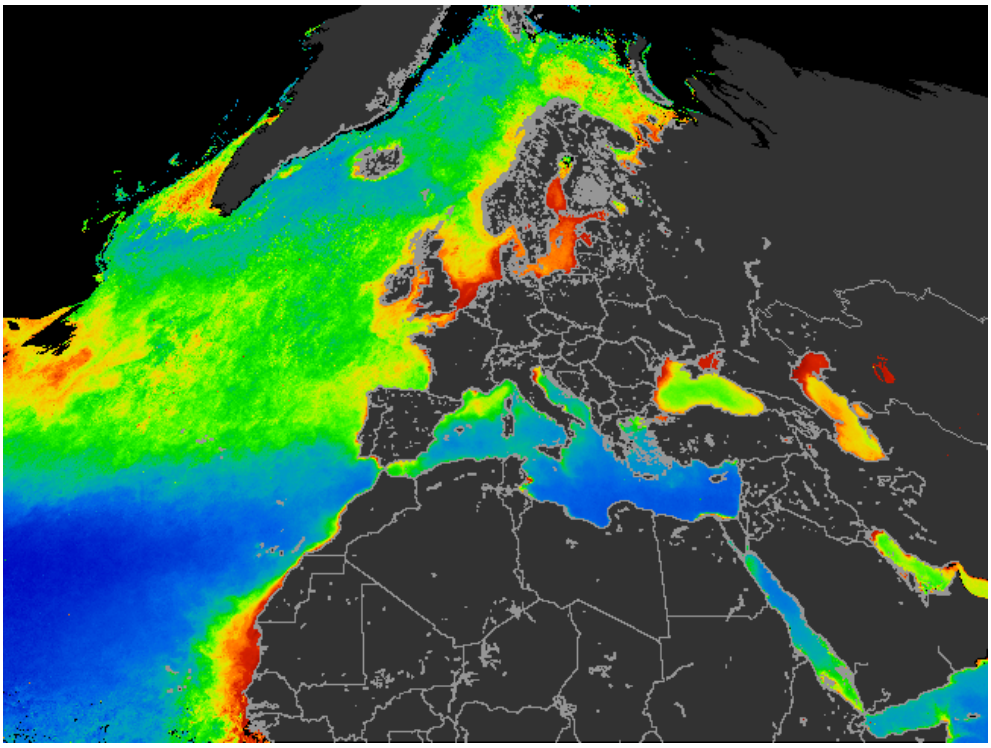

EUR 22916 EN - 2007

JRC EUROPEAN COMMISSION

ies Institute for Environment and Sustainability

The mission of the Institute for Environment and Sustainability is to provide scientific-technical support to the European Union's Policies for the protection and sustainable development of the European and global environment.

European Commission
Joint Research Centre
Institute for Environment and Sustainability

Contact information
Address: F. Mélin, JRC, TP272, 21020, Ispra, Italy
E-mail: frederic.melin@jrc.it
Tel.: (+39)-0332-785627
Fax: (+39)-0332-789034

http://ies.jrc.ec.europa.eu
http://www.jrc.ec.europa.eu

JRC 40253

EUR 22916 EN

ISSN 1018-5593

Luxembourg: Office for Official Publications of the European Communities

Printed in Italy

Abstract

A 10-year time series of ocean colour products has been assembled for the European Seas from the SeaWiFS and MODIS full resolution satellite imagery. The JRC ocean colour archive is first briefly described. Then the study focuses on the analysis of the spatial and temporal variability of standard products such as the chlorophyll *a* pigment concentration and the diffuse attenuation coefficient. The European seas are partitioned into a set of specific regions for which average time series are derived and analysed in terms of seasonal and inter-annual variability. Finally, a statistical analysis yields a decomposition of the series into seasonal, irregular and linear trend components, thus providing a classification of the European waters on the basis of their temporal variations.

Contents

Introduction

Optical remote sensing (ocean color) has demonstrated a capability to provide synoptic descriptions of the optical and biological properties of the oceans. This technique is based on the determination of the spectrum of water leaving radiance, i.e., the radiance emerging from below the sea surface. The amplitude and spectral shape of this primary geophysical ocean color product subsequently can be interpreted in terms of derived products such as concentrations of optically significant constituents or inherent optical properties for biogeochemical and environmental applications at global or regional scales. Particularly, satellite ocean color has given another dimension to marine biology and ecosystem studies, providing key information for instance on the timing and spatial distribution of phytoplankton blooms, and the magnitude of primary production.

The Coastal Zone Color Scanner (CZCS, Hovis et al., 1980) experiment first illustrated the potential of optical remote sensing (Feldman et al., 1989), including the first global view of the annual phytoplankton chlorophyll *a* pigment concentration (Yoder et al., 1993). The ocean color record was renewed twenty years after the end of the CZCS mission, mainly with the beginning of the SeaWiFS mission (Hooker et al., 1992). For global scale applications, the associated data record is now reaching a 10 year time span, and has been complemented by additional space missions. For the specific purpose of studies focused on European regional seas, for which full resolution imagery should be preferred, the SeaWiFS data series stops in December 2004. However, this 7-year series, considering its overall quality and consistency, already offers a resource particularly appropriate for multi-annual analysis of bio-optical properties (McClain et al., 2004).

The present study is a first contribution to the exploitation of satellite derived bio-optical time series for the European oceanic domain, with an initial focus on the chlorophyll *a* pigment concentration and the diffuse attenuation coefficient obtained from SeaWiFS. For the sake of completeness and future developments, the data archive derived from ocean color hosted at JRC is first briefly introduced, as well as the approach to comprehensively analyzing the data set. Subsequently, the time series are shown for the various areas constitutive of the European seas, with a focus on year-to-year differences. The MODIS derived equivalents are also presented, as a first illustration of the differences characterizing the two data sets. Considering the importance of assessing the creation of multi-mission data sets for long-term analysis, this aspect is being carefully considered in parallel efforts.

This report corresponds to the JRC Deliverable of WP3250 of the MARine and COASTal Environmental Information Services (MarCoast) - Water Quality Assessment Service.

Section 1

Data and Methods

1.1 Satellite Data and Processing

In view of generating an archive of ocean color derived products for the European marine domain, a raw data system has been assembled. The main sensors considered are the Sea-viewing Wide Field-of-view Sensor (SeaWiFS, Hooker et al., 1992) onboard the OrbView-2 spacecraft, and the Moderate Resolution Imaging Spectroradiometer (MODIS, Salomonson et al., 1989) onboard the Aqua platform.

The satellite level-1A imagery (raw data) from SeaWiFS and MODIS has been acquired from the Goddard Space Flight Center of the U.S. National Aeronautics and Space Administration (GSFC-NASA). In the case of SeaWiFS, only Local Area Coverage (LAC) full-resolution imagery is considered for the generation of a high-resolution data set. This fixes the time periods covered by the satellite data, from October 1997 to December 2004 for SeaWiFS and July 2002 to present for MODIS (the analysis in this document include data up to June 2007). The two sensors and associated software codes provide a similar suite of data products. An exception is the distribution of Photosynthetically Available Radiation (PAR), only available from SeaWiFS. Low-resolution SeaWiFS data (based on Global Area Coverage imagery) have been used to complete the time series for PAR over the European domain.

All satellite scenes have been processed with the SeaWiFS Data Analysis System (SeaDAS, Fu et al., 1998) software package (versions 4.9 and above). For both sensor products, the atmospheric correction scheme is based on the work by Gordon and Wang (1994) and subsequent developments (e.g., Patt et al., 2003, Wang et al., 2005, and references therein). Bio-optical algorithms provide a suite of variables that are briefly described in the following section. Both ends of the processing chains are kept on-line, which means Level-1A and Level-3 files, and all intermediary products (like Level-2) are deleted. The main steps of the processing chain are illustrated on Figure 1.1.

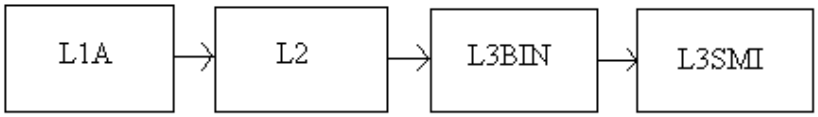

Figure 1.1: Processing chain schematic. L1A stands for Level-1A data, un-calibrated top-of-atmosphere radiances; L2 are Level-2 processed imagery; L3BIN are binned Level-3 data files organized on a sinusoidal grid; L3SMI are Level-3 data files organized as Standard Mapped Images (see next section).

1.2 Archive Description

The products are stored in four sets of files. The atmospheric correction scheme uses top-of-atmosphere radiances to produce an aerosol characterization and the spectrum of water leaving radiance (one category of products). The spectrum of top-of-atmosphere radiances is also used to derive the photosynthetically available radiation (PAR) using the method of Frouin et al. (2003), that is stored in separate files. A third category of products is made of derived concentrations of optically significant constituents (chlorophyll *a* Chl*a* and total suspended matter TSM) and apparent optical properties (diffuse attenuation coefficient K_d). A fourth category includes inherent optical properties for total absorption a_t, absorption by phytoplankton a_{ph}, absorption due to detritus and chromophoric dissolved organic matter (CDOM) a_{dg}, and back-scattering by particles b_{bp}. Table 1.1 lists information on these four categories of products.

The temporal binning includes daily, 8-day and monthly averages. All products are stored for all three temporal scales as sinusoidal projection data files, so-called binned files (L3BIN), at a resolution of 2-km. This storage format is particularly convenient in terms of data volume and organization. On the other hand, the data sets are not readily accessible without further re-mapping. Therefore, additional Level-3 data files are generated onto regular grids, designated standard mapped images (L3SMI). Practically, these latter files are those of interest for actual analysis and for the users. The temporal binning is identical for these independent windows, that similarly contain all variables for the 8-day and monthly composites, whereas the sets of inherent optical properties are available on a daily basis presently only for the windows associated with the Mediterranean and Black Seas. Clearly, a daily frequency could be easily achieved for all basins (L3SMI) using the L3BIN data files. The same is true for the generation of a new L3SMI window, which is straightforward if its geographic domain is included in the extent of the L3BIN (40°W-55°E and 10°N-80°N). The time and space binning follows the principles given in the *ad hoc* IOCCG report (number 4, 2004). Each pixel information is associated with the nearest grid cell (or bin), and subsequently simple averaging is used for temporal binning. The 7-year monthly time series available from SeaWiFS is used to compute a monthly climatology (December 1997 - November 2004) as well as monthly anomalies. A first climatology has also been derived from the 5-year time series obtained from MODIS (July 2002 - June 2007).

Table 1.1: List of fields included in the JRC archive for SeaWiFS (SWF) and MODIS (MOD). References: [1] Frouin et al. (2003); [2] Gordon and Wang (1994); [3] O'Reilly et al. (2000); [4] Clark; [5] Werdell (2005); [6] Lee et al. (2005); [7] Lee et al. (2002). dl stands for dimensionless.

Notation	Units	Description	Wavelength domain	Ref.
PAR	E m^{-2} d^{-1}	photosynthetically available radiation	spectrally integrated	[1]
L_{WN}	mW cm^{-2} μm^{-1} sr^{-1}	normalized water leaving radiance	SWF: 412, 443, 490 510, 555, 670	[2]
			MOD: 412, 443, 488 531, 551, 667	[2]
τ_a	dl	aerosol optical thickness	SWF: 443, 865	[2]
			MOD: 443, 869	
α	dl	Ångström exponent	SWF: 510-865	[2]
			MOD: 531-869	
Chl$a$	mg m^{-3}	chlorophyll a concentration		[3]
TSM	g m^{-3}	total suspended matter concentration		[4]
K_d	m^{-1}	diffuse attenuation coefficient	490	[5]
K_d	m^{-1}	diffuse attenuation coefficient	SWF: 412, 490, 555	[6]
			MOD: 412, 488, 551	
a_t	m^{-1}	total absorption coefficient	SWF: 412, 490, 555	[7]
			MOD: 412, 488, 551	
a_{ph}	m^{-1}	phytoplankton absorption coef.	SWF: 443, 490	[7]
			MOD: 443, 488	
a_{dg}	m^{-1}	detritus + CDOM absorption coef.	412, 443	[7]
$b_{b,p}$	m^{-1}	particulate back-scattering coefficient	SWF: 412, 490, 555	[7]
			MOD: 412, 488, 551	

The overall window for the L3BIN archive, considered as the European marine macro-region, covers the square 40°W-55°E and 10°N-80°N. The definition of the L3SMI windows is given in Table 1.2.

Table 1.2: Definition of the L3SMI windows for the JRC European archive. Ny and Nx are the number of lines and columns of the data files, respectively. Eq. Cyl. stands for Equidistant Cylindrical; Az. Iso. stands for Azimuthal Isotropic. All resolutions are approximately 2-km.

Notation	Description	Latitude	Longitude	Ny	Nx	Projection
BALT	Baltic Sea	52.75°N-66°N	3.5°E-30.5°E	736	764	Eq. Cyl.
BSEA	Black Sea	40.75°N-47.5°N	27.25°E-42°E	375	588	Eq. Cyl.
CASP	Caspian Sea	36.5°N-47.25°N	46.5°E-55°E	598	352	Eq. Cyl.
MEDI	Mediterranean Sea	30°N-46°N	6°W-36.5°E	889	1860	Eq. Cyl.
NADR	NE Atlantic	35°N-65°N	40°W-12.5°E	1666	1875	Eq. Cyl.
NASE	NE Subtrop. Atlantic	10°N-45°N	40°W-5°W	1944	1725	Eq. Cyl.
SARC	NE Subarctic Atlantic	50°N-80°N	40°W-40°E	1519	2501	Az. Iso.

For reference, the volume of data is already quite significant, as of September 2006, for Level-1A files:

- SeaWiFS: 400 Gb
- MODIS: 2700 Gb

for Level-3 files:

- SeaWiFS L3BIN: 785 Gb
- SeaWiFS L3SMI: 280 Gb
- MODIS L3BIN: 350 Gb
- MODIS L3SMI: 120 Gb

In the case of SeaWiFS, an agreement with the European Space Agency (ESA, third-party mission agreement) has given access to LAC data obtained at three receiving stations located in Norway, Italy and the Canary Islands, after March 2006. Although this data series does not provide a space and time coverage as complete as before December 2004, it is extremely precious as a complement to check the consistency with MODIS data in latter years. Together with the on-board registered LAC data still freely available for the northern Adriatic Sea, this data source also supplements the SeaWiFS validation activities. As for MODIS, the series is expanding; on the other hand, the data volume for Level-1A files is being slightly reduced by data delivery extracted on the European macro-region.

1.3 Validation with Field Data

It is challenging to provide uncertainty estimates for the various products over the European area, an effort which is out of the scope of the present text. JRC is contributing to the validation of ocean color products for the European waters by collection of accurate bio-optical measurements, mostly at the site of the Acqua Alta Oceanographic Tower (AAOT), a platform located in the north Adriatic Sea (Zibordi et al., 2002, Berthon et al., 2002). Validation results of ocean color products and/or algorithms have been presented in various analyzes (Zibordi et al., 2004a,b, Mélin et al., 2005, Zibordi et al., 2006a,b, Mélin and Zibordi, 2007, Mélin et al., 2007a,b). Additional radiometric data have been used to validate the spectra of normalized water leaving radiance L_{WN} at other sites, including the Baltic Sea (Zibordi et al., 2006c,d).

1.4 Data Analysis

The SeaWiFS and MODIS monthly time series are both used in this work but for consistency the statistical analysis mainly relies on the 7-year series provided by the SeaWiFS mission. In order to derive representative values for the European marine domain, the various European seas have been further partitioned into smaller areas (see following sections). This distribution is based on conventional regions, common knowledge or bathymetry. Depth topography is based on the General Bathymetric Chart of the Oceans (GEBCO) one-minute grid distributed by the British Oceanographic Data Centre.

For each of these areas and each month, the average value and standard deviation of a given variable have been computed from the satellite data set. The associated datum is computed as arithmetic or geometric (i.e., using log-transformed values) average. Typically, statistics calculated for the normalized water leaving radiances are based on un-transformed data whereas log-transformed data are used for other optical variables on the basis of the assumption of log-normal distributions (Campbell, 1995). If the data available for a given month cover less than 10% of the surface area, the corresponding monthly average is discarded. Even with a similar threshold, some caution is still needed when interpreting area-averaged values for regions where significant data gaps occur, like in the high-latitude regions. Moreover, data points lying beyond ± 3 standard deviations are excluded as a coarse quality check aiming at discarding unrealistic outliers.

The analysis in this report almost exclusively deals with the concentration of chlorophyll *a* Chl*a*, taken as an indicator of trophic conditions, and the coefficient of attenuation for diffuse light K_d at 490 nm, considered as a proxy for water turbidity. These products are obtained from the OC4v4 and OBPG algorithms, respectively (O'Reilly et al., 2000, Werdell, 2005). In the subsequent sections, multi-year time series of these two products are given for each area. Additionally, a table is provided, giving the climatological SeaWiFS Chl*a* cycle and the ratios of monthly averages with respect to the associated climatological value, as a simple way of summarizing the main inter-annual signals. The last section attempts a brief synthesis of the temporal variability observed for all the European marine regions considered in this report.

Section 2

Baltic Sea

The partition of the Baltic Sea is shown on Figure 2.1 with, from the North Sea to the northern end of the Baltic Sea, Skaggerak, Kattegat, Belt Sea, Arkona Basin, the western and eastern Southern Baltic Proper, the Gulf of Gdansk, the western and eastern Central Baltic Proper (or Gotland Basin), the Gulf of Riga, the Northern Baltic Proper, the Gulf of Finland, the Aland Sea, the Archipelago region, the Bothnian Sea, and the Bothnian Bay. The western and eastern Southern Baltic Proper, as well as the western and eastern parts of the Gotland Basin are aggregated for the presentation of the results.

This partition results from a synthesis of regions proposed by the International Council for the Exploration of the Sea (ICES) and the Helsinki Commission (HELCOM), as well as common knowledge of the basin features (S. Kaitala, personal communication). For each domain, the time series of Chl$a$ and $K_d(490)$ are given for the years 1997 to 2004 using SeaWiFS (lines with open circles) and for years 2002 to 2007 for MODIS (filled circles with dotted line). The climatologies from SeaWiFS (Dec. 1997-Nov. 2004, continuous line) and MODIS (Jul. 2002 - Jun. 2007, dashed line) are over-plotted for reference.

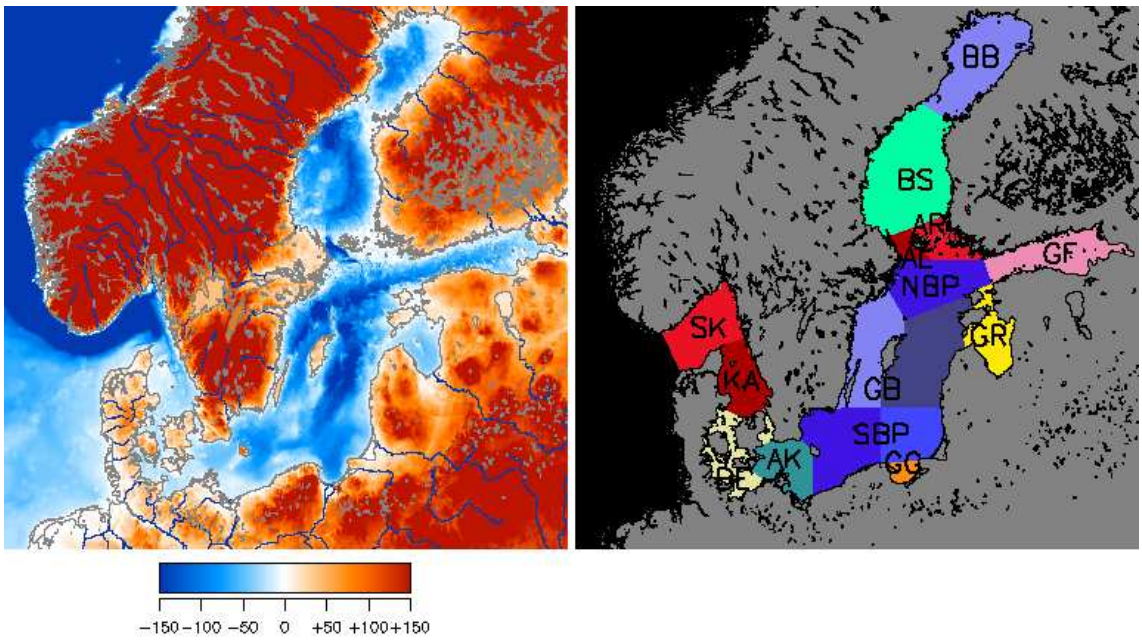

Figure 2.1: Distribution of Baltic Sea bathymetry and regions. **SK**: Skagerrak; **KA**: Kattegat; **BE**: Belt Sea; **AK**: Arkona Basin; **SBP**: Southern Baltic Proper (west and east); **GG**: Gulf of Gdansk; **GB**: Gotland Basin (west and east); **GR**: Gulf of Riga; **NBP**: Northern Baltic Proper; **GF**: Gulf of Finland; **AL**: Aland Sea; **AR**: Archipelago region; **BS**: Bothnian Sea; **BB**: Bothnian Bay.

2.1 Skagerrak

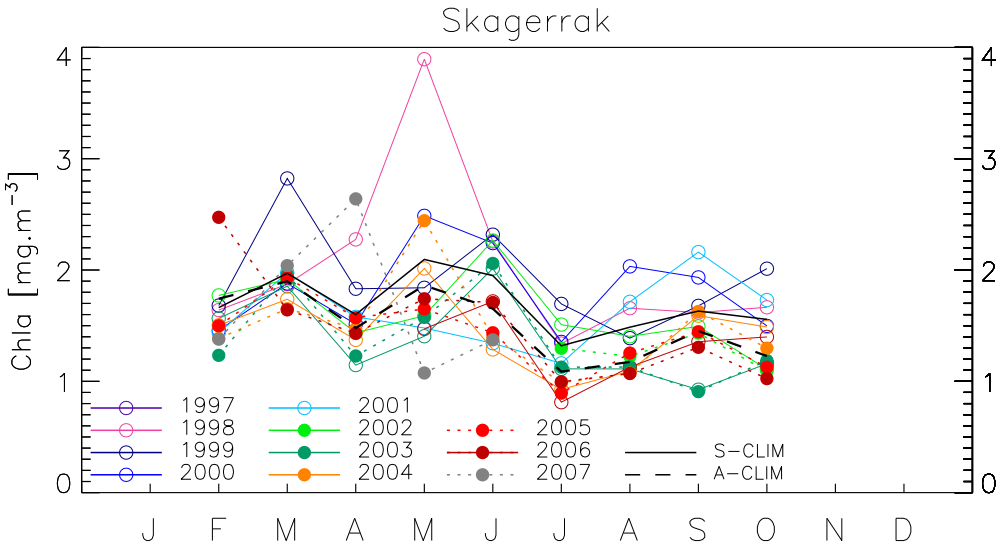

Figure 2.2: Chl*a* multi-annual time series for SeaWiFS (lines with open circles) and MODIS (filled circles with dotted line) and associated climatologies (black line and dashed line, respectively).

The Skagerrak is here included in the Baltic domain for convenience. The SeaWiFS climatological record indicates only a slight seasonal variability. Large inter-annual peaks for Chl*a* and K_d can be noticed in spring in 1998 (April-May) and 1999 (March). Conversely, the Chl*a* levels show a low in autumn 2003. Overall, the agreement with MODIS is satisfactory. The MODIS Chl*a* climatology is below that of SeaWiFS almost for the entire year.

Table 2.1: Skagerrak; SeaWiFS Chl*a* inter-annual anomalies, computed as ratio of area-averaged Chl*a* concentrations. The 2^{nd} column gives the SeaWiFS climatological Chl*a* (in mg m^{-3}). In bold, anomalies below 0.8 or above 1.2. A datum of 1 means a regional monthly value close to climatology.

Month	mg m^{-3}	1998	1999	2000	2001	2002	2003	2004
J	-	-	-	-	-	-	-	-
F	1.662	0.99	1.01	0.88	0.86	1.07	0.94	0.90
M	1.971	0.95	**1.43**	0.95	1.00	0.97	0.94	0.88
A	1.600	**1.42**	1.14	0.95	0.99	0.90	**0.72**	0.86
M	2.095	**1.86**	0.88	1.19	**0.71**	**0.76**	**0.67**	0.96
J	1.950	1.16	1.19	1.15	**0.69**	1.16	1.03	**0.66**
J	1.319	1.01	**1.29**	1.03	0.88	1.14	0.84	**0.70**
A	1.486	1.11	0.93	**1.37**	1.15	0.94	**0.75**	**0.73**
S	1.631	0.99	1.03	1.19	**1.33**	0.92	**0.57**	0.97
O	1.556	1.07	**1.29**	0.96	1.11	**0.71**	**0.74**	0.96
N	-	-	-	-	-	-	-	-
D	-	-	-	-	-	-	-	-

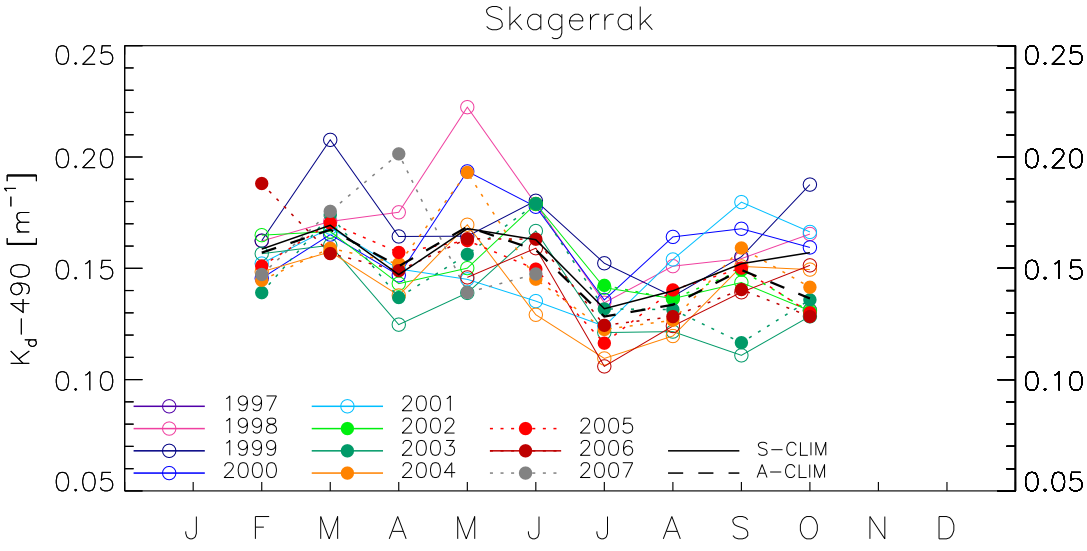

Figure 2.3: $K_d(490)$ multi-annual time series for SeaWiFS (lines with open circles) and MODIS (filled circles with dotted line) and associated climatologies (black line and dashed line, respectively).

2.2 Kattegat

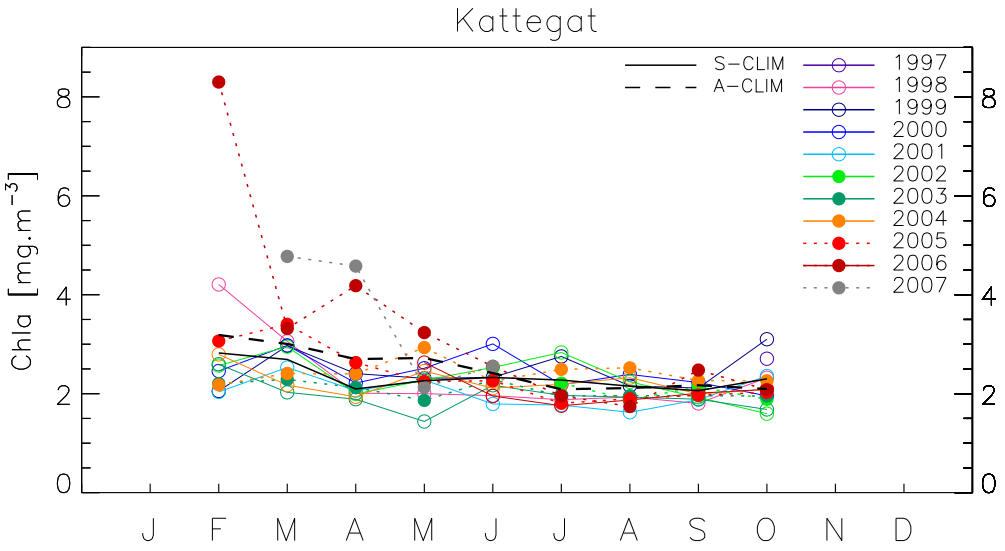

Figure 2.4: Chl*a* multi-annual time series for SeaWiFS (lines with open circles) and MODIS (filled circles with dotted line) and associated climatologies (black line and dashed line, respectively).

The SeaWiFS seasonal cycle for the Kattegat region does not appear marked, but there are pronounced variations from month to month. The Chl*a* levels seem to be below average for the whole year. As a seasonal anomaly, summer 2001 stands out as a strong negative signal. It is however underlined that most monthly averages are in the interval 1.5-3 mg m^{-3}. Significant differences, positive or negative, are noticed with respect to MODIS Chl*a*. The SeaWiFS K_d climatology appears higher than that of SeaWiFS for most of the year. This is also true for Chl*a* for the first half of the year.

Table 2.2: Kattegat; SeaWiFS Chl*a* inter-annual anomalies, computed as ratio of area-averaged Chl*a* concentrations. The 2^{nd} column gives the SeaWiFS climatological Chl*a* (in mg m^{-3}). In bold, anomalies below 0.8 or above 1.2. A datum of 1 means a regional monthly value close to climatology.

Month	mg m^{-3}	1998	1999	2000	2001	2002	2003	2004
J	-	-	-	-	-	-	-	-
F	2.824	**1.49**	**0.73**	0.87	**0.72**	0.91	0.92	0.99
M	2.691	1.14	1.10	1.11	0.94	1.10	**0.75**	0.81
A	2.096	0.96	1.15	1.06	0.98	0.95	0.90	0.92
M	2.262	0.88	1.02	1.11	1.01	1.00	**0.64**	1.09
J	2.328	0.84	1.00	**1.29**	**0.77**	1.09	0.93	0.91
J	2.275	0.83	**1.21**	0.96	**0.78**	**1.25**	0.86	0.96
A	2.151	0.90	1.00	1.11	**0.75**	1.04	0.90	1.08
S	2.060	0.88	1.03	1.08	0.91	0.93	0.92	0.97
O	2.300	1.01	**1.35**	0.85	1.02	**0.69**	**0.73**	0.91
N	-	-	-	-	-	-	-	-
D	-	-	-	-	-	-	-	-

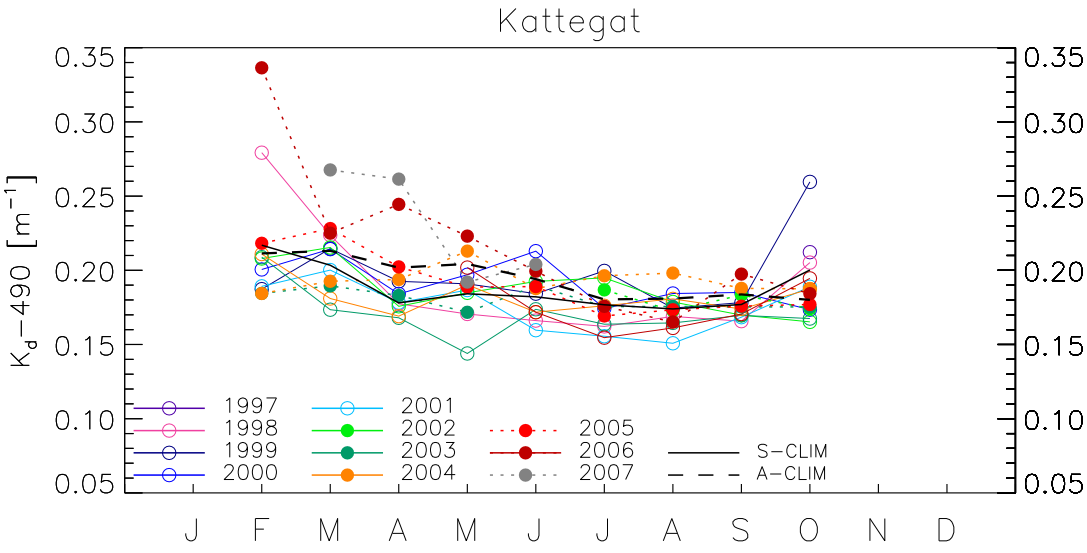

Figure 2.5: $K_d(490)$ multi-annual time series for SeaWiFS (lines with open circles) and MODIS (filled circles with dotted line) and associated climatologies (black line and dashed line, respectively).

2.3 Belt Sea

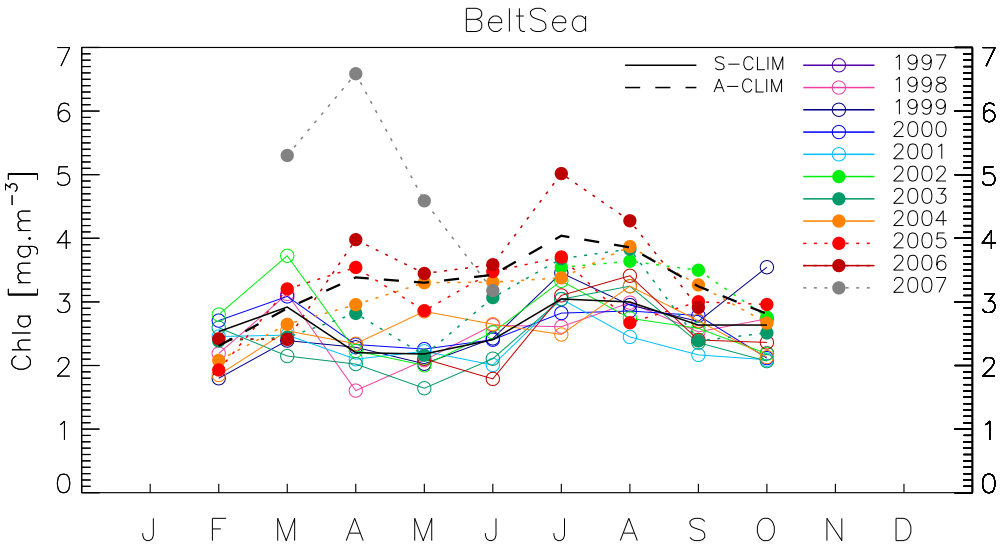

Figure 2.6: Chl*a* multi-annual time series for SeaWiFS (lines with open circles) and MODIS (filled circles with dotted line) and associated climatologies (black line and dashed line, respectively).

Like in the Kattegat, the average SeaWiFS seasonal cycle in the Belt Sea does not appear marked, but there are pronounced variations from month to month. The spring seasons of 2001 and 2003 appear below the climatological average for both Chl*a* and K_d. Significant differences appear with respect to MODIS, with an overall positive bias, also apparent for the climatological values.

Table 2.3: Belt Sea; SeaWiFS Chl$a$ inter-annual anomalies, computed as ratio of area-averaged Chl$a$ concentrations. The 2^{nd} column gives the SeaWiFS climatological Chl$a$ (in mg m^{-3}). In bold, anomalies below 0.8 or above 1.2. A datum of 1 means a regional monthly value close to climatology.

Month	mg m^{-3}	1998	1999	2000	2001	2002	2003	2004
J	-	-	-	-	-	-	-	-
F	2.532	0.86	**0.71**	1.07	0.97	1.11	1.02	**0.73**
M	2.918	1.07	0.82	1.06	0.85	**1.28**	**0.74**	0.87
A	2.201	**0.73**	1.04	1.06	0.95	1.01	0.92	1.06
M	2.180	0.96	0.93	1.04	1.02	0.92	**0.75**	**1.31**
J	2.406	1.09	1.01	1.00	0.83	1.05	0.88	1.10
J	3.045	0.86	1.13	0.93	1.00	1.09	1.00	0.82
A	2.998	1.00	0.98	0.95	0.82	0.91	1.08	1.08
S	2.636	0.96	1.02	1.06	0.82	0.98	0.89	1.03
O	2.635	1.04	**1.35**	0.80	**0.79**	0.83	**0.79**	0.81
N	-	-	-	-	-	-	-	-
D	-	-	-	-	-	-	-	-

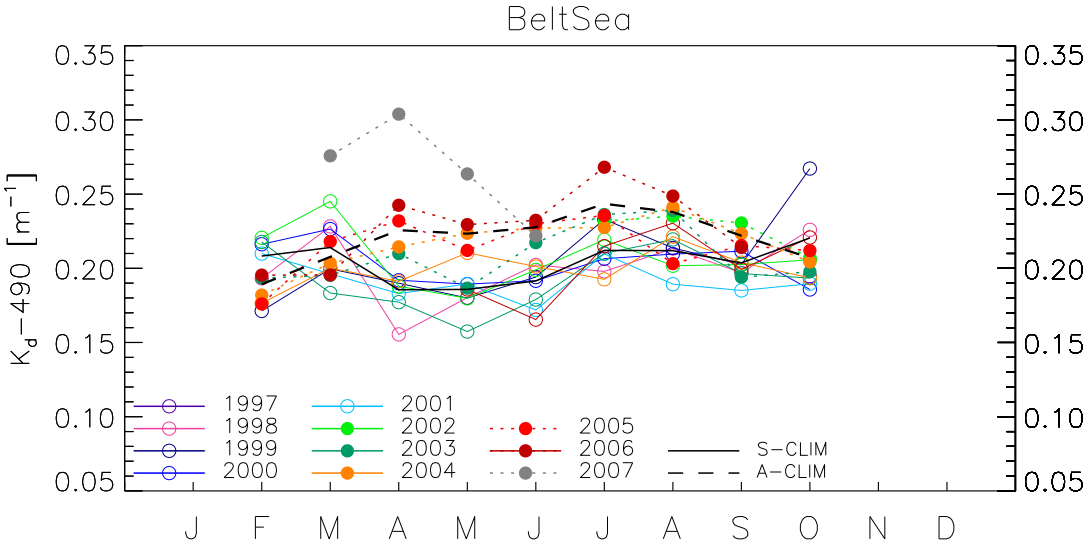

Figure 2.7: $K_d(490)$ multi-annual time series for SeaWiFS (lines with open circles) and MODIS (filled circles with dotted line) and associated climatologies (black line and dashed line, respectively).

2.4 Arkona Sea

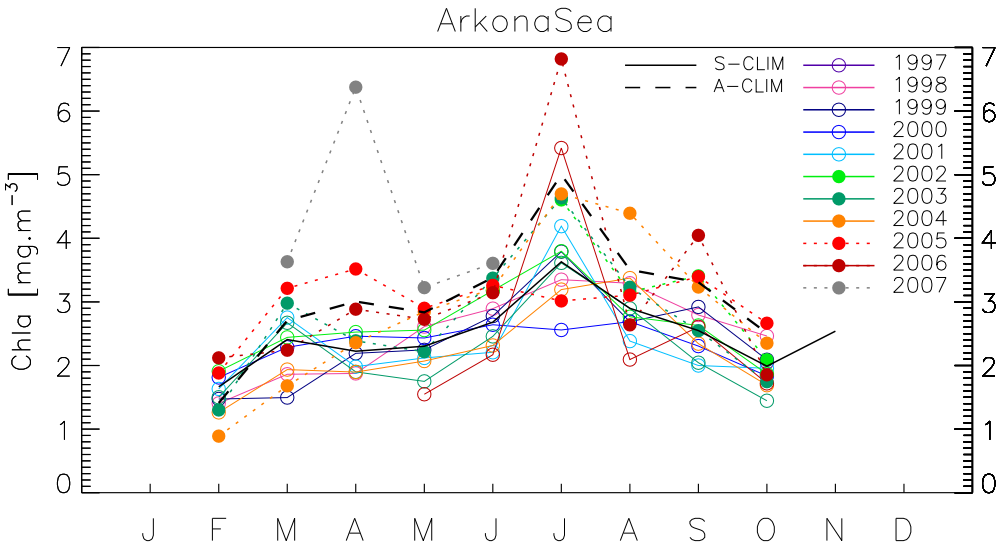

Figure 2.8: Chl*a* multi-annual time series for SeaWiFS (lines with open circles) and MODIS (filled circles with dotted line) and associated climatologies (black line and dashed line, respectively).

In the Arkona Sea, the Chl*a* cycle shows a slight local maximum in spring, in March or April, and a clearer maximum around July. This peak is also apparent for K_d. The summer 2000 is evident as an outlier for this pattern, failing to produce any increase in mean monthly Chl*a* or K_d in summer. Conversely, the July Chl*a* maximum was strong in 2001, in the middle of negative anomalies. The entire period from autumn 2003 to July 2004 is characterized by negative Chl*a* anomalies. The summer Chl*a* peaks reproduced by the MODIS product are higher than the SeaWiFS equivalents, as is the associated climatology. Interestingly, the strong summer peak exhibited by the MODIS series in 2006 is also apparent in the SeaWiFS record, even though with a smaller magnitude for Chl*a*. This underlines the value of the additional SeaWiFS data in evaluating the quality of the emerging MODIS series.

Table 2.4: Arkona Sea; SeaWiFS Chl*a* inter-annual anomalies, computed as ratio of area-averaged Chl*a* concentrations. The 2^{nd} column gives the SeaWiFS climatological Chl*a* (in mg m^{-3}). In bold, anomalies below 0.8 or above 1.2. A datum of 1 means a regional monthly value close to climatology.

Month	mg m^{-3}	1998	1999	2000	2001	2002	2003	2004
J	-	-	-	-	-	-	-	-
F	1.665	0.84	0.88	1.09	0.98	1.15	0.90	**0.76**
M	2.408	**0.77**	**0.62**	0.95	1.14	1.01	1.11	0.80
A	2.224	0.84	0.99	1.11	0.89	1.14	0.85	0.85
M	2.303	1.13	0.98	1.06	0.92	1.11	**0.76**	0.90
J	2.680	1.08	1.04	0.99	0.82	1.19	0.92	0.86
J	3.629	0.92	1.04	**0.71**	1.15	1.05	1.00	0.88
A	2.898	1.14	0.93	0.93	0.82	0.95	1.00	1.16
S	2.548	1.10	1.15	0.90	**0.78**	1.03	0.80	0.92
O	1.989	**1.24**	1.05	0.92	0.98	0.94	**0.73**	0.85
N	2.539	-	-	-	-	-	-	-
D	-	-	-	-	-	-	-	-

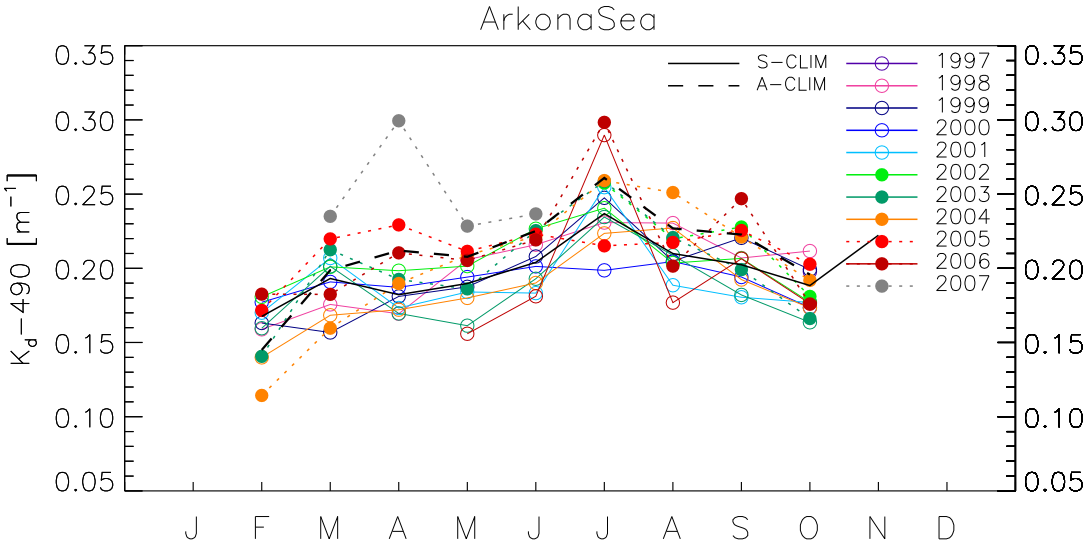

Figure 2.9: $K_d(490)$ multi-annual time series for SeaWiFS (lines with open circles) and MODIS (filled circles with dotted line) and associated climatologies (black line and dashed line, respectively).

2.5 Gulf of Gdansk

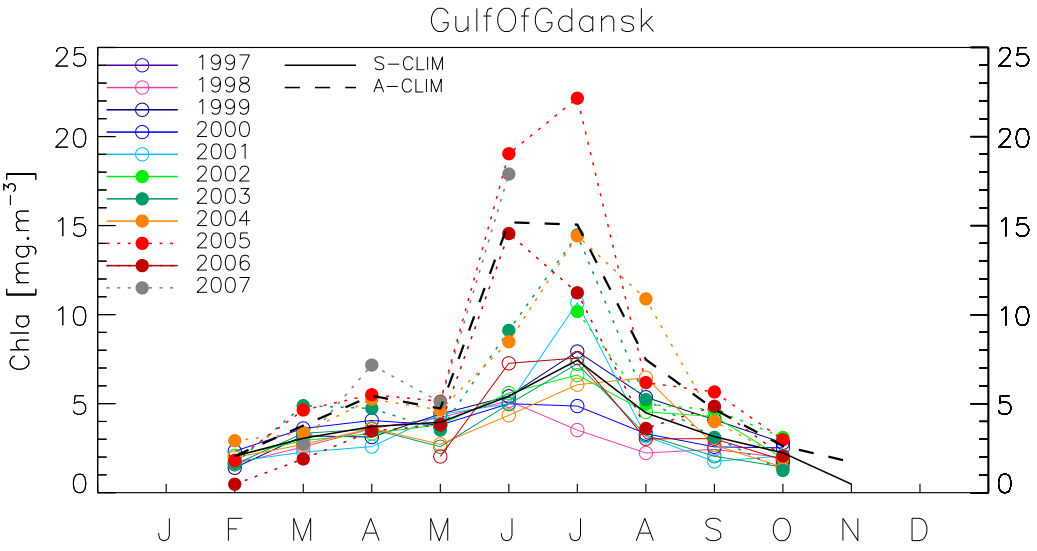

Figure 2.10: Chl*a* multi-annual time series for SeaWiFS (lines with open circles) and MODIS (filled circles with dotted line) and associated climatologies (black line and dashed line, respectively).

In the Gulf of Gdansk, the yearly Chl*a* maximum is found usually from June to August. This is modulated by a large dispersion of the monthly average values in July and August (for instance a ratio to the climatological value from 0.47 to 1.43 for July). The summer *Chla* levels appear rather low in 1998 and 2000. Furthermore, the MODIS Chl*a* concentration values are clearly much elevated with respect to those of SeaWiFS. Even though less pronounced, this is also true for K_d.

Table 2.5: Gulf of Gdansk; SeaWiFS Chl*a* inter-annual anomalies, computed as ratio of area-averaged Chl*a* concentrations. The 2^{nd} column gives the SeaWiFS climatological Chl*a* (in mg m^{-3}). In bold, anomalies below 0.8 or above 1.2. A datum of 1 means a regional monthly value close to climatology.

Month	mg m^{-3}	1998	1999	2000	2001	2002	2003	2004
J	-	-	-	-	-	-	-	-
F	2.048	**0.79**	**0.68**	1.14	0.85	1.01	**0.78**	0.97
M	3.053	0.84	1.05	1.18	**0.75**	0.96	1.09	0.89
A	3.709	0.97	0.84	1.09	**0.70**	0.90	0.96	0.97
M	3.954	1.07	1.12	0.96	1.11	0.97	**0.65**	**0.69**
J	5.416	0.95	1.00	0.92	0.92	1.03	0.92	0.80
J	7.441	**0.47**	1.07	**0.65**	**1.43**	0.89	0.97	0.82
A	4.478	**0.50**	1.20	**0.74**	**0.71**	1.01	**0.72**	**1.44**
S	3.148	**0.77**	**1.30**	0.82	**0.56**	**1.36**	**0.65**	0.85
O	2.239	0.88	**1.25**	1.12	0.92	0.87	**0.64**	**0.64**
N	0.481	-	-	-	-	-	-	-
D	-	-	-	-	-	-	-	-

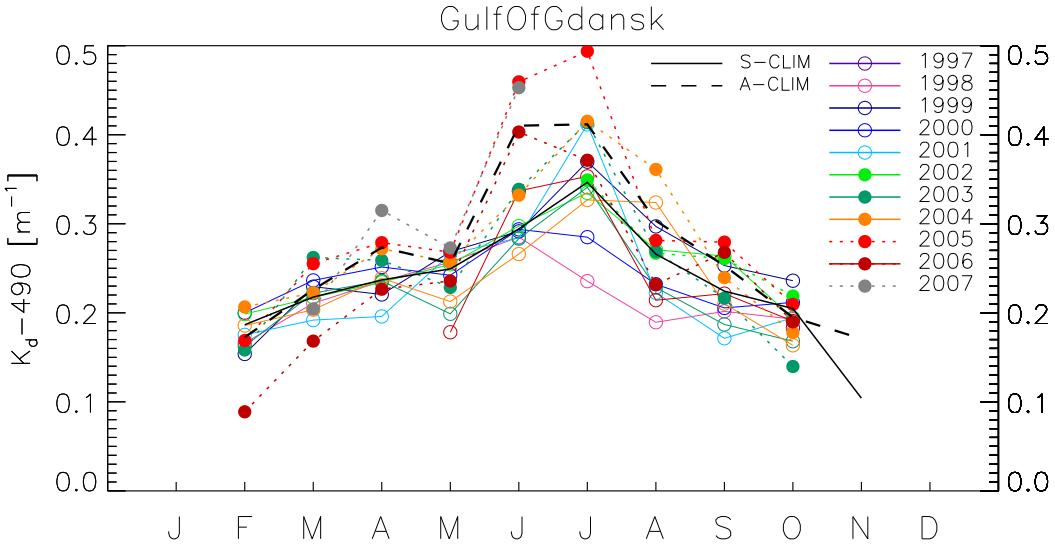

Figure 2.11: $K_d(490)$ multi-annual time series for SeaWiFS (lines with open circles) and MODIS (filled circles with dotted line) and associated climatologies (black line and dashed line, respectively).

2.6 Southern Baltic Proper

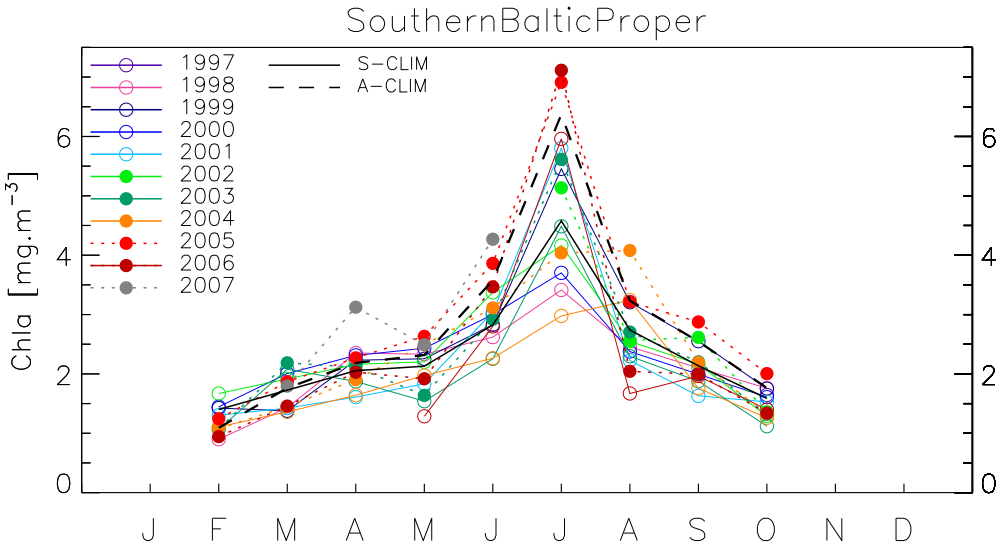

Figure 2.12: Chl*a* multi-annual time series for SeaWiFS (lines with open circles) and MODIS (filled circles with dotted line) and associated climatologies (black line and dashed line, respectively).

The two Southern Baltic Proper areas have here been aggregated into one region. After the initial increase in biomass from February to the successive months, the SeaWiFS Chl*a* maximum is clearly in July. A similar pattern is displayed for K_d. The period from spring 1999 to June 2000 displays above average Chl*a* values, whereas the converse is true from April 2003 to July 2004 (that is associated with the lowest July value, 0.65 times the climatological level). Importantly, the Chl*a* averages provided by MODIS are clearly higher than the contemporaneous SeaWiFS monthly averages. Differences between the two data records are somewhat reduced for K_d.

Table 2.6: Southern Baltic Proper; SeaWiFS Chl$a$ inter-annual anomalies, computed as ratio of area-averaged Chl$a$ concentrations. The 2^{nd} column gives the SeaWiFS climatological Chl$a$ (in mg m^{-3}). In bold, anomalies below 0.8 or above 1.2. A datum of 1 means a regional monthly value close to climatology.

Month	mg m^{-3}	1998	1999	2000	2001	2002	2003	2004
J	-	-	-	-	-	-	-	-
F	1.399	**0.64**	1.02	1.03	0.93	1.19	**0.76**	**0.79**
M	1.727	0.83	**0.80**	1.16	0.83	1.11	**1.20**	**0.79**
A	2.055	1.14	1.09	1.13	**0.78**	1.05	0.91	**0.80**
M	2.130	1.09	1.06	1.14	0.86	1.03	**0.72**	0.93
J	2.825	0.93	1.00	1.06	1.08	1.19	**0.80**	0.80
J	4.578	**0.75**	1.19	0.81	**1.27**	0.91	0.98	**0.65**
A	2.738	0.90	1.17	0.87	0.81	0.93	0.84	1.18
S	2.138	0.98	1.19	0.93	**0.76**	1.01	0.88	0.82
O	1.588	1.11	1.10	1.01	0.96	0.81	**0.71**	**0.79**
N	-	-	-	-	-	-	-	-
D	-	-	-	-	-	-	-	-

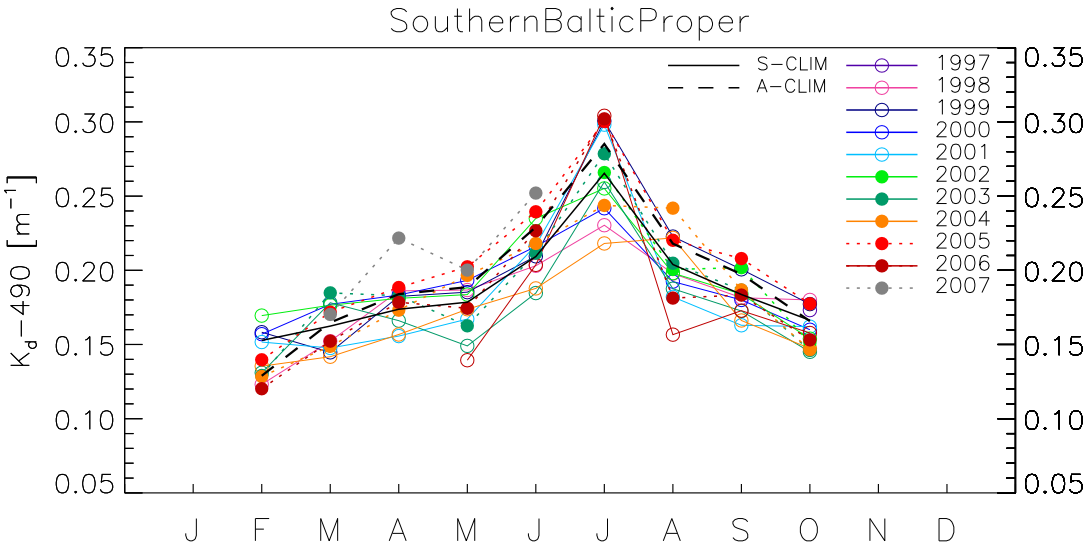

Figure 2.13: $K_d(490)$ multi-annual time series for SeaWiFS (lines with open circles) and MODIS (filled circles with dotted line) and associated climatologies (black line and dashed line, respectively).

2.7 Gotland Basin

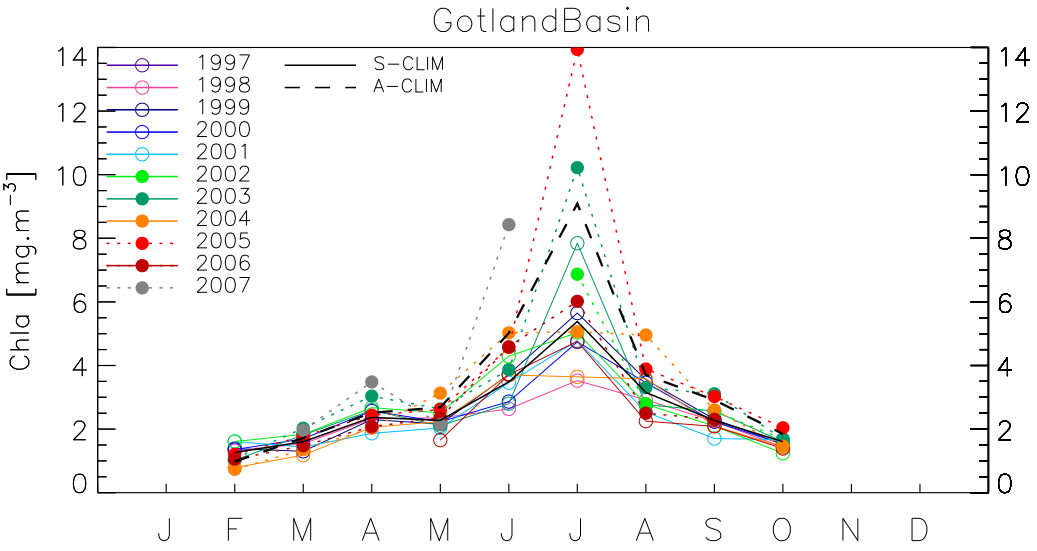

Figure 2.14: Chl*a* multi-annual time series for SeaWiFS (lines with open circles) and MODIS (filled circles with dotted line) and associated climatologies (black line and dashed line, respectively).

The results for the Gotland Basin are somewhat similar to those of the Southern Baltic Proper. For that region also, the maximum Chl*a* and K_d values are usually found in July. The inter-annual variability seems however reduced. The lowest anomaly is found for the summer (June-July) 1998. The Chl*a* levels are somewhat low in 2004. As for the adjacent southern region, the MODIS products are characterized by higher levels. The July maximum is very high in 2003 and even more in 2005. The LAC product for SeaWiFS in 2003 shows the highest monthly value in the entire record (1.46 times the climatological value). The latter MODIS peak is associated with a basin wide cyanobacteria bloom with an accumulation of associated material at the sea surface (Zibordi et al., 2006d). The peaks for both SeaWiFS and MODIS are much lower in 2006. SeaWiFS and MODIS K_d products are clearly more coincident than for Chl*a*.

Table 2.7: Gotland Basin; SeaWiFS Chl*a* inter-annual anomalies, computed as ratio of area-averaged Chl*a* concentrations. The 2^{nd} column gives the SeaWiFS climatological Chl*a* (in mg m^{-3}). In bold, anomalies below 0.8 or above 1.2. A datum of 1 means a regional monthly value close to climatology.

Month	mg m^{-3}	1998	1999	2000	2001	2002	2003	2004
J	-	-	-	-	-	-	-	-
F	1.262	1.04	1.10	1.07	**1.27**	**1.27**	0.81	**0.62**
M	1.603	0.96	0.81	1.06	0.89	1.14	1.13	**0.74**
A	2.369	0.98	0.97	1.08	**0.79**	1.13	1.10	0.87
M	2.275	1.03	0.95	0.98	0.89	1.10	0.92	0.98
J	3.484	**0.76**	1.07	0.82	0.99	**1.23**	0.80	1.06
J	5.384	**0.65**	1.05	0.88	0.89	0.94	**1.46**	**0.68**
A	3.151	0.93	1.13	1.10	0.80	0.88	0.88	1.14
S	2.272	0.99	1.02	0.98	**0.75**	0.92	1.13	0.92
O	1.605	0.89	0.95	0.95	1.04	**0.77**	1.00	0.89
N	-	-	-	-	-	-	-	-
D	-	-	-	-	-	-	-	-

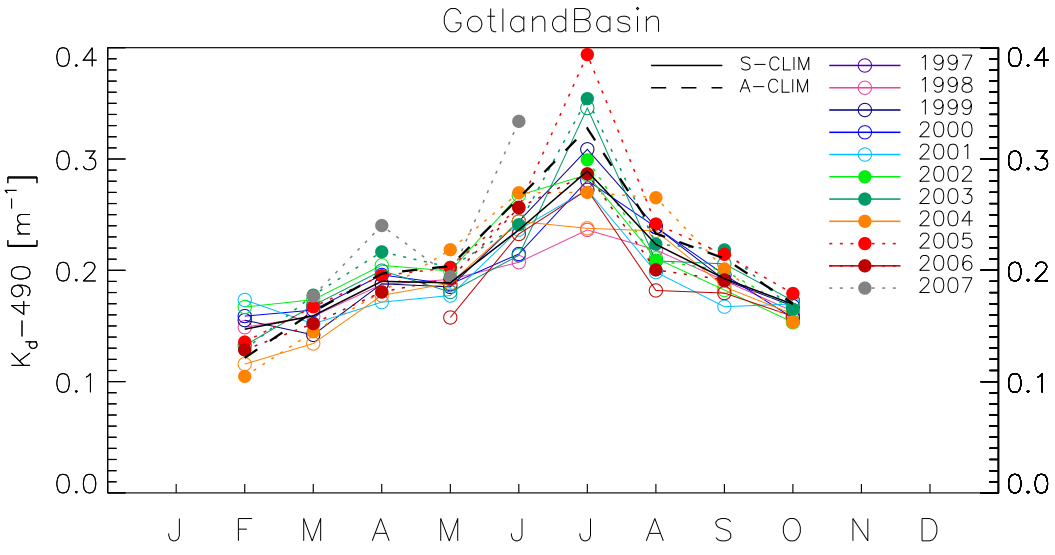

Figure 2.15: $K_d(490)$ multi-annual time series for SeaWiFS (lines with open circles) and MODIS (filled circles with dotted line) and associated climatologies (black line and dashed line, respectively).

2.8 Northern Baltic Proper

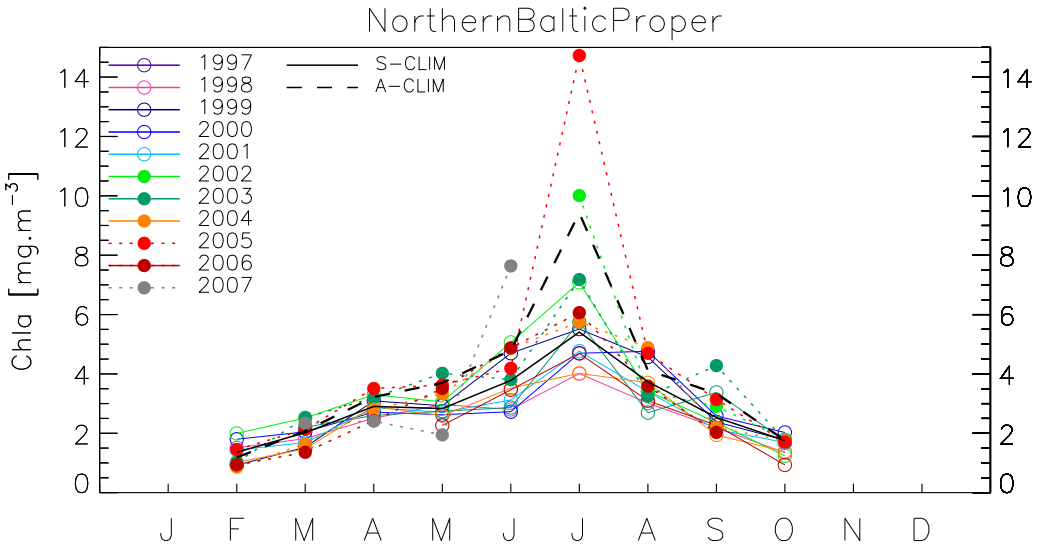

Figure 2.16: Chl*a* multi-annual time series for SeaWiFS (lines with open circles) and MODIS (filled circles with dotted line) and associated climatologies (black line and dashed line, respectively).

The results described for the Gotland Basin are mostly applicable to the northern Baltic Sea. However, the high values of the summer 2003 are much less prominent whereas the first MODIS Chl*a* monthly average (July 2002) is high. As for the Gotland Basin, both Chl*a* and K_d from MODIS hint at high values for the summer 2007.

Table 2.8: Northern Baltic Proper; SeaWiFS Chl$a$ inter-annual anomalies, computed as ratio of area-averaged Chl$a$ concentrations. The 2^{nd} column gives the SeaWiFS climatological Chl$a$ (in mg m^{-3}). In bold, anomalies below 0.8 or above 1.2. A datum of 1 means a regional monthly value close to climatology.

Month	mg m^{-3}	1998	1999	2000	2001	2002	2003	2004
J	-	-	-	-	-	-	-	-
F	1.357	1.11	**0.68**	**1.32**	1.06	**1.47**	-	**0.75**
M	2.021	0.90	**0.76**	1.01	0.83	**1.25**	1.09	**0.73**
A	2.903	0.86	1.06	0.93	0.99	1.14	0.90	1.00
M	2.832	1.05	1.03	0.93	0.96	1.08	0.97	0.91
J	3.779	**0.74**	**1.24**	**0.72**	0.83	**1.34**	**0.76**	0.93
J	5.408	**0.74**	1.02	0.87	0.88	**1.31**	1.06	**0.74**
A	3.735	0.81	**1.22**	**1.27**	0.91	0.92	**0.72**	0.99
S	2.533	0.86	0.94	1.02	0.84	0.93	**1.33**	**0.77**
O	1.751	**0.77**	1.01	1.16	0.97	**0.71**	0.99	**0.79**
N	-	-	-	-	-	-	-	-
D	-	-	-	-	-	-	-	-

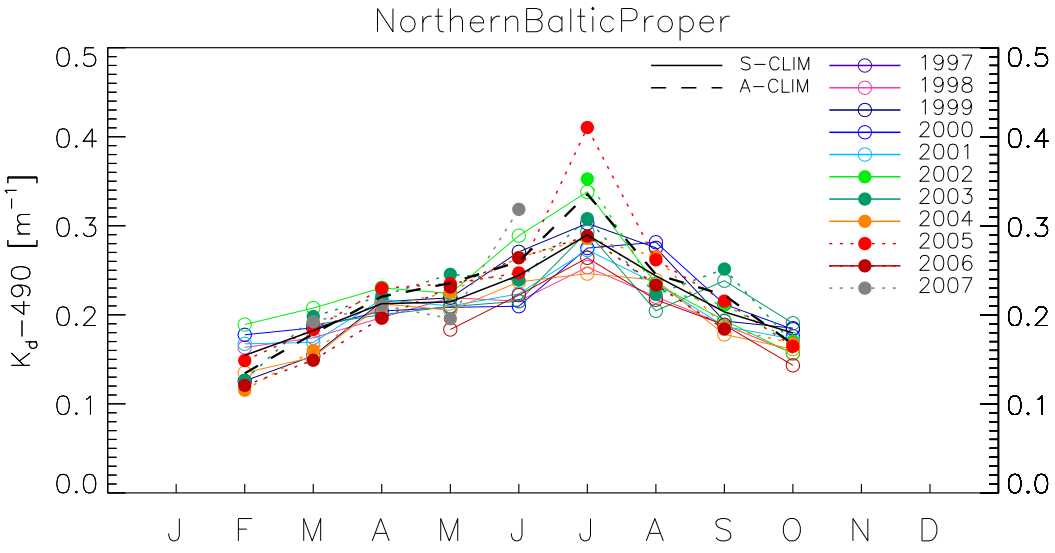

Figure 2.17: $K_d(490)$ multi-annual time series for SeaWiFS (lines with open circles) and MODIS (filled circles with dotted line) and associated climatologies (black line and dashed line, respectively).

2.9 Gulf of Riga

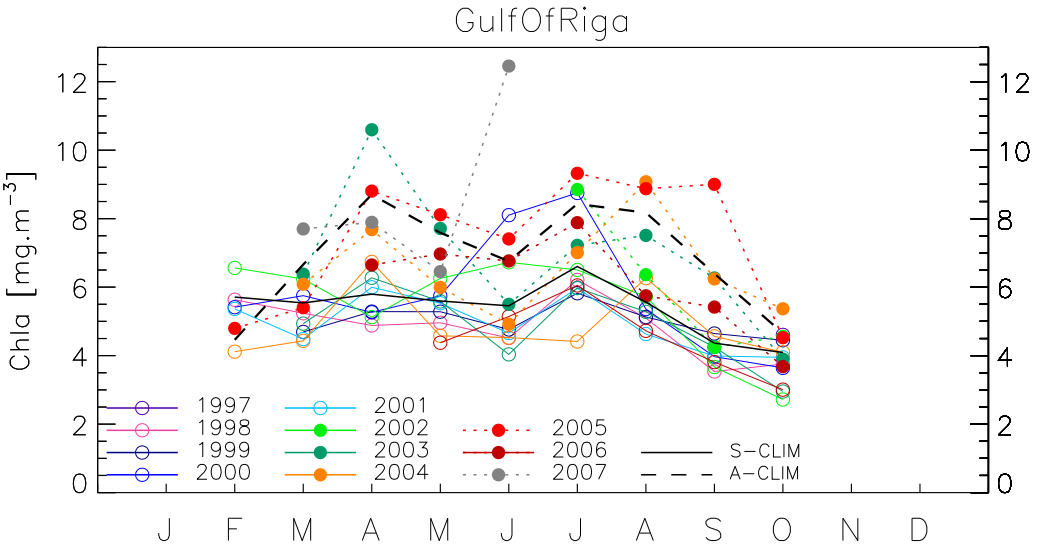

Figure 2.18: Chl*a* multi-annual time series for SeaWiFS (lines with open circles) and MODIS (filled circles with dotted line) and associated climatologies (black line and dashed line, respectively).

Monthly Chl*a* and K_d averages are extremely variable from one month to the next. On the other hand, the inter-annual variability is rather constrained, with some exceptions, like the low values of June 2003 and July 2004, and the peak of June-July 2000. For both Chl*a* and K_d, large differences can be found between SeaWiFS and MODIS.

Table 2.9: Gulf of Riga; SeaWiFS Chl*a* inter-annual anomalies, computed as ratio of area-averaged Chl*a* concentrations. The 2^{nd} column gives the SeaWiFS climatological Chl*a* (in mg m^{-3}). In bold, anomalies below 0.8 or above 1.2. A datum of 1 means a regional monthly value close to climatology.

Month	mg m^{-3}	1998	1999	2000	2001	2002	2003	2004
J	-	-	-	-	-	-	-	-
F	5.709	0.99	-	0.95	0.94	1.15	-	**0.72**
M	5.540	0.95	0.85	1.04	0.81	1.13	0.89	**0.80**
A	5.796	0.84	0.91	0.91	1.03	0.88	1.08	1.16
M	5.594	0.89	0.94	1.03	0.99	1.12	1.00	0.82
J	5.454	0.83	0.87	**1.49**	0.85	**1.23**	**0.74**	0.83
J	6.604	0.94	0.88	**1.33**	0.90	0.98	0.91	**0.67**
A	5.562	0.92	0.92	0.96	0.83	1.03	0.95	1.13
S	4.364	0.81	1.06	0.91	0.91	0.84	0.97	1.05
O	4.090	0.92	1.09	0.89	0.97	**0.67**	**0.72**	1.00
N	-	-	-	-	-	-	-	-
D	-	-	-	-	-	-	-	-

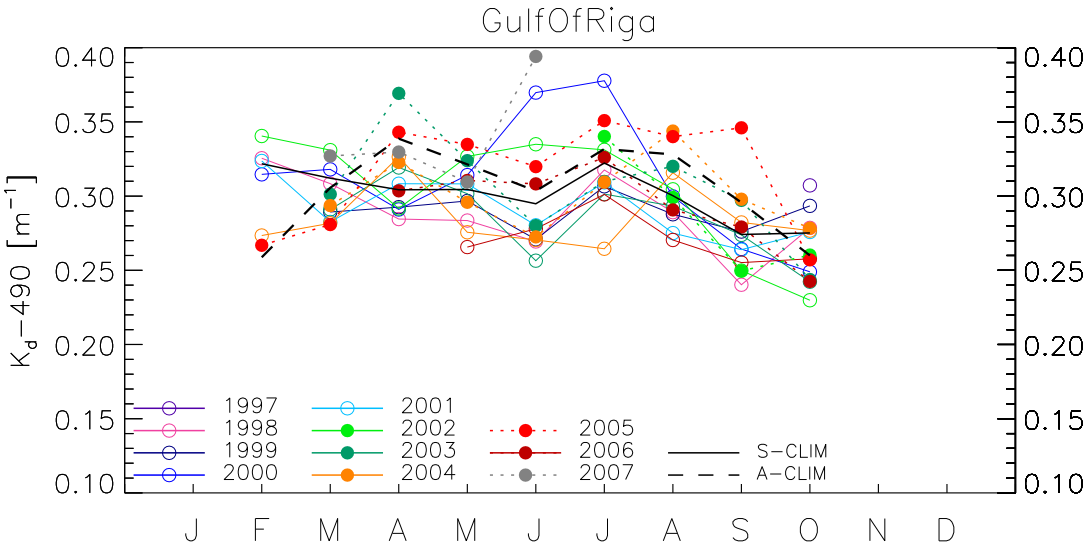

Figure 2.19: $K_d(490)$ multi-annual time series for SeaWiFS (lines with open circles) and MODIS (filled circles with dotted line) and associated climatologies (black line and dashed line, respectively).

2.10 Gulf of Finland

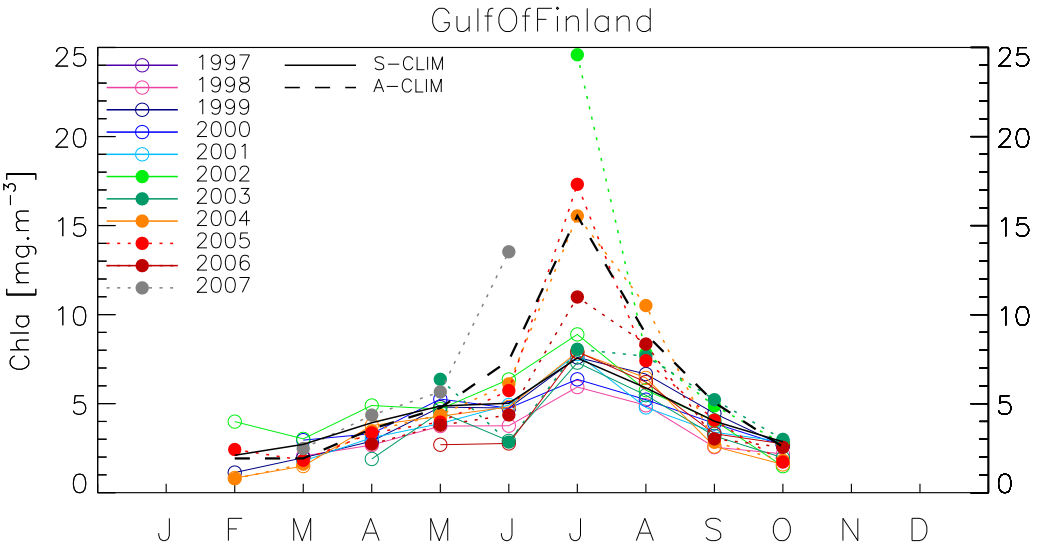

Figure 2.20: Chl*a* multi-annual time series for SeaWiFS (lines with open circles) and MODIS (filled circles with dotted line) and associated climatologies (black line and dashed line, respectively).

After the initial increase from February to May, the most prominent feature in the SeaWiFS record is the July Chl*a* maximum. For K_d, there is a first maximum in May followed by a larger one in July. The inter-annual variability is more pronounced than in the Baltic Proper. The whole years 1998 and 2003 are associated with Chl*a* that are below climatological average. Conversely, the year 2002 is characterized by significant positive anomalies. A noticeable feature is again the large MODIS estimates in summer.

Table 2.10: Gulf of Finland; SeaWiFS Chl*a* inter-annual anomalies, computed as ratio of area-averaged Chl*a* concentrations. The 2^{nd} column gives the SeaWiFS climatological Chl*a* (in mg m^{-3}). In bold, anomalies below 0.8 or above 1.2. A datum of 1 means a regional monthly value close to climatology.

Month	mg m^{-3}	1998	1999	2000	2001	2002	2003	2004
J	-	-	-	-	-	-	-	-
F	2.102	-	**0.54**	-	-	**1.90**	-	**0.39**
M	2.714	**0.76**	**0.72**	1.09	**0.65**	1.11	-	**0.55**
A	3.929	**0.68**	**0.74**	0.84	**0.79**	**1.25**	**0.48**	0.96
M	4.867	**0.77**	0.99	1.08	**0.80**	0.96	0.93	0.88
J	5.024	**0.75**	0.95	0.95	0.98	**1.27**	**0.58**	0.96
J	7.558	**0.78**	1.00	0.84	1.03	1.18	0.97	1.05
A	5.885	0.83	1.13	0.89	0.81	0.98	0.93	1.10
S	4.012	**0.64**	1.11	0.97	0.85	1.01	**0.79**	**0.65**
O	2.858	**0.76**	0.93	0.93	1.00	**0.52**	**0.69**	**0.56**
N	-	-	-	-	-	-	-	-
D	-	-	-	-	-	-	-	-

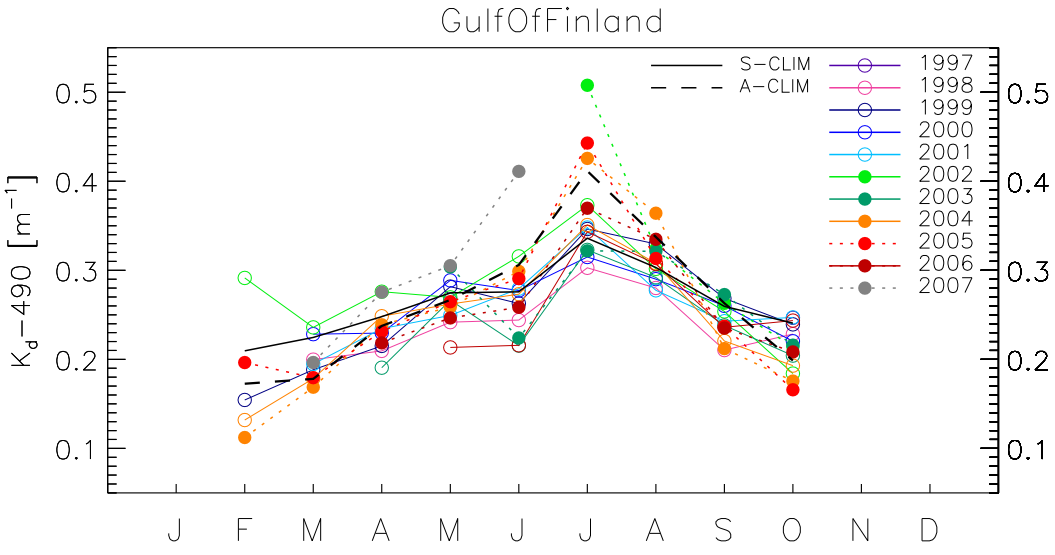

Figure 2.21: $K_d(490)$ multi-annual time series for SeaWiFS (lines with open circles) and MODIS (filled circles with dotted line) and associated climatologies (black line and dashed line, respectively).

2.11 Aland Sea

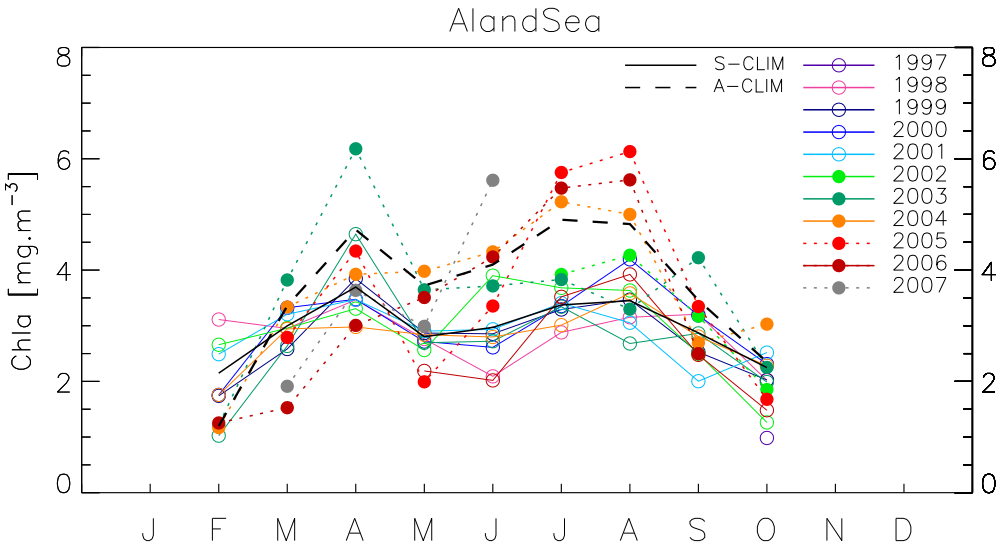

Figure 2.22: Chl*a* multi-annual time series for SeaWiFS (lines with open circles) and MODIS (filled circles with dotted line) and associated climatologies (black line and dashed line, respectively).

The regional averages tend to show a slight double-peak feature, with maxima around April and July-August, and lower values in May-June. There are exceptions to this pattern, like the strong positive anomaly in June 2002. MODIS climatologies of Chl*a* nd K_d are consistently higher than the SeaWiFS counterparts.

Table 2.11: Aland Sea; SeaWiFS Chl*a* inter-annual anomalies, computed as ratio of area-averaged Chl*a* concentrations. The 2^{nd} column gives the SeaWiFS climatological Chl*a* (in mg m^{-3}). In bold, anomalies below 0.8 or above 1.2. A datum of 1 means a regional monthly value close to climatology.

Month	mg m^{-3}	1998	1999	2000	2001	2002	2003	2004
J	-	-	-	-	-	-	-	-
F	2.148	**1.45**	0.81	0.82	1.16	**1.24**	**0.48**	0.82
M	2.998	0.98	0.86	1.11	1.07	0.99	0.88	0.98
A	3.694	0.94	1.04	0.94	0.94	0.90	**1.26**	0.81
M	2.803	0.99	1.02	0.97	1.04	0.91	0.96	1.01
J	2.970	**0.70**	0.96	0.88	0.99	**1.31**	0.92	0.94
J	3.373	0.85	0.98	0.99	1.01	1.09	0.99	0.89
A	3.449	0.91	1.01	**1.22**	0.89	1.05	**0.78**	1.04
S	2.872	1.12	0.88	1.11	**0.70**	0.87	1.00	0.98
O	2.248	0.90	0.90	1.03	1.12	**0.56**	0.88	1.01
N	-	-	-	-	-	-	-	-
D	-	-	-	-	-	-	-	-

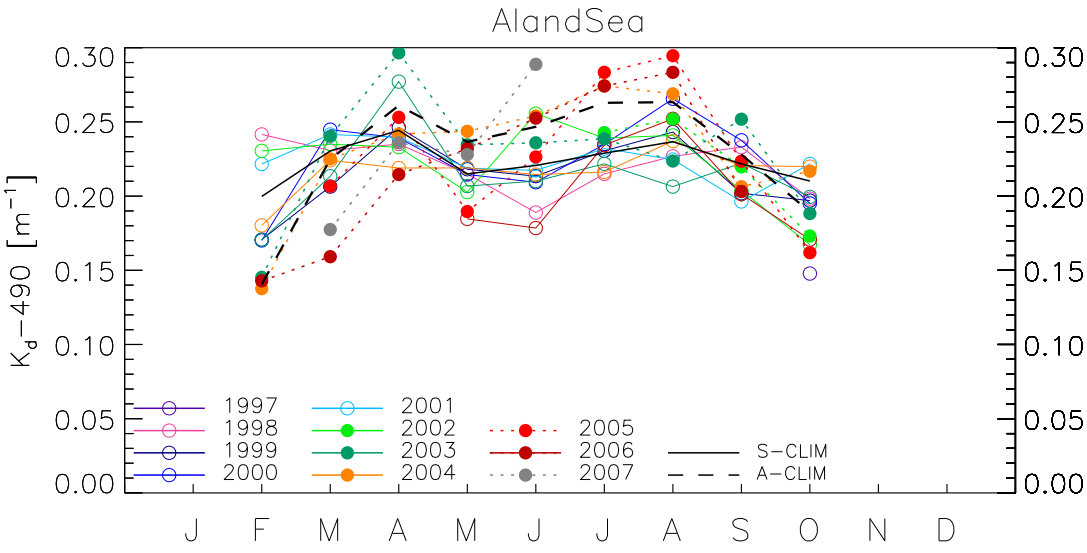

Figure 2.23: $K_d(490)$ multi-annual time series for SeaWiFS (lines with open circles) and MODIS (filled circles with dotted line) and associated climatologies (black line and dashed line, respectively).

2.12 Archipelago Region

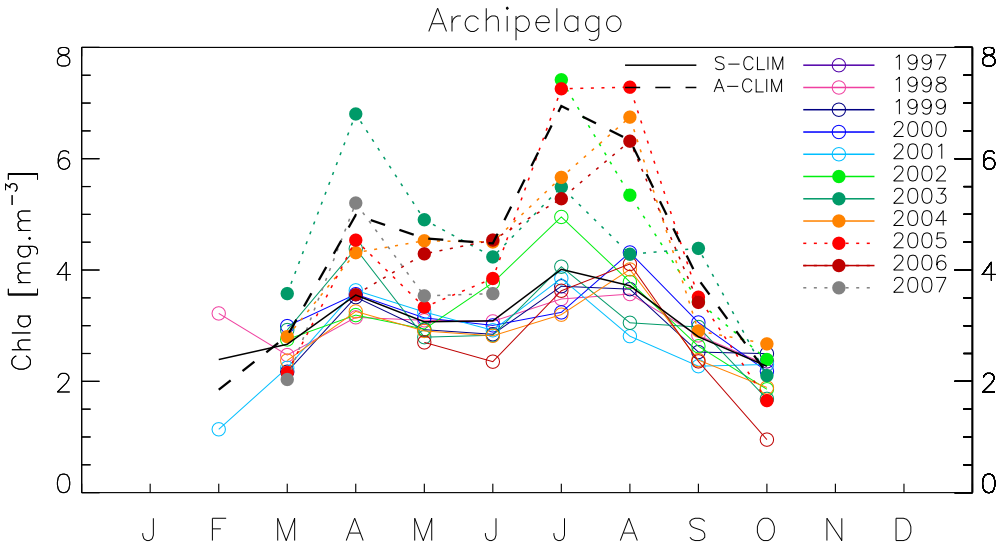

Figure 2.24: Chl*a* multi-annual time series for SeaWiFS (lines with open circles) and MODIS (filled circles with dotted line) and associated climatologies (black line and dashed line, respectively).

The data records for the Archipelago region are rather close to those shown for the Aland Sea.

Table 2.12: Archipelago Region; SeaWiFS Chl*a* inter-annual anomalies, computed as ratio of area-averaged Chl*a* concentrations. The 2^{nd} column gives the SeaWiFS climatological Chl*a* (in mg m^{-3}). In bold, anomalies below 0.8 or above 1.2. A datum of 1 means a regional monthly value close to climatology.

Month	mg m^{-3}	1998	1999	2000	2001	2002	2003	2004
J	-	-	-	-	-	-	-	-
F	2.391	**1.35**	-	-	**0.48**	-	-	-
M	2.666	0.93	0.81	1.12	0.84	1.03	1.10	0.89
A	3.550	0.89	0.99	1.00	1.02	0.90	**1.23**	0.92
M	3.069	1.01	0.95	1.02	1.06	0.96	0.91	0.95
J	3.086	1.00	0.92	0.97	0.95	**1.22**	0.92	0.91
J	4.012	0.87	0.92	0.81	0.96	**1.23**	1.01	**0.80**
A	3.717	0.96	0.98	1.16	**0.76**	1.02	0.82	1.08
S	2.801	1.01	0.90	1.09	0.81	0.94	1.06	0.85
O	2.270	1.01	1.10	0.96	1.01	0.82	**0.74**	0.83
N	-	-	-	-	-	-	-	-
D	-	-	-	-	-	-	-	-

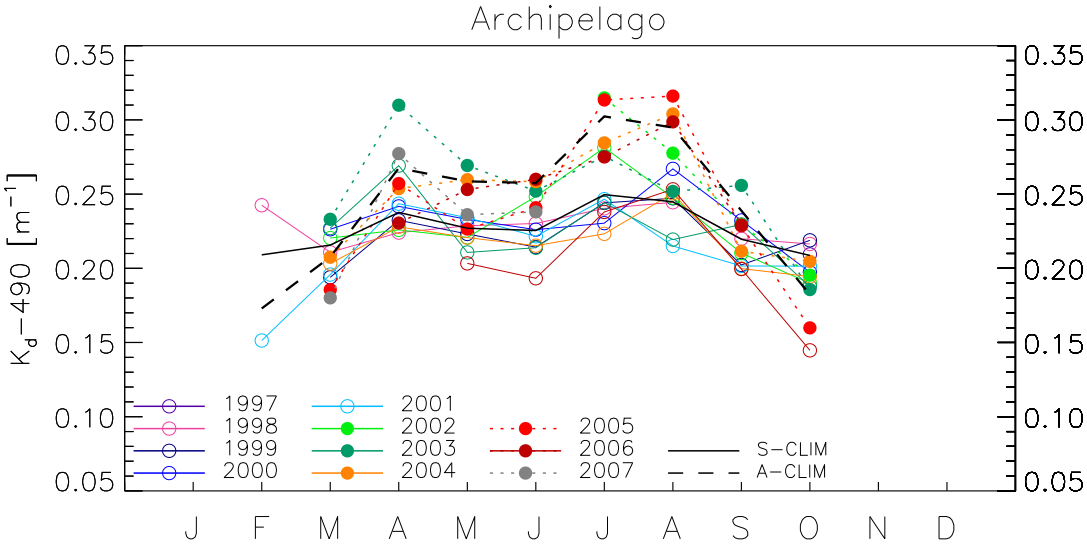

Figure 2.25: $K_d(490)$ multi-annual time series for SeaWiFS (lines with open circles) and MODIS (filled circles with dotted line) and associated climatologies (black line and dashed line, respectively).

2.13 Bothnian Sea

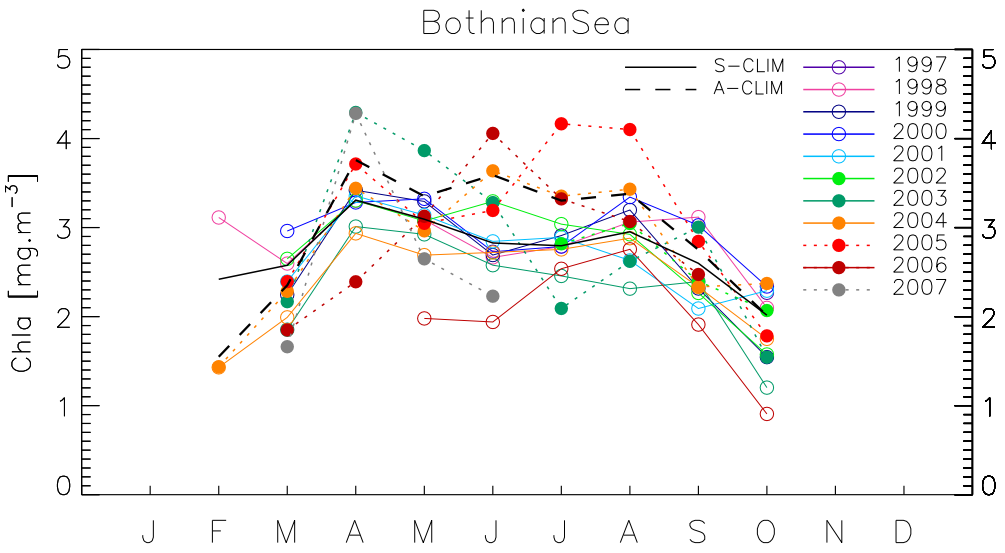

Figure 2.26: Chl*a* multi-annual time series for SeaWiFS (lines with open circles) and MODIS (filled circles with dotted line) and associated climatologies (black line and dashed line, respectively).

Even though there is a large variability on this pattern, the SeaWiFS Chl*a* cycle for the Bothnian Sea shows a maximum around April, and for some years a secondary peak in August. Overall, the Chl*a* levels as documented by the SeaWiFS data seem to have been lower since autumn 2002. On the other hand, the MODIS data indicate fairly high values for the last 3 years, but low Chl*a* concentrations in May-June 2007. The levels of attenuation are rather constant with higher levels from April to August. The K_d climatologies provided by the two sensors are similar.

Table 2.13: Bothnian Sea; SeaWiFS Chl*a* inter-annual anomalies, computed as ratio of area-averaged Chl*a* concentrations. The 2^{nd} column gives the SeaWiFS climatological Chl*a* (in mg m^{-3}). In bold, anomalies below 0.8 or above 1.2. A datum of 1 means a regional monthly value close to climatology.

Month	mg m^{-3}	1998	1999	2000	2001	2002	2003	2004
J	-	-	-	-	-	-	-	-
F	2.420	**1.29**	-	-	-	-	-	**0.59**
M	2.576	1.01	0.87	1.15	0.93	1.03	**0.72**	**0.77**
A	3.308	1.00	1.03	0.99	1.01	1.00	0.91	0.89
M	3.094	1.00	1.06	1.07	1.01	0.99	0.95	0.87
J	2.827	0.94	0.95	0.97	1.01	1.17	0.91	0.96
J	2.796	1.00	1.04	1.00	1.03	1.09	0.88	0.99
A	2.953	1.04	1.08	1.13	0.89	0.99	**0.78**	0.98
S	2.599	1.20	0.89	1.16	0.80	0.87	0.92	0.90
O	2.016	1.04	**0.77**	1.16	1.14	**0.78**	**0.60**	0.87
N	-	-	-	-	-	-	-	-
D	-	-	-	-	-	-	-	-

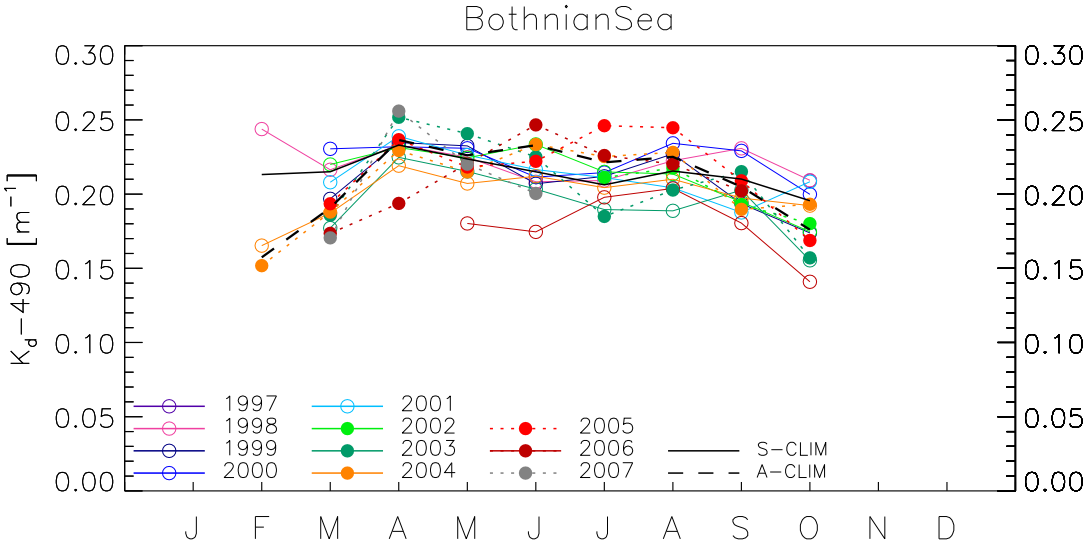

Figure 2.27: $K_d(490)$ multi-annual time series for SeaWiFS (lines with open circles) and MODIS (filled circles with dotted line) and associated climatologies (black line and dashed line, respectively).

2.14 Bothnian Bay

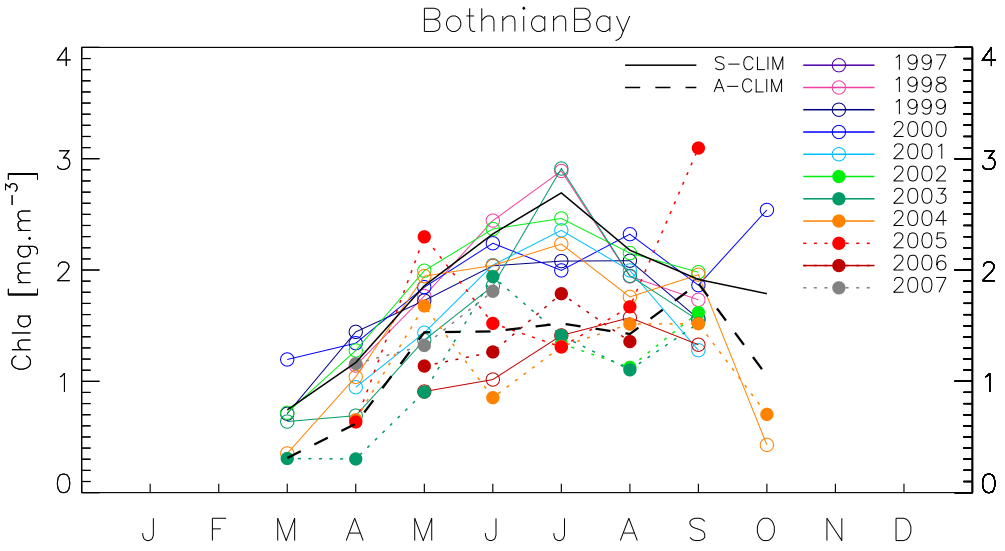

Figure 2.28: Chl*a* multi-annual time series for SeaWiFS (lines with open circles) and MODIS (filled circles with dotted line) and associated climatologies (black line and dashed line, respectively).

The growing season is reduced in the Bothnian Bay with respect to the region lying further south. The biomass levels increase steadily up to June-July, with a peak in July. An exception is the year 2000, with higher Chl*a* in June and August. In general, the series appear lower in 1999, 2001 and 2003. Interestingly, the MODIS data (Chl*a* and K_d) are found mostly below the SeaWiFS data.

Table 2.14: Bothnian Bay; SeaWiFS Chl*a* inter-annual anomalies, computed as ratio of area-averaged Chl*a* concentrations. The 2^{nd} column gives the SeaWiFS climatological Chl*a* (in mg m^{-3}). In bold, anomalies below 0.8 or above 1.2. A datum of 1 means a regional monthly value close to climatology.

Month	mg m^{-3}	1998	1999	2000	2001	2002	2003	2004
J	-	-	-	-	-	-	-	-
F	-	-	-	-	-	-	-	-
M	0.743	-	0.95	**1.61**	-	0.97	0.86	**0.47**
A	1.169	0.98	**1.24**	1.15	0.81	1.09	**0.59**	0.89
M	1.858	0.95	0.93	0.99	**0.77**	1.07	**0.74**	1.05
J	2.324	1.05	0.88	0.96	0.88	1.02	**0.80**	0.88
J	2.693	1.07	**0.77**	**0.74**	0.88	0.91	1.08	0.83
A	2.178	0.89	0.96	1.07	0.92	0.99	0.89	0.81
S	1.915	0.90	0.82	0.97	**0.67**	1.03	0.81	1.02
O	1.787	-	-	**1.42**	-	-	-	**0.24**
N	-	-	-	-	-	-	-	-
D	-	-	-	-	-	-	-	-

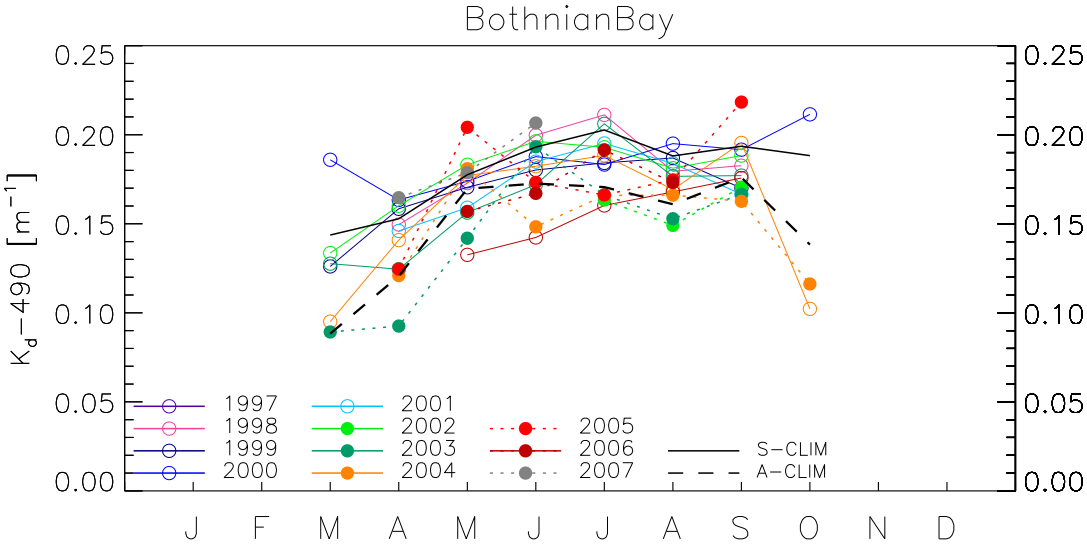

Figure 2.29: $K_d(490)$ multi-annual time series for SeaWiFS (lines with open circles) and MODIS (filled circles with dotted line) and associated climatologies (black line and dashed line, respectively).

Section 3

Mediterranean Sea

The partition of the Mediterranean Sea is shown on Figure 3.1 with, from northwest to southeast, Adriatic Sea, Gulf of Lions, Ligurian Sea, Balearic Sea, Provencal Basin, Alboran Sea, Algerian Basin, Tyrrhenian Sea, northern and southern Ionian Sea, Aegean Sea, northern and southern Levantine Basin. It reproduces that chosen by Bricaud et al. (2002).

For each domain, the time series of Chl$a$ and $K_d(490)$ are given for the years 1997 to 2004 using SeaWiFS (lines with open circles) and for years 2002 to 2007 for MODIS (filled circles with dotted line). The climatologies from SeaWiFS (Dec. 1997-Nov. 2004, continuous line) and MODIS (Jul. 2002-Jun. 2007, dashed line) are over-plotted for reference.

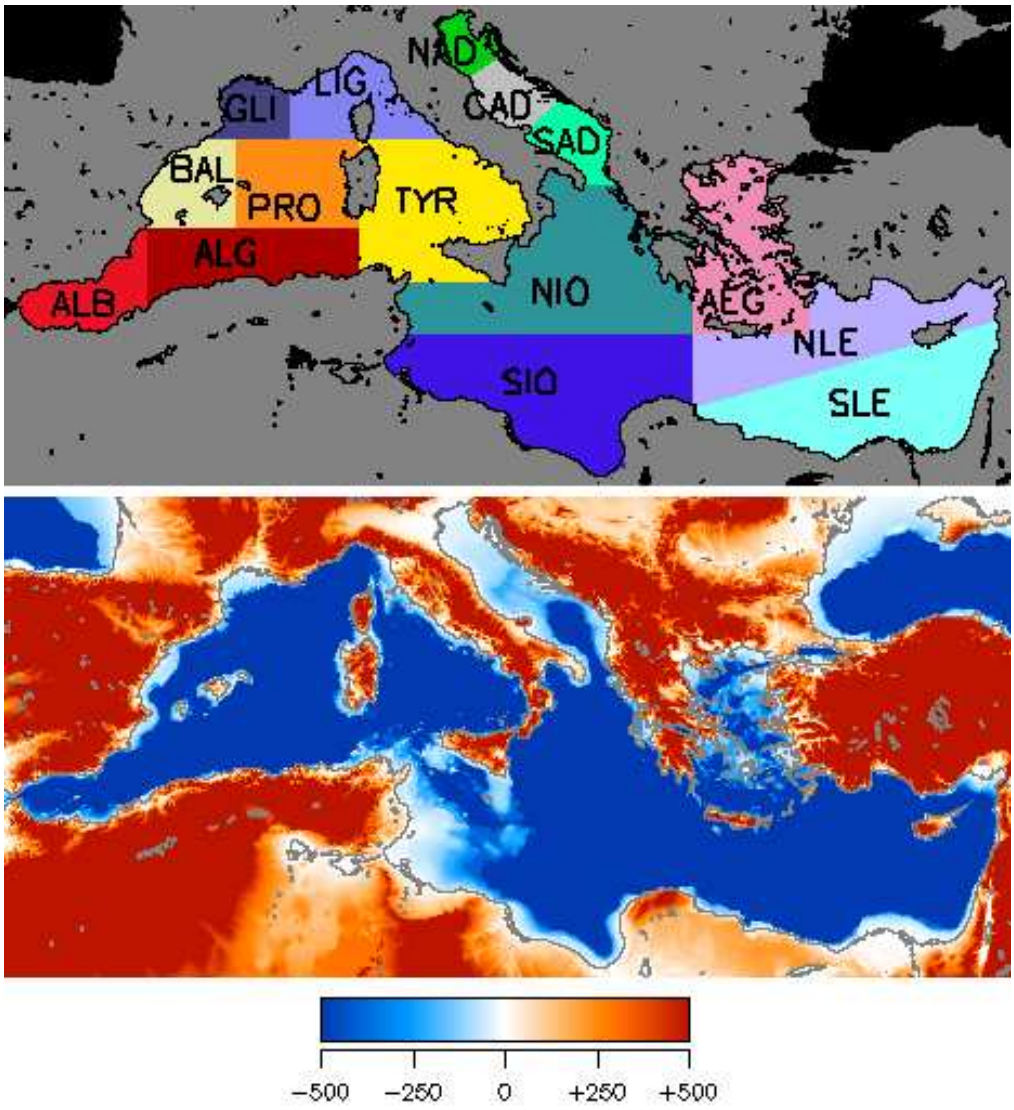

Figure 3.1: Distribution of Mediterranean Sea bathymetry and partition. **NAD**: Northern Adriatic Sea; **CAD**: Central Adriatic Sea; **SAD**: Southern Adriatic Sea; **ALB**: Alboran Sea; **GLI**: Gulf of Lions; **LIG**: Ligurian Sea; **BAL**: Balearic Sea; **PRO**: Provencal Basin; **ALG**: Algerian Basin; **TYR**: Tyrrhenian Sea; **NIO**: North Ionian Sea; **SIO**: South Ionian Sea; **AEG**: Aegean Sea; **NLE** and **SLE**: North and South Levantine Basin:

3.1 Northern Adriatic Sea

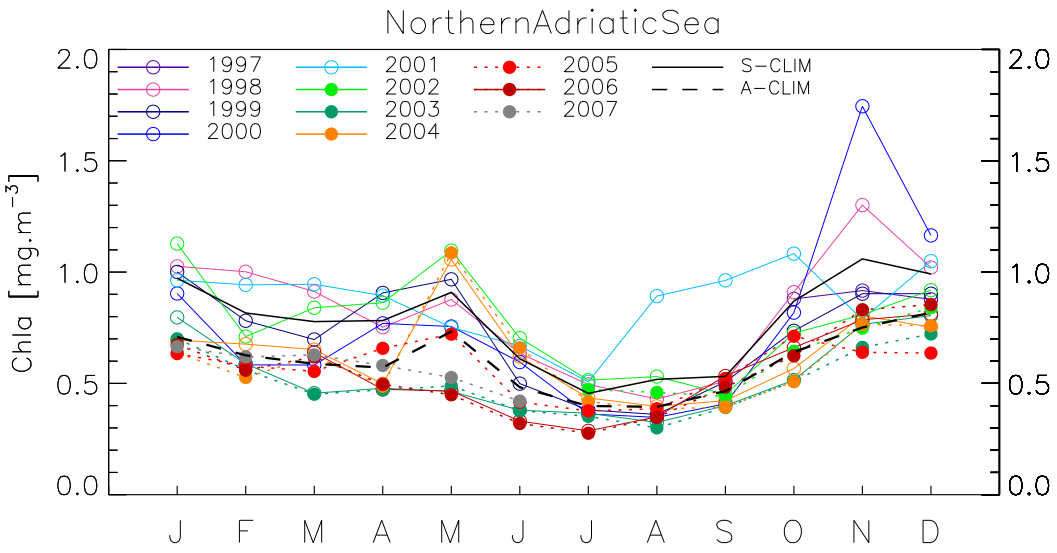

Figure 3.2: Chl*a* multi-annual time series for SeaWiFS (lines with open circles) and MODIS (filled circles with dotted line) and associated climatologies (black line and dashed line, respectively).

The northern part of the Adriatic Sea has the highest regional levels of Chl*a* in the Mediterranean Sea, with a seasonal cycle displaying a minimum in summer. Interestingly, after autumn 2002, the monthly anomalies were mostly negative for more than 2 years (except in May-June 2004), and rather low concentrations are shown in 2006-2007. The period from summer 1999 to October 2000 was also characterized by concentrations lower than the climatological average. Conversely, particularly high Chl*a* values are noticed for late winter and autumn 1998, autumn 2000, and late summer 2001. For this optically complex system, the agreement between SeaWiFS and MODIS data appears satisfactory. The inter-annual variability is translated by the differences observed between the SeaWiFS and MODIS climatologies. The attenuation K_d record shows similar variations with a clear seasonal minimum in July-August, maxima in winter and May.

Table 3.1: Northern Adriatic Sea; SeaWiFS Chl*a* inter-annual anomalies, computed as ratio of area-averaged Chl*a* concentrations. The 2^{nd} column gives the SeaWiFS climatological Chl*a* (in mg m^{-3}). In bold, anomalies below 0.8 or above 1.2. A datum of 1 means a regional monthly value close to climatology.

Month	mg m^{-3}	1998	1999	2000	2001	2002	2003	2004
J	0.972	1.05	1.03	0.93	0.99	1.16	0.82	**0.71**
F	0.816	**1.23**	0.96	**0.71**	1.15	0.87	**0.72**	0.83
M	0.777	1.17	0.90	**0.75**	**1.22**	1.08	**0.59**	0.84
A	0.782	0.96	1.16	0.98	1.14	1.10	**0.61**	**0.64**
M	0.909	0.96	1.06	0.83	0.83	**1.21**	**0.51**	1.16
J	0.610	1.04	0.82	0.98	1.09	1.15	**0.62**	1.02
J	0.455	1.09	0.84	**0.80**	1.11	1.13	0.80	0.95
A	0.518	0.83	**0.70**	**0.67**	**1.72**	1.02	**0.63**	**0.77**
S	0.532	0.96	0.95	**0.77**	**1.81**	0.85	**0.75**	**0.79**
O	0.869	1.05	0.85	0.94	**1.25**	0.83	**0.59**	**0.65**
N	1.059	**1.23**	0.85	**1.65**	**0.74**	**0.76**	**0.72**	**0.76**
D	0.992	1.03	0.91	1.17	1.06	0.93	0.81	**0.76**

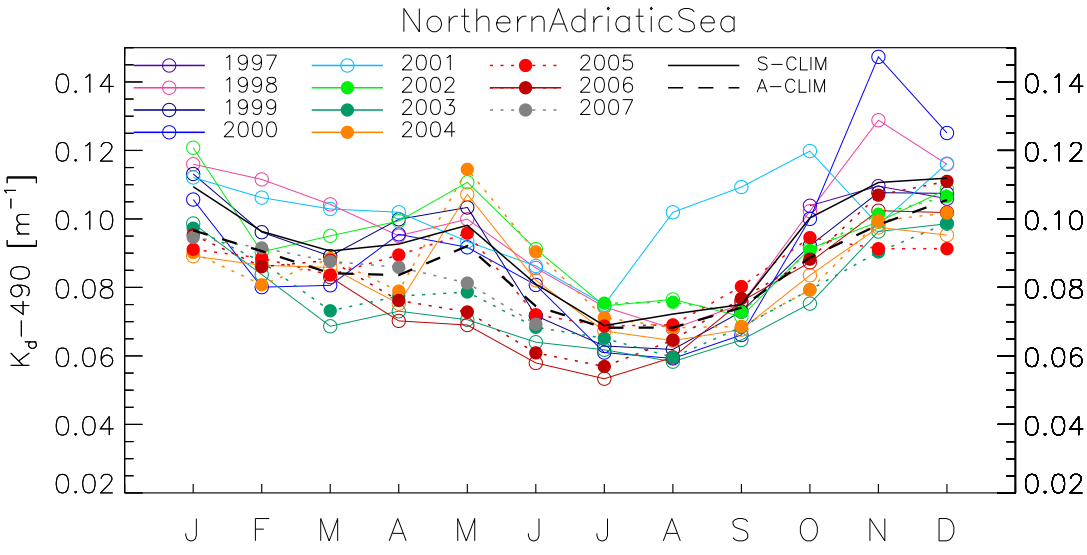

Figure 3.3: $K_d(490)$ multi-annual time series for SeaWiFS (lines with open circles) and MODIS (filled circles with dotted line) and associated climatologies (black line and dashed line, respectively).

3.2 Central Adriatic Sea

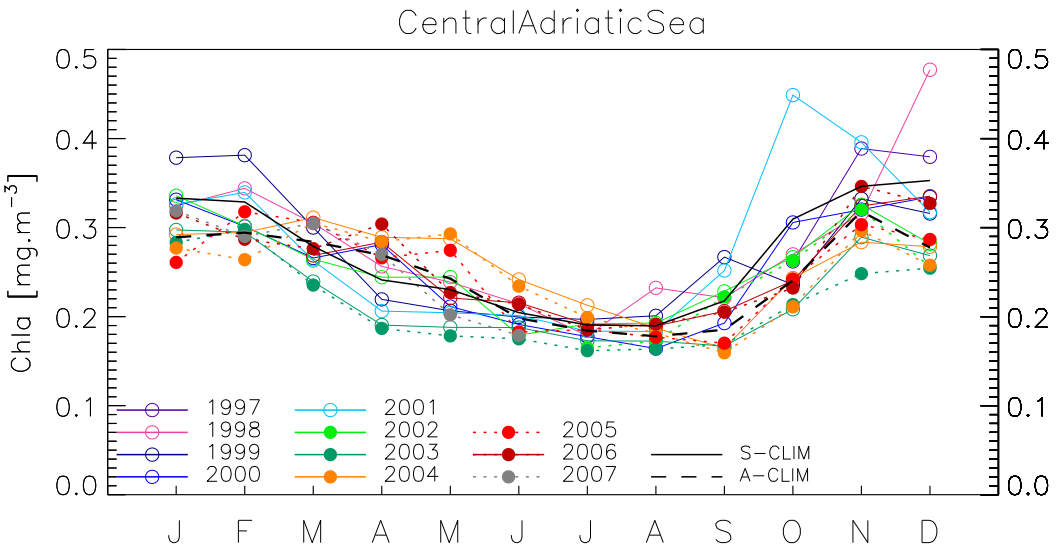

Figure 3.4: Chl*a* multi-annual time series for SeaWiFS (lines with open circles) and MODIS (filled circles with dotted line) and associated climatologies (black line and dashed line, respectively).

In the central Adriatic Sea, the seasonal cycle resembles that in the northern part, with a minimum in summer, but the average Chl*a* and K_d are lower and the inter-annual variability is dampened. A difference is the consistent positive Chl*a* anomaly for the period March-July 2004, contrasting with the mostly negative anomalies for the period autumn 2002 to December 2004 in the northern Adriatic. Based on the MODIS record, rather high K_d values can also be noticed in the spring seasons between 2004 and 2006.

Table 3.2: Central Adriatic Sea; SeaWiFS Chl*a* inter-annual anomalies, computed as ratio of area-averaged Chl*a* concentrations. The 2^{nd} column gives the SeaWiFS climatological Chl*a* (in mg m^{-3}). In bold, anomalies below 0.8 or above 1.2. A datum of 1 means a regional monthly value close to climatology.

Month	mg m^{-3}	1998	1999	2000	2001	2002	2003	2004
J	0.333	0.97	1.14	0.99	0.98	1.01	0.89	0.88
F	0.329	1.05	1.16	0.92	1.03	0.92	0.90	0.90
M	0.279	1.09	1.08	0.95	0.94	0.95	0.86	1.12
A	0.241	1.06	0.91	1.16	0.85	1.01	**0.79**	1.20
M	0.230	1.04	0.90	0.92	0.89	1.06	0.82	**1.25**
J	0.204	1.05	0.98	0.93	0.98	0.88	0.92	1.18
J	0.191	0.94	1.03	0.93	0.96	1.01	0.91	1.12
A	0.190	**1.22**	1.06	0.86	0.97	1.02	0.91	0.99
S	0.218	1.02	**1.23**	0.89	1.16	1.05	**0.77**	**0.76**
O	0.309	0.87	**0.76**	0.99	**1.45**	0.86	**0.67**	**0.79**
N	0.346	0.91	0.96	0.92	1.14	0.94	0.84	0.82
D	0.353	**1.35**	0.90	0.95	0.90	**0.80**	**0.76**	**0.79**

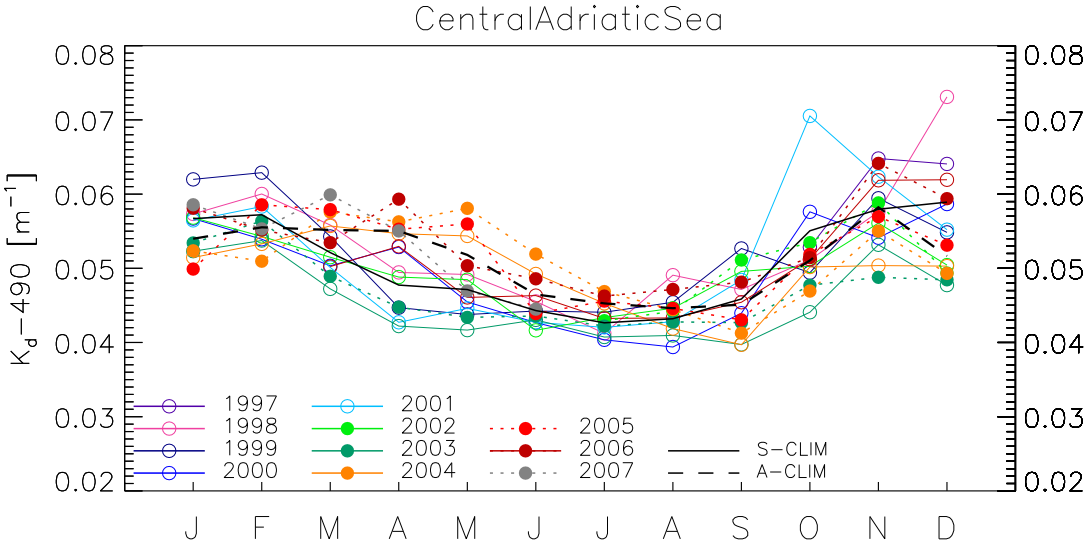

Figure 3.5: $K_d(490)$ multi-annual time series for SeaWiFS (lines with open circles) and MODIS (filled circles with dotted line) and associated climatologies (black line and dashed line, respectively).

3.3 Southern Adriatic Sea

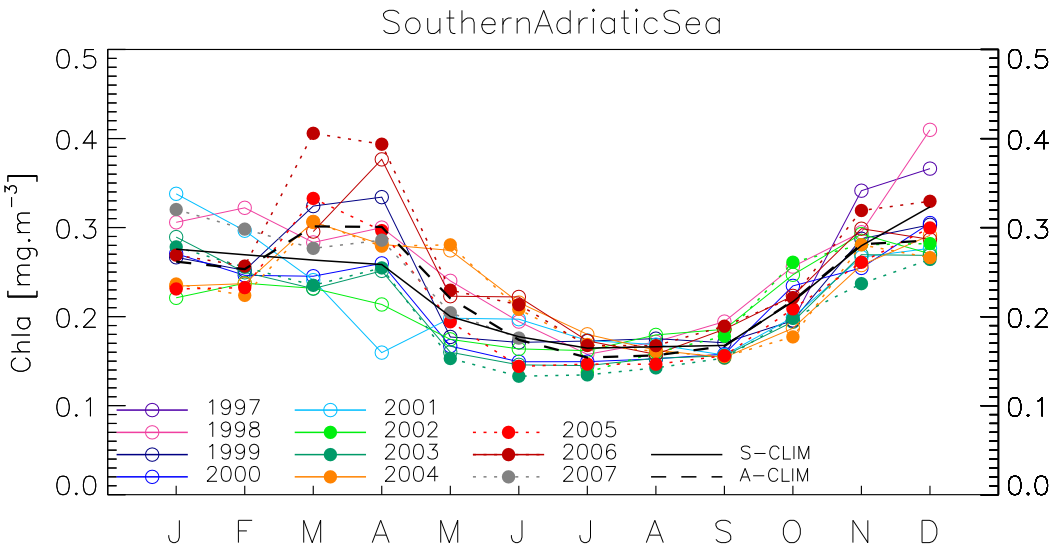

Figure 3.6: Chl*a* multi-annual time series for SeaWiFS (lines with open circles) and MODIS (filled circles with dotted line) and associated climatologies (black line and dashed line, respectively).

The southern part of the Adriatic Sea shows an evolution compared to the temporal patterns characterizing the central area. A late winter maximum is more marked and the summer minimum is longer. The inter-annual variability is still diminished with few instances of anomalies outside the 0.8-1.2 bounds. In fact, most of the inter-annual variations are found in the timing and amplitude of the late winter maximum. In that respect, the low values of April 2001 for Chl*a* and K_d are particularly noticeable. As in the rest of the basin, the year 2003 is characterized by relatively low Chl*a* levels. This is also partly true for 2004, with the notable exception of larger values from March to June 2004. The MODIS and SeaWiFS records compare favorably. The large Chl*a* values given by MODIS for the spring 2006, and by SeaWiFS in April 2006, can be considered as a clear departure with respect to climatology.

Table 3.3: Southern Adriatic Sea; SeaWiFS Chl*a* inter-annual anomalies, computed as ratio of area-averaged Chl*a* concentrations. The 2^{nd} column gives the SeaWiFS climatological Chl*a* (in mg m^{-3}). In bold, anomalies below 0.8 or above 1.2. A datum of 1 means a regional monthly value close to climatology.

Month	C, mg m^{-3}	1998	1999	2000	2001	2002	2003	2004
J	0.276	1.11	0.97	0.98	**1.23**	0.80	1.05	0.85
F	0.269	1.20	0.93	0.91	1.10	0.88	0.93	0.88
M	0.264	1.07	**1.23**	0.93	0.91	0.88	0.88	1.16
A	0.259	1.16	**1.29**	1.00	**0.62**	0.83	0.97	1.09
M	0.200	**1.20**	0.89	0.83	0.99	0.87	**0.80**	**1.37**
J	0.177	1.10	0.96	0.84	1.11	0.92	0.82	**1.22**
J	0.165	0.96	1.05	0.91	1.05	0.98	0.88	1.09
A	0.166	1.03	1.06	0.92	1.01	1.08	0.92	0.98
S	0.168	1.16	1.02	0.94	0.94	1.11	0.93	0.92
O	0.217	1.18	0.90	1.08	0.92	1.14	0.90	0.86
N	0.280	1.05	1.03	0.91	0.95	1.05	0.96	0.92
D	0.323	**1.27**	0.94	0.94	0.86	0.84	0.83	0.90

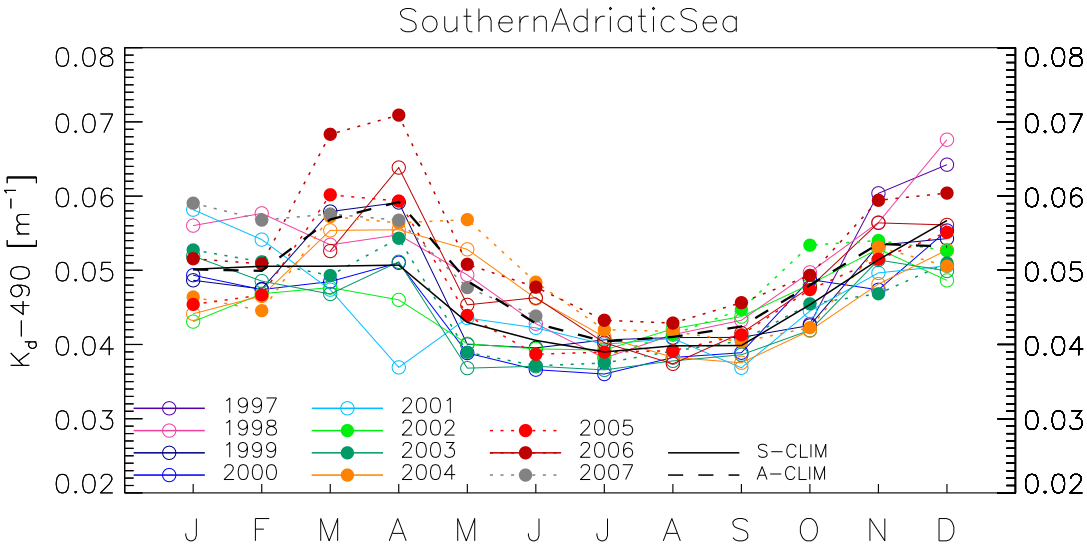

Figure 3.7: $K_d(490)$ multi-annual time series for SeaWiFS (lines with open circles) and MODIS (filled circles with dotted line) and associated climatologies (black line and dashed line, respectively).

3.4 Alboran Sea

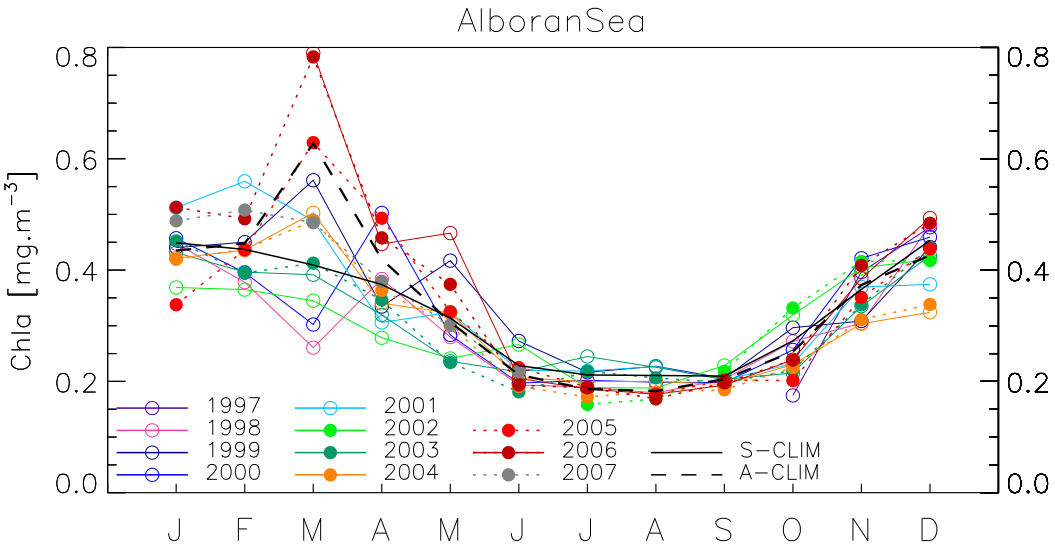

Figure 3.8: Chl*a* multi-annual time series for SeaWiFS (lines with open circles) and MODIS (filled circles with dotted line) and associated climatologies (black line and dashed line, respectively).

Averaged over the region, the spatial variability characteristic of the Alboran Sea is integrated into a rather stable seasonal cycle. The spring period is that associated with most inter-annual variations. For instance, the lowest and highest Chl*a* anomalies (0.64 and 1.36 times the climatological value) are both found in March (1998 and 1999, respectively). This is continued by large anomalies displayed by MODIS in March 2005 and 2006, and by SeaWiFS in March 2006. Higher spring values in recent years give a higher climatological level for MODIS derived Chl*a* and K_d.

Table 3.4: Alboran Sea; SeaWiFS Chl*a* inter-annual anomalies, computed as ratio of area-averaged Chl*a* concentrations. The 2^{nd} column gives the SeaWiFS climatological Chl*a* (in mg m^{-3}). In bold, anomalies below 0.8 or above 1.2. A datum of 1 means a regional monthly value close to climatology.

Month	mg m^{-3}	1998	1999	2000	2001	2002	2003	2004
J	0.449	1.00	0.98	1.02	1.14	0.82	0.96	0.94
F	0.437	0.87	1.03	0.90	**1.28**	0.83	0.91	1.00
M	0.409	**0.64**	**1.37**	**0.74**	1.19	0.84	0.96	**1.23**
A	0.374	1.03	0.89	**1.34**	0.82	**0.74**	0.85	0.91
M	0.314	0.89	**1.33**	0.90	1.03	**0.77**	**0.75**	1.03
J	0.228	0.85	1.19	0.86	0.96	1.17	0.95	0.90
J	0.212	0.90	1.02	0.95	1.03	0.89	1.16	0.94
A	0.211	0.85	1.08	0.94	1.08	0.89	1.07	0.95
S	0.210	0.97	0.98	0.94	0.97	1.09	0.97	0.93
O	0.273	1.00	1.09	0.94	0.85	1.17	**0.79**	0.84
N	0.365	0.83	0.84	1.15	1.01	1.11	0.92	0.83
D	0.453	1.06	0.97	1.01	0.83	0.92	0.94	**0.71**

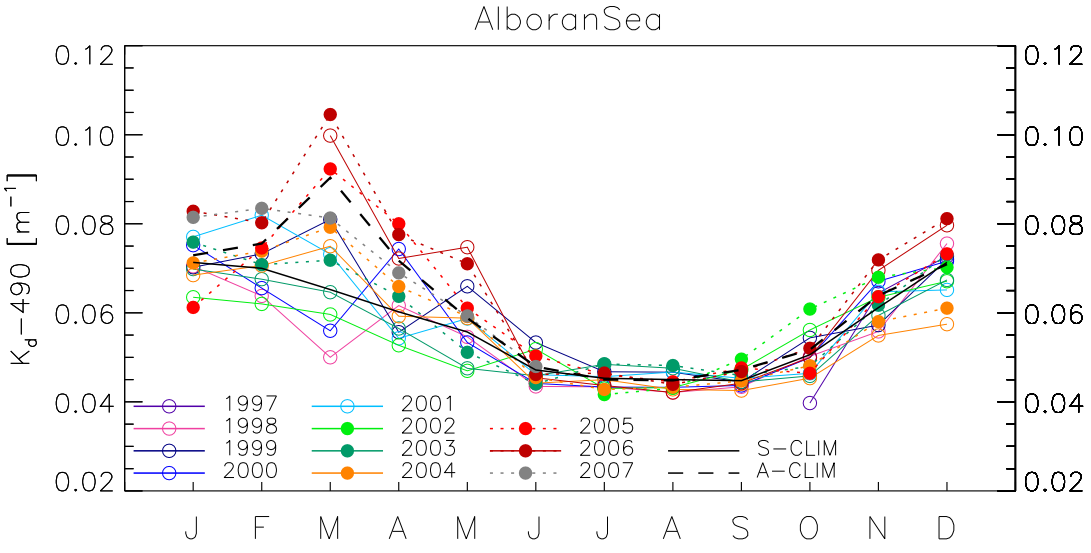

Figure 3.9: $K_d(490)$ multi-annual time series for SeaWiFS (lines with open circles) and MODIS (filled circles with dotted line) and associated climatologies (black line and dashed line, respectively).

3.5 Gulf of Lions

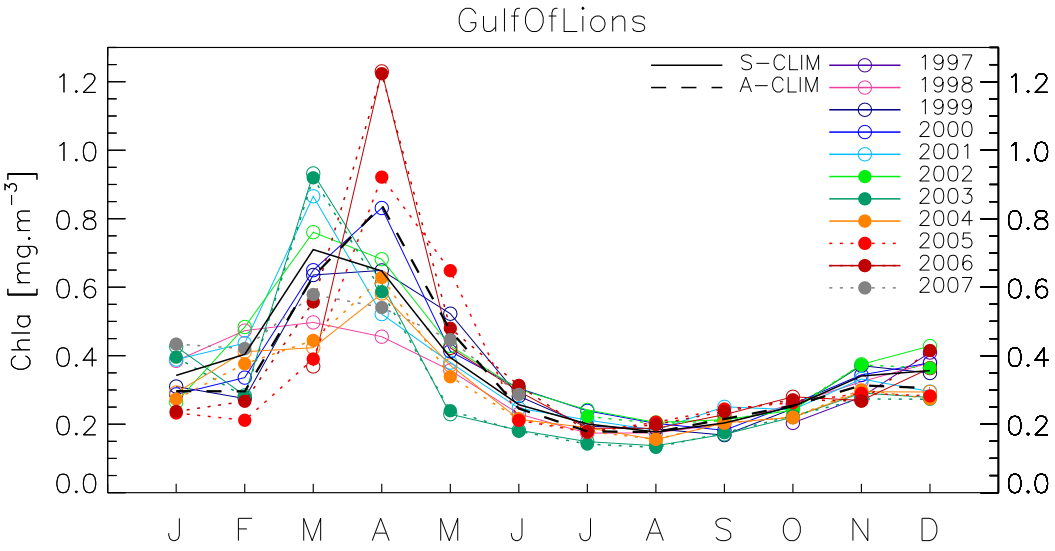

Figure 3.10: Chl*a* multi-annual time series for SeaWiFS (lines with open circles) and MODIS (filled circles with dotted line) and associated climatologies (black line and dashed line, respectively).

The seasonal cycle in the Gulf of Lions is well marked, with a spring bloom (March-April) and an extended summer minimum. Most of the inter-annual variability is found in spring, particularly in the amplitude and timing of the bloom. For instance, the bloom peak was seen in March from 2001 to 2003, and in April in 2000 and 2004, whereas the bloom amplitude was very low in 1998. The last 2 years (2005 and 2006 with MODIS data) indicate a rather high peak centered on April and a weaker signal in 2007.

Table 3.5: Gulf of Lions; SeaWiFS Chl*a* inter-annual anomalies, computed as ratio of area-averaged Chl*a* concentrations. The 2^{nd} column gives the SeaWiFS climatological Chl*a* (in mg m^{-3}). In bold, anomalies below 0.8 or above 1.2. A datum of 1 means a regional monthly value close to climatology.

Month	mg m^{-3}	1998	1999	2000	2001	2002	2003	2004
J	0.342	1.12	0.91	0.84	1.13	**0.77**	**1.25**	0.85
F	0.404	1.17	**0.68**	0.83	1.08	1.20	**0.70**	1.02
M	0.710	**0.70**	0.90	0.92	**1.22**	1.07	**1.31**	**0.60**
A	0.647	**0.70**	1.00	**1.28**	0.81	1.05	0.94	0.90
M	0.395	0.91	**1.32**	1.05	0.96	1.09	**0.58**	0.94
J	0.257	0.89	1.10	1.19	0.96	1.17	**0.71**	0.83
J	0.201	0.87	0.97	1.19	1.06	**1.20**	**0.74**	0.95
A	0.177	0.99	1.05	1.14	1.03	1.16	**0.77**	0.87
S	0.204	0.99	0.83	0.89	**1.23**	1.05	0.84	1.00
O	0.252	1.03	0.98	1.03	0.96	0.96	0.88	0.87
N	0.341	0.95	1.09	1.01	0.97	1.10	0.85	0.86
D	0.357	1.06	0.98	1.06	0.83	**1.20**	**0.78**	0.82

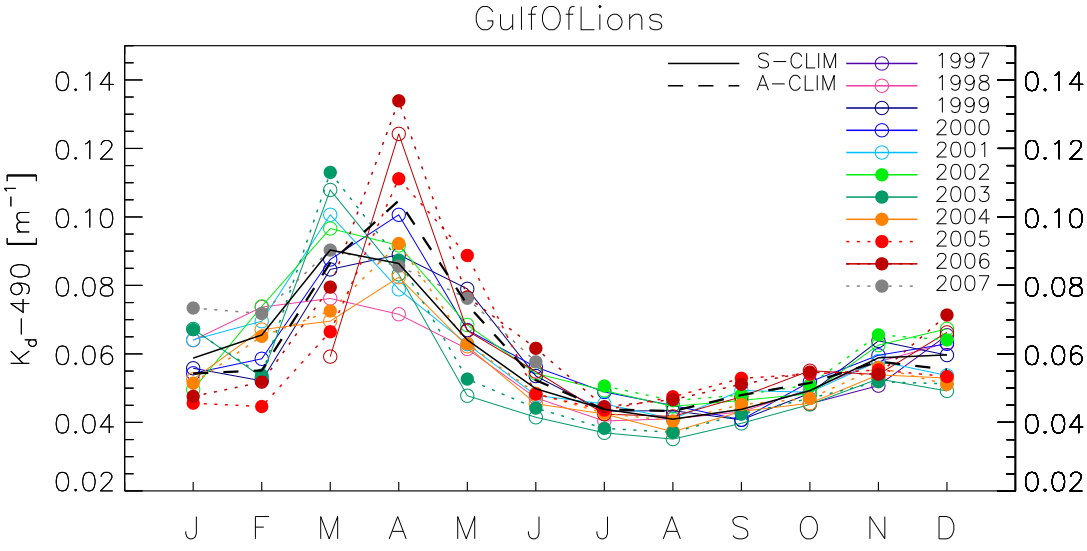

Figure 3.11: $K_d(490)$ multi-annual time series for SeaWiFS (lines with open circles) and MODIS (filled circles with dotted line) and associated climatologies (black line and dashed line, respectively).

3.6 Ligurian Sea

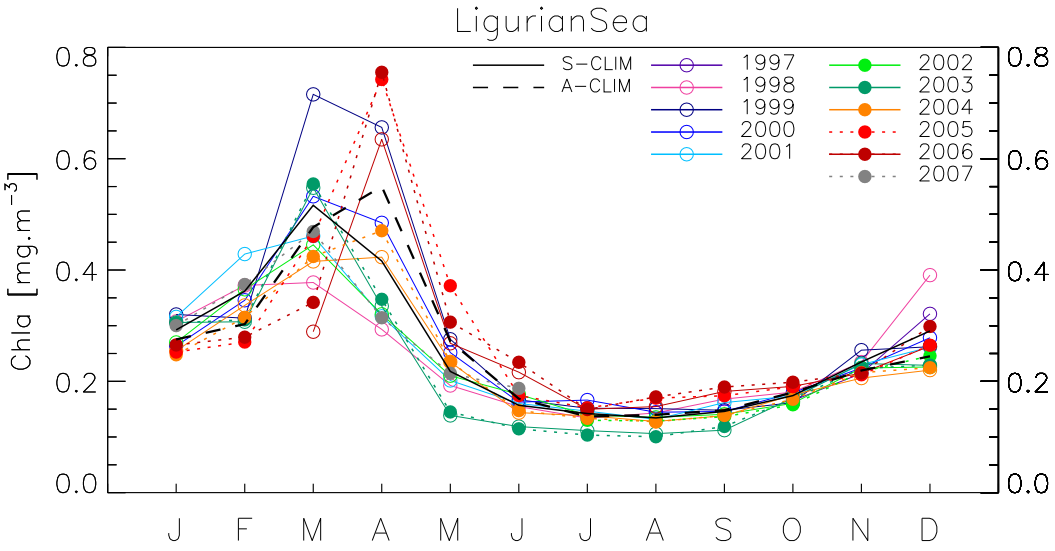

Figure 3.12: Chl*a* multi-annual time series for SeaWiFS (lines with open circles) and MODIS (filled circles with dotted line) and associated climatologies (black line and dashed line, respectively).

The results for the Gulf of Lions partly apply to the Ligurian Sea. The year 1998 saw a low intensity of the bloom, whereas the following year 1999 had clearly the largest amplitude of the SeaWiFS record (in terms of Chl*a* and K_d). The MODIS Chl*a* also shows large peaks in April, after relatively low values in early spring.

Table 3.6: Ligurian Sea; SeaWiFS Chl*a* inter-annual anomalies, computed as ratio of area-averaged Chl*a* concentrations. The 2^{nd} column gives the SeaWiFS climatological Chl*a* (in mg m^{-3}). In bold, anomalies below 0.8 or above 1.2. A datum of 1 means a regional monthly value close to climatology.

Month	mg m^{-3}	1998	1999	2000	2001	2002	2003	2004
J	0.292	1.05	1.10	0.90	1.08	0.92	1.05	0.87
F	0.362	1.03	0.87	0.95	1.18	1.01	0.85	0.93
M	0.516	**0.73**	**1.39**	1.03	0.89	0.86	1.06	0.80
A	0.416	**0.70**	**1.58**	1.17	**0.76**	**0.77**	0.81	1.02
M	0.218	0.88	**1.27**	1.16	0.93	0.96	**0.64**	1.08
J	0.157	0.99	1.06	1.04	1.02	1.12	**0.76**	0.92
J	0.142	0.94	1.07	1.17	1.03	0.98	**0.78**	0.97
A	0.134	1.07	1.12	1.08	0.98	1.01	**0.79**	0.95
S	0.146	1.15	1.01	1.00	1.11	0.97	**0.77**	0.95
O	0.174	1.04	0.93	1.03	1.00	0.92	0.98	1.01
N	0.235	1.00	1.09	0.95	0.98	0.95	0.99	0.88
D	0.290	**1.35**	0.90	0.96	0.90	**0.78**	**0.79**	**0.76**

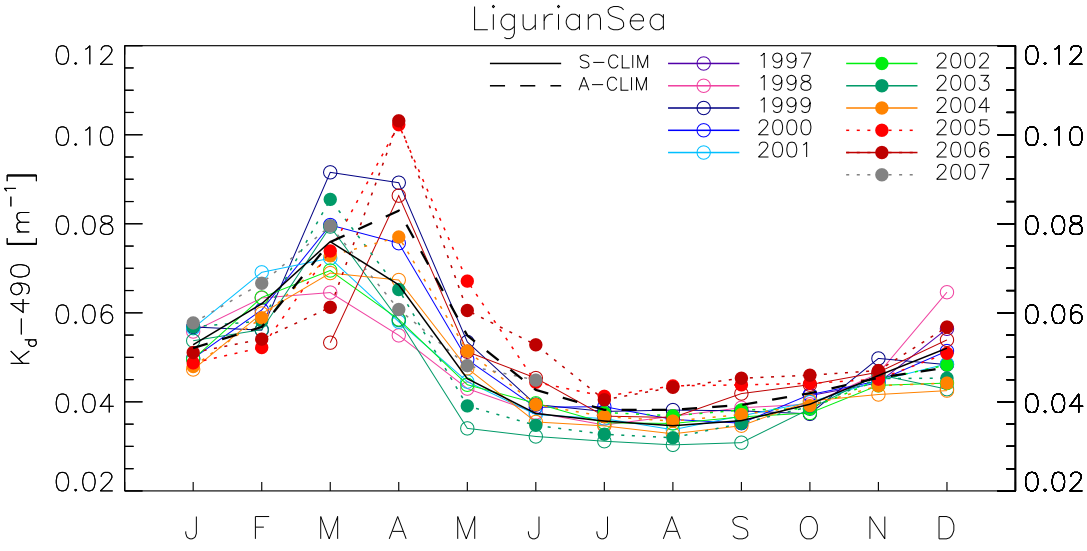

Figure 3.13: $K_d(490)$ multi-annual time series for SeaWiFS (lines with open circles) and MODIS (filled circles with dotted line) and associated climatologies (black line and dashed line, respectively).

3.7 Balearic Sea

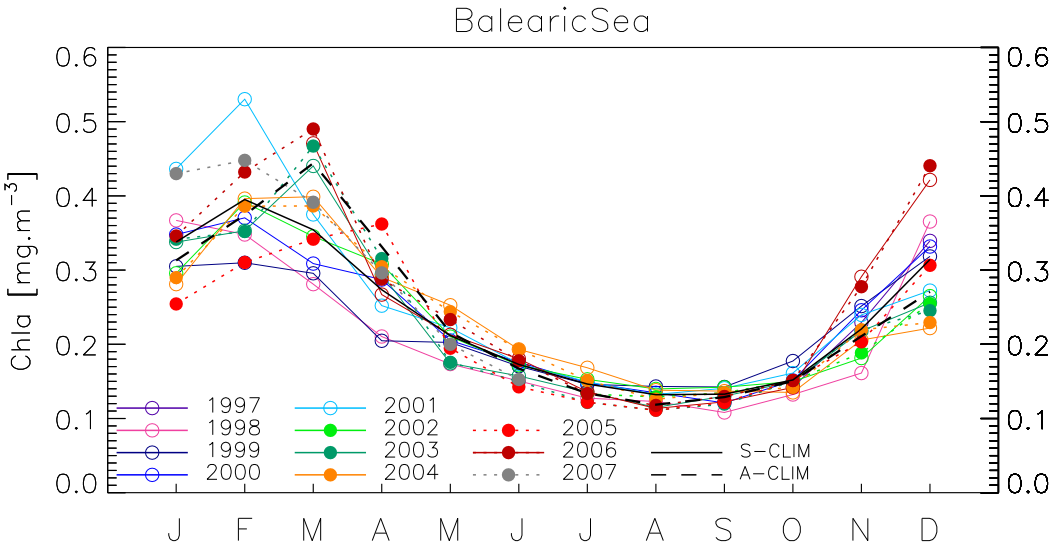

Figure 3.14: Chl*a* multi-annual time series for SeaWiFS (lines with open circles) and MODIS (filled circles with dotted line) and associated climatologies (black line and dashed line, respectively).

The seasonal cycle appears fairly stable in the Balearic region. The spring maxima in 1998 and 1999 are characterized by negative anomalies (actually, almost the whole 1998 had Chl*a* lower than climatology). Conversely, the spring bloom of 2001 was early and of high intensity. The signals for spring 2006 and 2007 appear in the high range.

Table 3.7: Balearic Sea; SeaWiFS Chl*a* inter-annual anomalies, computed as ratio of area-averaged Chl*a* concentrations. The 2^{nd} column gives the SeaWiFS climatological Chl*a* (in mg m^{-3}). In bold, anomalies below 0.8 or above 1.2. A datum of 1 means a regional monthly value close to climatology.

Month	mg m^{-3}	1998	1999	2000	2001	2002	2003	2004
J	0.338	1.09	0.90	1.03	**1.29**	0.87	1.00	0.83
F	0.395	0.88	**0.78**	0.94	**1.34**	0.99	0.89	1.00
M	0.354	**0.79**	0.83	0.87	1.06	0.97	**1.24**	1.13
A	0.274	**0.77**	**0.75**	1.05	0.92	1.13	1.08	1.06
M	0.212	0.82	0.96	0.97	1.05	0.99	0.82	1.19
J	0.173	0.87	0.99	1.02	1.01	0.99	0.91	1.12
J	0.146	0.87	1.00	1.01	1.02	1.04	0.92	1.15
A	0.132	0.93	1.08	1.02	1.00	1.06	0.87	1.05
S	0.133	0.81	1.07	0.91	1.06	1.07	0.98	1.03
O	0.152	0.87	1.17	1.00	1.06	0.99	0.99	0.89
N	0.221	**0.73**	1.14	1.11	1.09	0.82	0.99	0.93
D	0.314	1.16	1.01	1.06	0.87	0.84	0.81	**0.71**

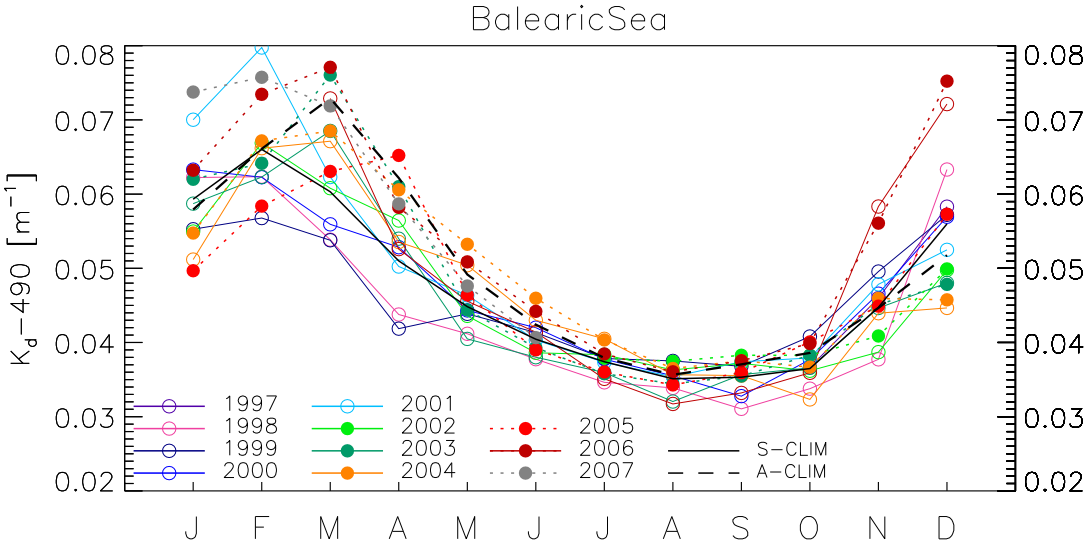

Figure 3.15: $K_d(490)$ multi-annual time series for SeaWiFS (lines with open circles) and MODIS (filled circles with dotted line) and associated climatologies (black line and dashed line, respectively).

3.8 Provencal Basin

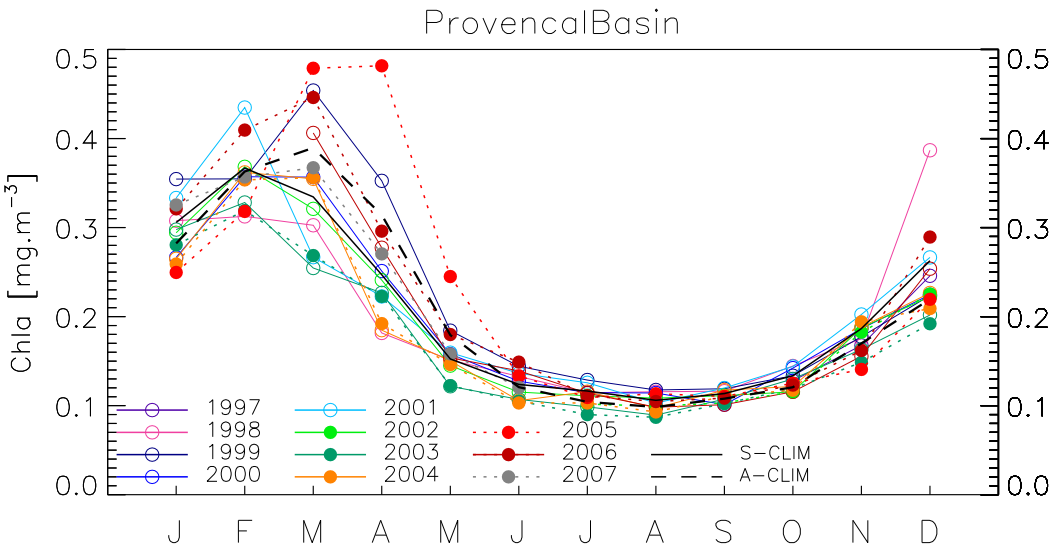

Figure 3.16: Chl*a* multi-annual time series for SeaWiFS (lines with open circles) and MODIS (filled circles with dotted line) and associated climatologies (black line and dashed line, respectively).

Noticeable inter-annual features can be distinguished in the Provencal Basin, mainly in the spring period, around a well defined seasonal cycle (maximum in early spring, February-March, and a minimum in summer). Spring 1998 and the whole 2003 are associated with negative anomalies. Opposite to this, the spring 1999 displayed high Chl*a* values. This is also true for February 2001, but the bloom had a fast demise after that. According to the MODIS series, the seasonal peak was quite late in 2005 and 2006 (April and March, respectively).

Table 3.8: Provencal Basin; SeaWiFS Chl$a$ inter-annual anomalies, computed as ratio of area-averaged Chl$a$ concentrations. The 2^{nd} column gives the SeaWiFS climatological Chl$a$ (in mg m^{-3}). In bold, anomalies below 0.8 or above 1.2. A datum of 1 means a regional monthly value close to climatology.

Month	mg m^{-3}	1998	1999	2000	2001	2002	2003	2004
J	0.306	1.01	1.16	0.87	1.09	0.96	0.97	0.87
F	0.367	0.85	0.97	0.97	1.19	1.00	0.89	0.99
M	0.334	0.90	**1.36**	1.07	**0.80**	0.96	**0.76**	1.06
A	0.247	**0.74**	**1.43**	1.02	0.90	0.98	0.92	**0.75**
M	0.152	0.99	**1.21**	1.04	1.05	0.95	**0.80**	0.99
J	0.124	1.07	1.17	1.03	1.10	0.93	0.86	0.85
J	0.116	0.98	1.11	0.98	1.08	0.95	0.85	0.99
A	0.106	1.09	1.11	1.08	0.97	1.02	0.84	0.92
S	0.114	1.02	1.05	0.89	1.06	0.98	0.95	1.03
O	0.134	1.08	1.00	1.06	1.08	0.87	0.97	0.91
N	0.187	0.94	0.95	1.00	1.08	1.00	0.87	1.01
D	0.263	**1.47**	0.85	0.85	1.01	0.85	**0.77**	0.86

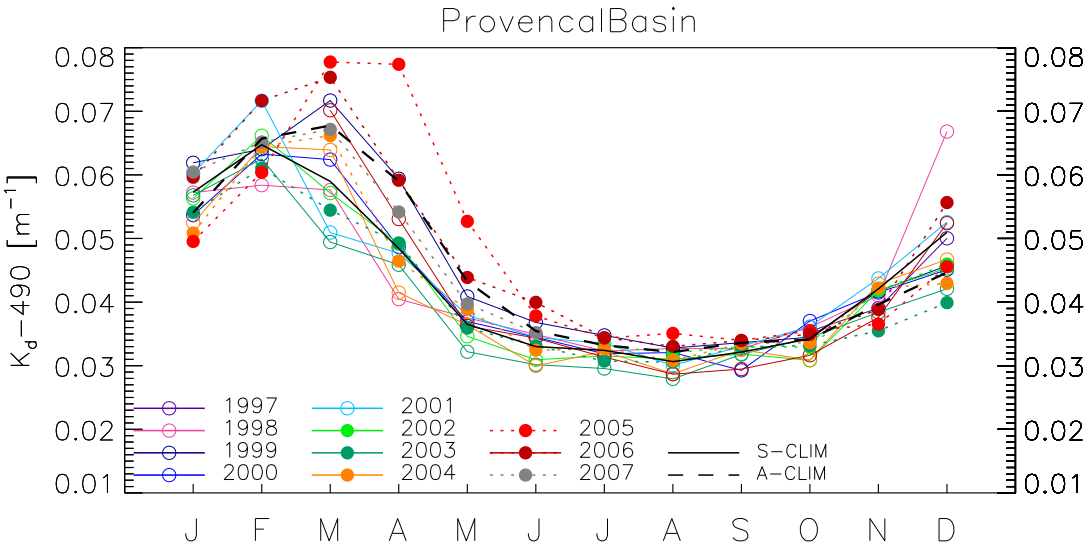

Figure 3.17: K$_d$(490) multi-annual time series for SeaWiFS (lines with open circles) and MODIS (filled circles with dotted line) and associated climatologies (black line and dashed line, respectively).

3.9 Algerian Basin

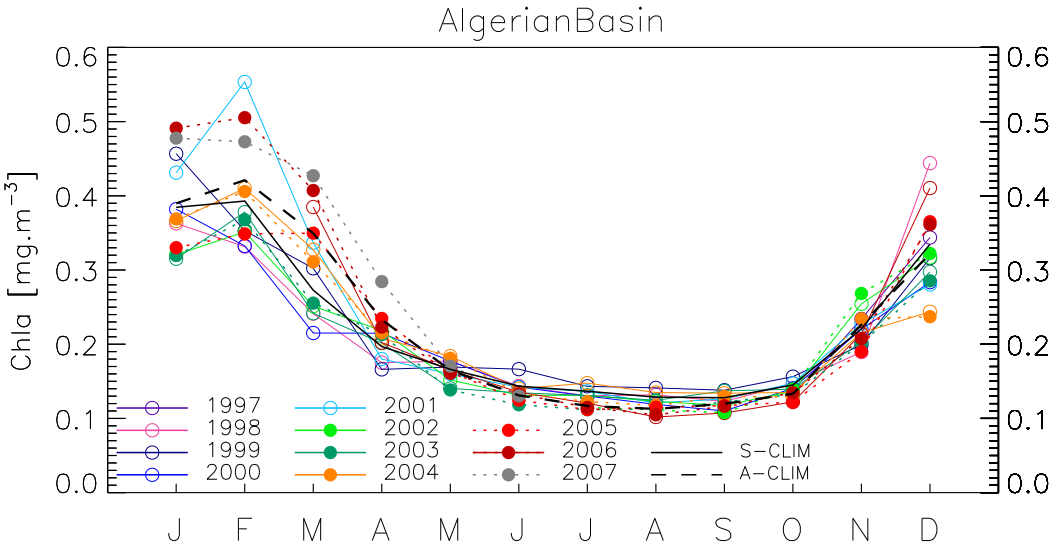

Figure 3.18: Chl*a* multi-annual time series for SeaWiFS (lines with open circles) and MODIS (filled circles with dotted line) and associated climatologies (black line and dashed line, respectively).

In the Algerian basin, there is a clear Chl*a* and K_d maximum at the beginning of the year (January-February) and a prolonged minimum from May to October. The level of inter-annual variations is low, with the exception of February 2001, and 2006-2007 (from MODIS) standing out with high anomalies.

Table 3.9: Algerian Basin; SeaWiFS Chl*a* inter-annual anomalies, computed as ratio of area-averaged Chl*a* concentrations. The 2^{nd} column gives the SeaWiFS climatological Chl*a* (in mg m^{-3}). In bold, anomalies below 0.8 or above 1.2. A datum of 1 means a regional monthly value close to climatology.

Month	mg m^{-3}	1998	1999	2000	2001	2002	2003	2004
J	0.385	0.94	1.19	0.99	1.12	0.83	0.82	0.95
F	0.393	0.84	0.90	0.85	**1.41**	0.89	0.96	1.04
M	0.273	0.88	1.11	**0.79**	**1.23**	0.92	0.89	**1.20**
A	0.197	0.89	0.84	1.09	0.91	1.11	1.02	1.05
M	0.166	1.07	1.02	1.07	0.96	0.91	0.84	1.11
J	0.143	1.00	1.16	0.99	0.99	0.91	0.94	0.98
J	0.137	0.95	1.05	0.95	1.00	0.96	0.96	1.08
A	0.129	1.02	1.10	0.92	0.94	0.96	0.97	1.05
S	0.128	0.96	1.08	0.86	0.99	0.92	1.07	1.05
O	0.145	1.02	1.08	0.97	1.01	0.94	0.96	0.93
N	0.221	0.86	0.90	1.00	1.03	1.15	0.92	0.98
D	0.335	**1.33**	0.94	0.85	0.84	0.95	0.89	**0.73**

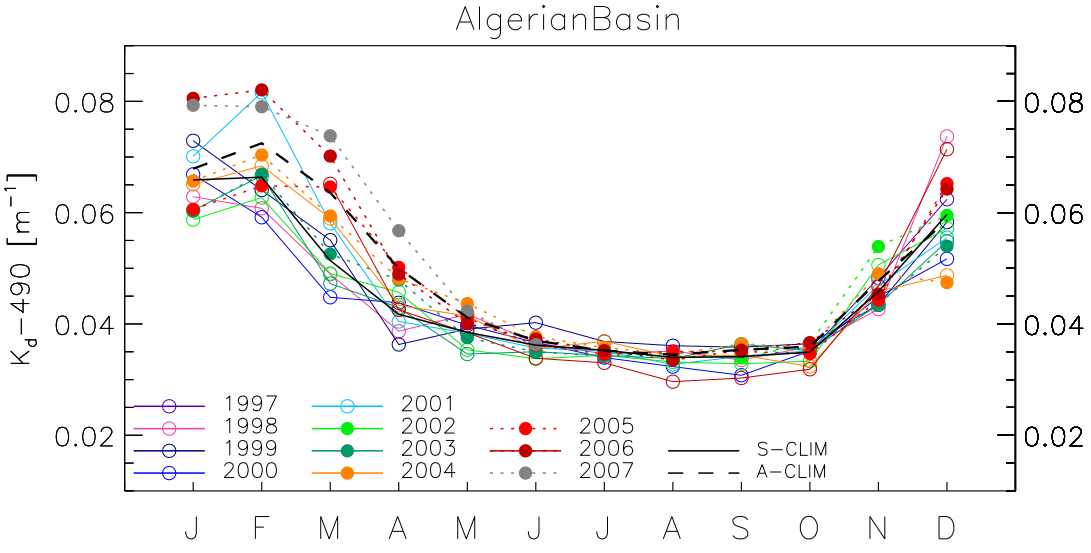

Figure 3.19: $K_d(490)$ multi-annual time series for SeaWiFS (lines with open circles) and MODIS (filled circles with dotted line) and associated climatologies (black line and dashed line, respectively).

3.10 Tyrrhenian Sea

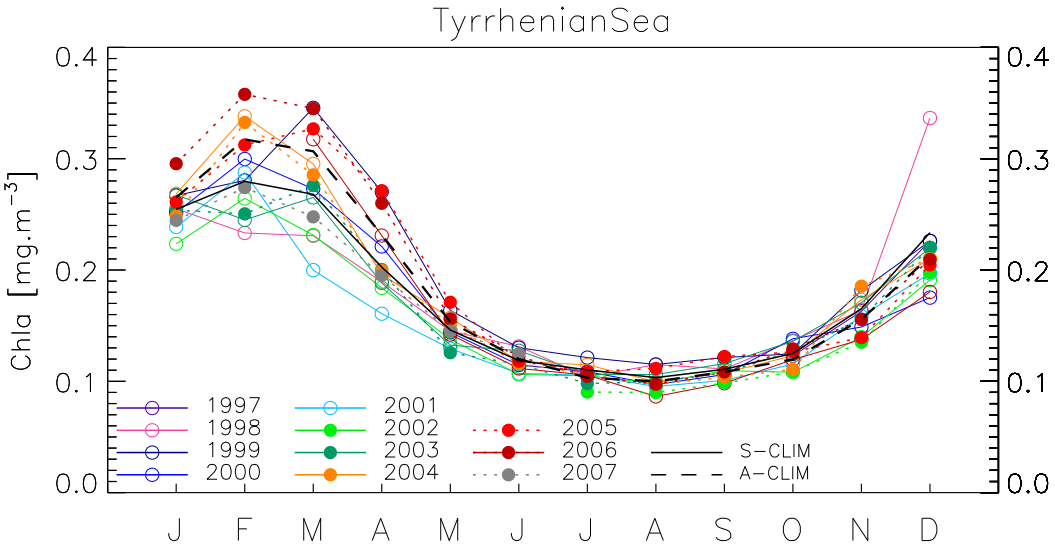

Figure 3.20: Chl*a* multi-annual time series for SeaWiFS (lines with open circles) and MODIS (filled circles with dotted line) and associated climatologies (black line and dashed line, respectively).

Year-to-year differences in the Tyrrhenian Sea are fairly limited. February-March maxima were elevated in 1999, 2004 and 2006, and relatively lower in 1998 and 2001. As in similar parts of the basin, the SeaWiFS and MODIS series agree well.

Table 3.10: Tyrrhenian Sea; SeaWiFS Chl$a$ inter-annual anomalies, computed as ratio of area-averaged Chl$a$ concentrations. The 2^{nd} column gives the SeaWiFS climatological Chl$a$ (in mg m^{-3}). In bold, anomalies below 0.8 or above 1.2. A datum of 1 means a regional monthly value close to climatology.

Month	mg m^{-3}	1998	1999	2000	2001	2002	2003	2004
J	0.254	1.00	1.05	0.99	0.94	0.88	1.05	1.05
F	0.280	0.83	1.00	1.07	1.03	0.95	0.88	**1.21**
M	0.268	0.86	**1.29**	1.02	**0.75**	0.86	0.99	1.10
A	0.203	0.94	**1.33**	1.09	**0.79**	0.91	0.93	0.97
M	0.146	0.99	1.12	0.99	0.89	0.94	0.91	1.07
J	0.119	1.11	1.10	0.97	0.90	0.89	1.07	0.99
J	0.110	0.94	1.10	0.99	0.96	0.95	0.96	1.04
A	0.103	1.11	1.11	0.94	0.92	0.95	1.03	0.96
S	0.111	1.00	1.10	0.96	0.91	0.99	1.05	0.97
O	0.125	1.09	1.00	1.11	0.92	0.86	1.09	0.98
N	0.165	0.99	1.10	0.90	0.96	0.85	1.03	1.05
D	0.234	**1.44**	0.97	**0.75**	0.84	0.82	0.94	0.90

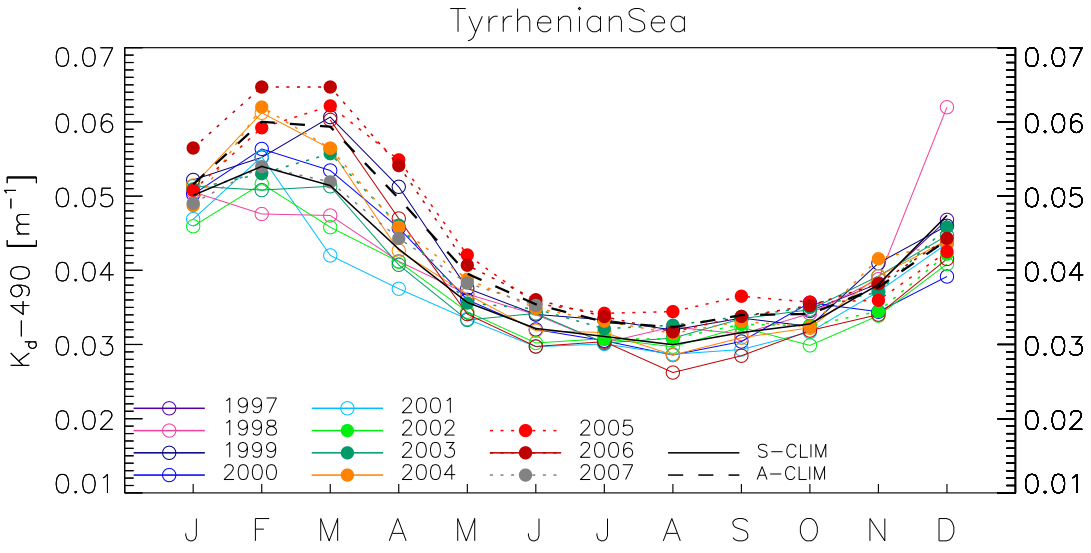

Figure 3.21: $K_d(490)$ multi-annual time series for SeaWiFS (lines with open circles) and MODIS (filled circles with dotted line) and associated climatologies (black line and dashed line, respectively).

3.11 Northern Ionian Sea

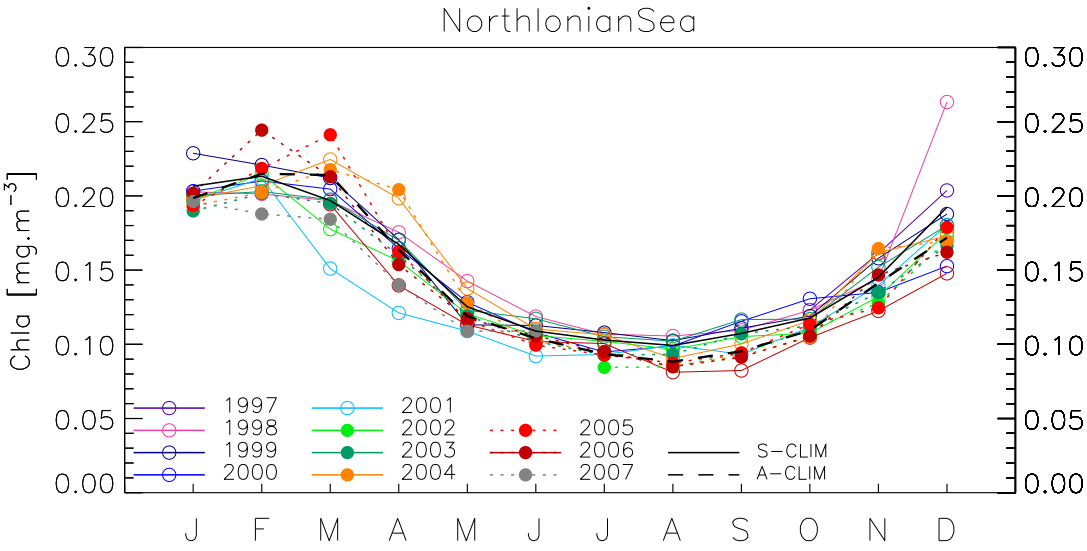

Figure 3.22: Chl*a* multi-annual time series for SeaWiFS (lines with open circles) and MODIS (filled circles with dotted line) and associated climatologies (black line and dashed line, respectively).

In the northern part of the Ionian Sea, the only inter-annual regional-scale signals worth mentioning are the low Chl*a* and K_d levels in the first half of 2001 and high values in December 1998-January 1999. The 2005 and 2006 maxima as given by MODIS (in March and February, respectively) are in the high range.

Table 3.11: Northern Ionian Sea; SeaWiFS Chl*a* inter-annual anomalies, computed as ratio of area-averaged Chl*a* concentrations. The 2^{nd} column gives the SeaWiFS climatological Chl*a* (in mg m^{-3}). In bold, anomalies below 0.8 or above 1.2. A datum of 1 means a regional monthly value close to climatology.

Month	mg m^{-3}	1998	1999	2000	2001	2002	2003	2004
J	0.207	0.98	1.11	0.98	0.95	0.95	0.97	0.96
F	0.213	0.94	1.04	0.98	0.99	1.01	0.95	0.97
M	0.197	1.00	1.08	1.04	**0.77**	0.90	1.00	1.14
A	0.167	1.05	1.02	0.98	**0.72**	0.93	1.02	1.19
M	0.125	1.14	0.90	1.02	0.87	0.96	0.98	1.10
J	0.109	1.09	1.04	0.99	0.85	0.97	1.08	1.01
J	0.103	1.04	1.05	0.92	0.91	0.99	1.02	1.03
A	0.099	1.06	1.03	1.00	1.00	0.97	1.03	0.91
S	0.107	1.02	1.03	1.08	0.87	0.98	1.09	0.93
O	0.118	1.04	1.01	1.11	0.95	0.91	0.99	0.99
N	0.145	0.99	1.09	0.93	0.96	0.91	1.05	1.11
D	0.192	**1.37**	0.98	**0.79**	0.94	0.91	0.94	0.90

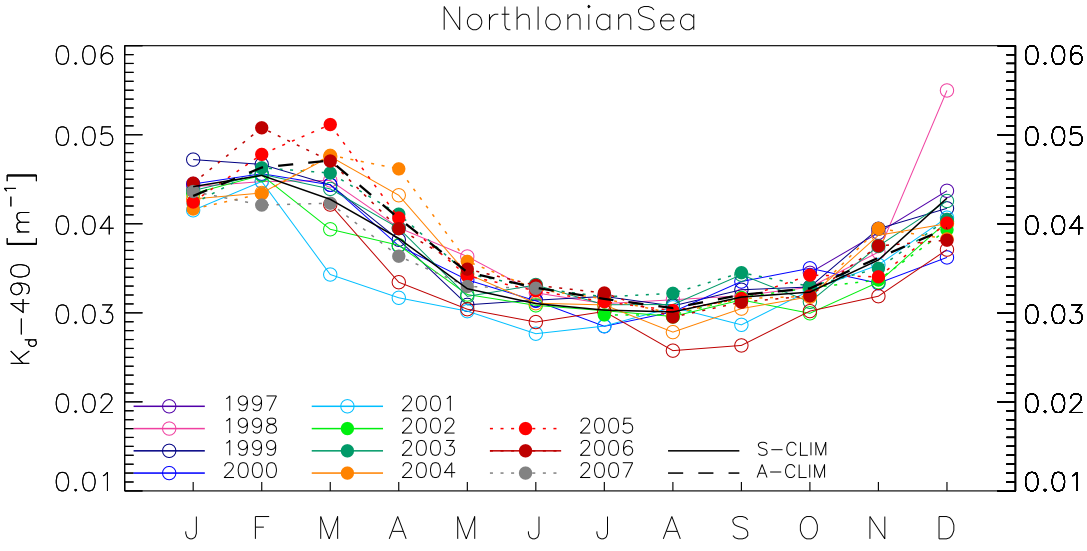

Figure 3.23: $K_d(490)$ multi-annual time series for SeaWiFS (lines with open circles) and MODIS (filled circles with dotted line) and associated climatologies (black line and dashed line, respectively).

3.12 Southern Ionian Sea

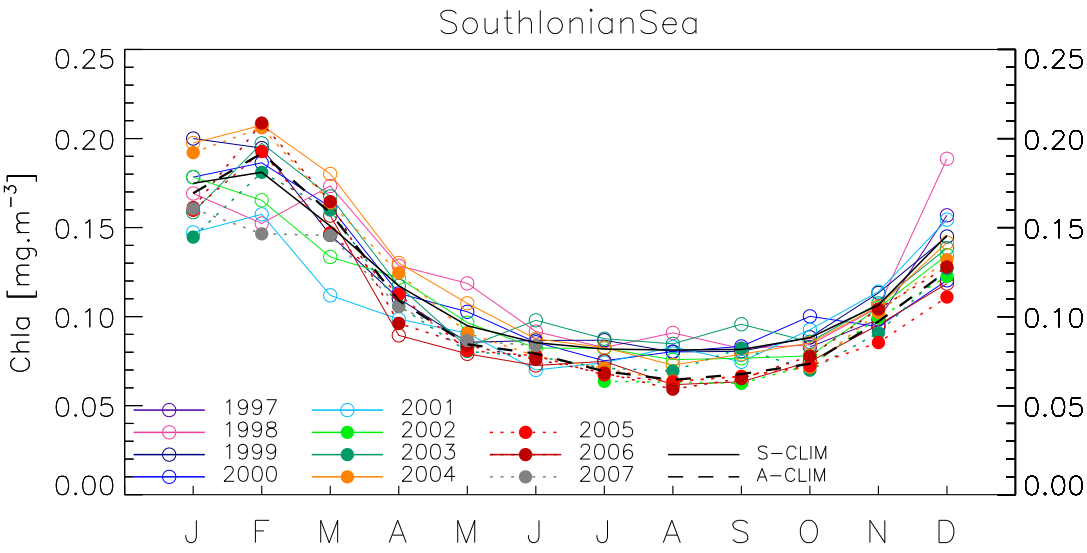

Figure 3.24: Chl*a* multi-annual time series for SeaWiFS (lines with open circles) and MODIS (filled circles with dotted line) and associated climatologies (black line and dashed line, respectively).

Except relatively low values in the first part of 2001, the seasonal evolutions of Chl*a* in the southern part of the Ionian Sea are very robust with respect to the SeaWiFS climatology.

Table 3.12: Southern Ionian Sea; SeaWiFS Chl*a* inter-annual anomalies, computed as ratio of area-averaged Chl*a* concentrations. The 2^{nd} column gives the SeaWiFS climatological Chl*a* (in mg m^{-3}). In bold, anomalies below 0.8 or above 1.2. A datum of 1 means a regional monthly value close to climatology.

Month	mg m^{-3}	1998	1999	2000	2001	2002	2003	2004
J	0.175	0.97	1.14	1.02	0.84	1.02	0.91	1.13
F	0.181	0.84	1.07	1.03	0.87	0.91	1.09	1.15
M	0.151	1.15	0.97	1.07	**0.74**	0.88	1.11	1.19
A	0.117	1.10	0.94	0.96	0.84	1.04	1.00	1.11
M	0.095	**1.25**	0.90	1.08	0.96	1.02	0.87	1.13
J	0.085	1.07	1.01	1.00	0.82	0.96	1.15	1.03
J	0.082	1.01	1.06	0.92	0.91	1.00	1.07	1.01
A	0.081	1.12	0.99	0.99	1.02	0.93	1.04	0.90
S	0.082	1.01	0.99	1.02	0.91	0.94	1.17	0.97
O	0.088	0.95	1.00	1.14	1.05	0.88	0.97	0.97
N	0.107	0.99	1.06	0.89	1.07	0.99	1.01	0.99
D	0.146	**1.30**	1.00	0.83	1.06	0.92	0.95	0.97

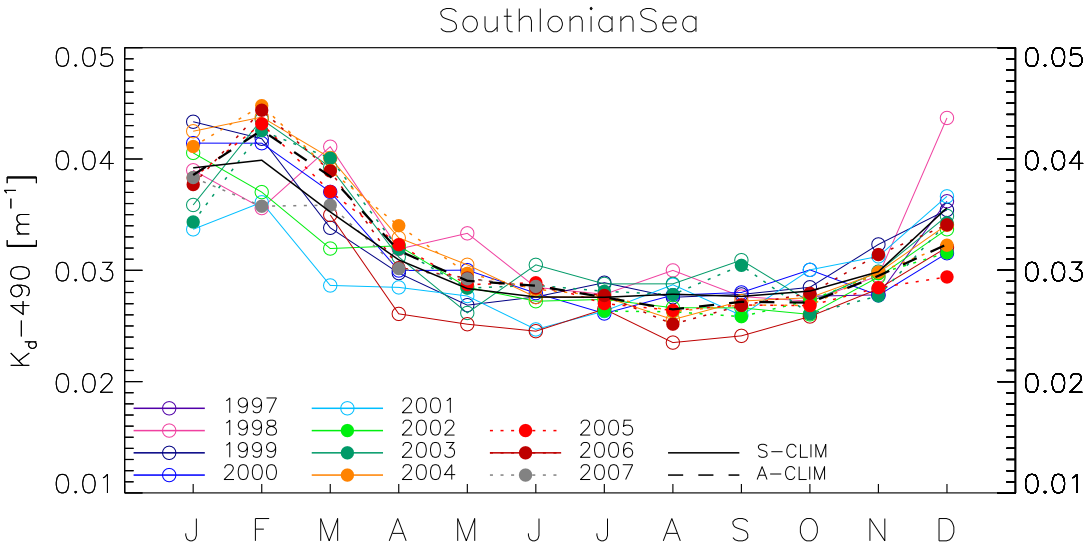

Figure 3.25: $K_d(490)$ multi-annual time series for SeaWiFS (lines with open circles) and MODIS (filled circles with dotted line) and associated climatologies (black line and dashed line, respectively).

3.13 Aegean Sea

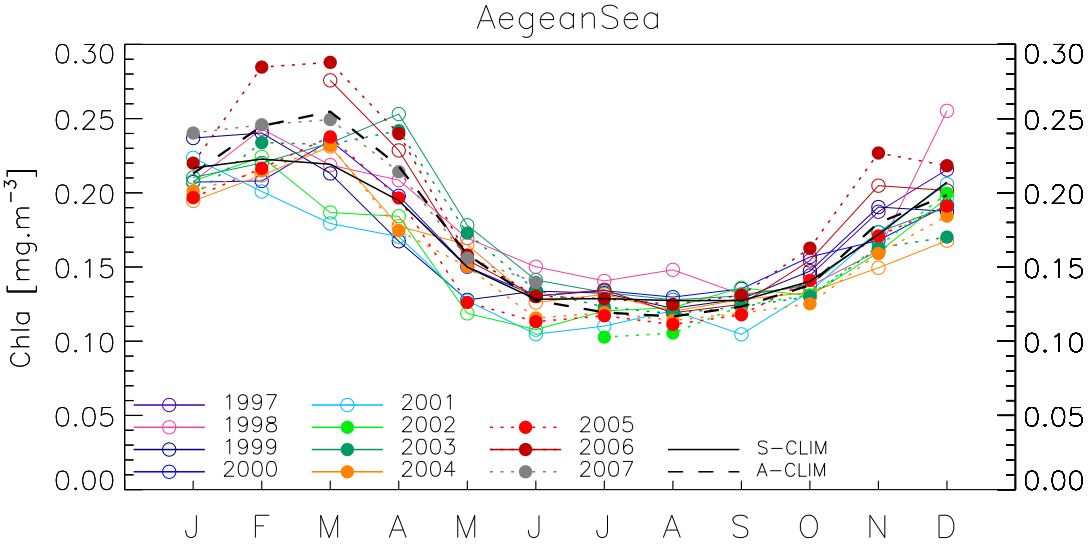

Figure 3.26: Chl*a* multi-annual time series for SeaWiFS (lines with open circles) and MODIS (filled circles with dotted line) and associated climatologies (black line and dashed line, respectively).

In the Aegean Sea, the seasonal maxima in winter-spring is slightly extended with respect to more oligotrophic regions of the basin. Inter-annual variations are restricted in a small range. There is an early decrease of Chl*a* towards the annual minimum in 2001 and 2002 (actually most of these 2 years are below climatological levels). The periods of winter 1998-1999 and late spring 2003 are characterized by relatively high Chl*a* and K_d values. An important feature could be the very large maximum illustrated by the MODIS record in 2006, confirmed by the available SeaWiFS LAC data for Chl*a*, but less so for K_d.

Table 3.13: Aegean Sea; SeaWiFS Chl*a* inter-annual anomalies, computed as ratio of area-averaged Chl*a* concentrations. The 2^{nd} column gives the SeaWiFS climatological Chl*a* (in mg m^{-3}). In bold, anomalies below 0.8 or above 1.2. A datum of 1 means a regional monthly value close to climatology.

Month	mg m^{-3}	1998	1999	2000	2001	2002	2003	2004
J	0.217	0.96	1.09	0.96	1.03	0.96	0.97	0.90
F	0.223	1.09	1.08	0.93	0.90	1.01	0.99	0.95
M	0.219	1.00	0.97	1.07	0.82	0.85	1.06	1.05
A	0.195	1.07	0.86	1.02	0.88	0.95	**1.30**	0.91
M	0.150	1.13	0.85	1.00	0.85	**0.79**	1.19	1.10
J	0.128	1.17	1.04	1.02	0.82	0.84	1.10	0.98
J	0.129	1.09	1.03	1.04	0.86	0.94	1.03	1.02
A	0.127	1.16	0.96	1.02	0.95	0.96	1.00	0.94
S	0.127	1.03	1.01	1.06	0.82	1.07	1.02	1.01
O	0.140	0.98	1.05	1.12	0.95	0.93	0.98	0.95
N	0.172	0.94	1.11	0.98	1.01	0.93	1.01	0.87
D	0.207	**1.23**	0.90	0.92	0.99	0.95	0.92	0.81

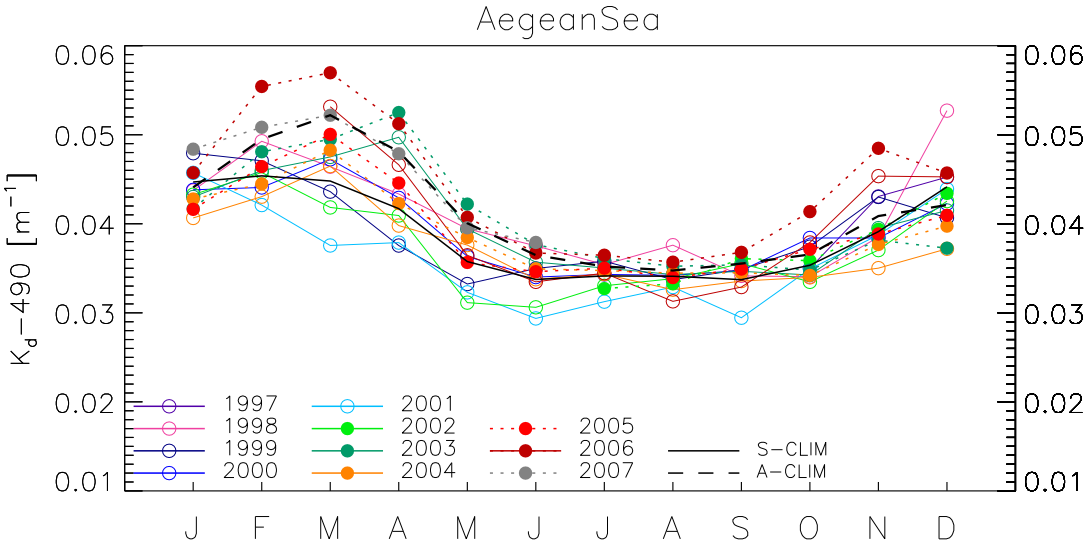

Figure 3.27: $K_d(490)$ multi-annual time series for SeaWiFS (lines with open circles) and MODIS (filled circles with dotted line) and associated climatologies (black line and dashed line, respectively).

3.14 Levantine Basin

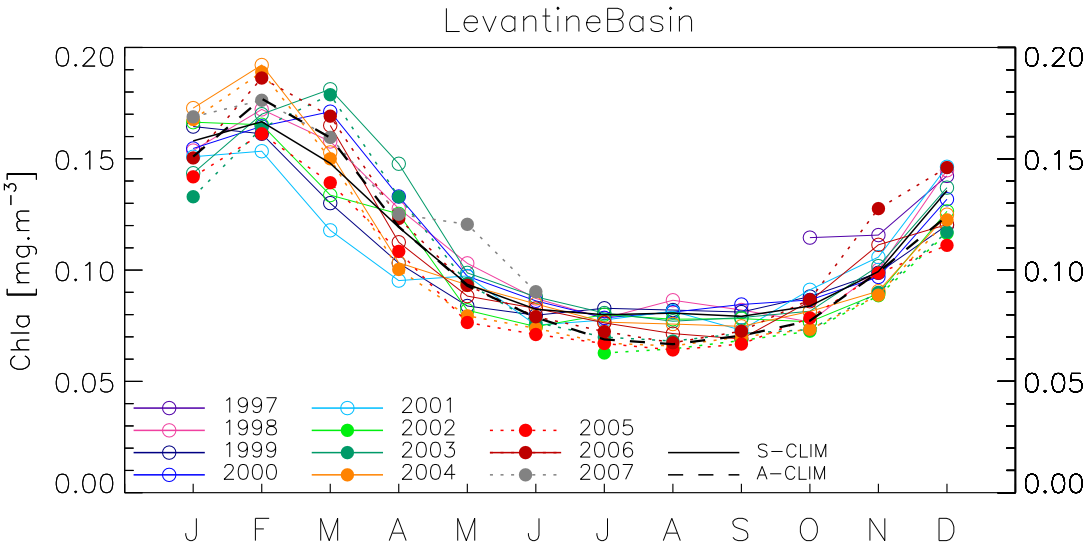

Figure 3.28: Chl*a* multi-annual time series for SeaWiFS (lines with open circles) and MODIS (filled circles with dotted line) and associated climatologies (black line and dashed line, respectively).

Interannual anomalies are very constrained in the Levantine basin. The spring periods of 2001 and 2003 can be mentioned for relatively low and high values, respectively. MODIS derived K_d values appear fairly high in 2006 and 2007.

Table 3.14: Northern Levantine Basin; SeaWiFS Chl*a* inter-annual anomalies, computed as ratio of area-averaged Chl*a* concentrations. The 2^{nd} column gives the SeaWiFS climatological Chl*a* (in mg m^{-3}). In bold, anomalies below 0.8 or above 1.2. A datum of 1 means a regional monthly value close to climatology.

Month	mg m^{-3}	1998	1999	2000	2001	2002	2003	2004
J	0.158	0.97	1.04	0.98	0.96	1.05	0.91	1.09
F	0.167	1.03	0.97	0.99	0.92	0.99	1.02	1.15
M	0.148	1.07	0.88	1.16	**0.80**	0.90	**1.22**	1.03
A	0.119	1.07	0.87	1.12	**0.80**	1.05	**1.24**	0.87
M	0.094	1.10	0.90	1.04	1.04	0.88	1.06	1.00
J	0.082	1.06	0.97	1.05	0.91	0.91	1.07	1.03
J	0.080	0.98	1.04	0.98	0.97	1.00	1.01	0.96
A	0.081	1.07	1.02	1.01	1.01	0.97	0.96	0.94
S	0.079	1.04	1.02	1.07	0.92	0.99	0.99	0.94
O	0.084	0.92	1.05	1.03	1.09	0.92	0.97	0.97
N	0.099	1.01	0.99	0.98	1.07	0.90	1.02	0.91
D	0.136	1.07	0.89	0.97	1.08	0.93	1.01	0.92

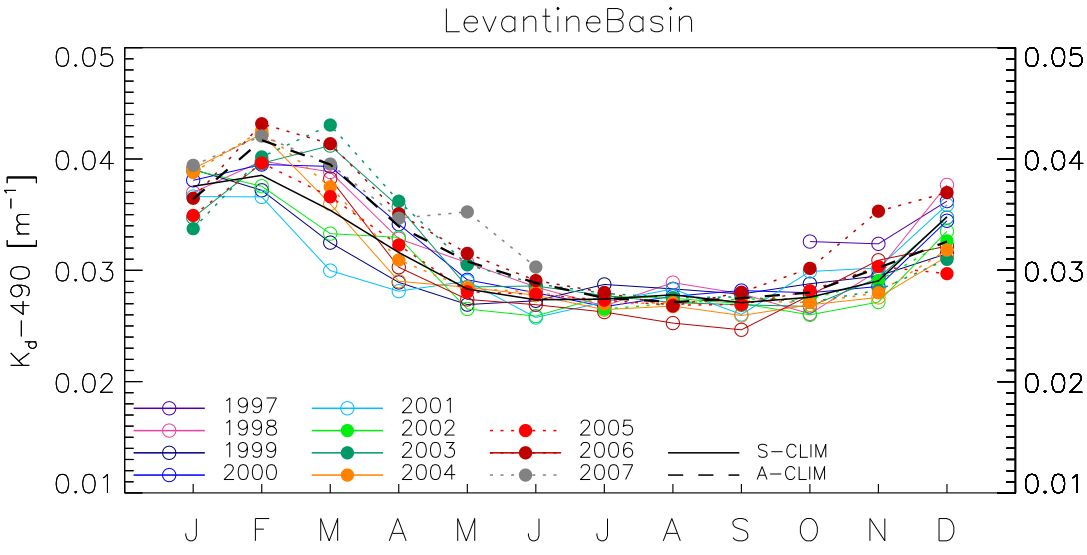

Figure 3.29: $K_d(490)$ multi-annual time series for SeaWiFS (lines with open circles) and MODIS (filled circles with dotted line) and associated climatologies (black line and dashed line, respectively).

Section 4

Black Sea

The partition of the Black Sea is shown on Figure 4.1. Besides the Azov Sea, the basin is partitioned on the basis of a division between western and eastern basin and bathymetry (200-m isobath). The results will be shown for the western Black Sea shelf, the western deep Black Sea, and the eastern deep Black Sea.

For each domain, the time series of Chl$a$ and $K_d(490)$ are given for the years 1997 to 2004 using SeaWiFS (lines with open circles) and for years 2002 to 2007 for MODIS (filled circles with dotted line). The climatologies from SeaWiFS (Dec. 1997-Nov. 2004, continuous line) and MODIS (Jul. 2002-Jun. 2007, dashed line) are over-plotted for reference.

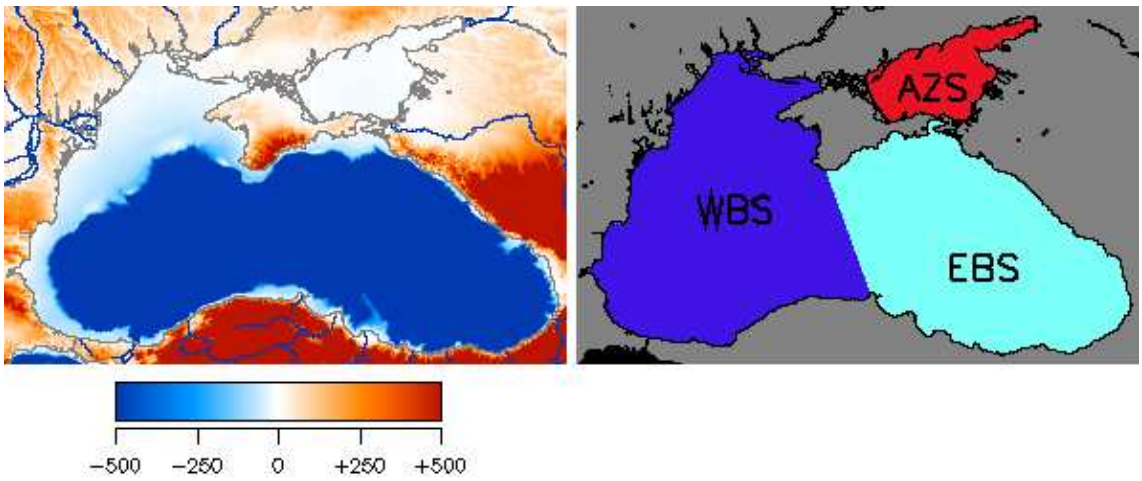

Figure 4.1: Distribution of Black Sea bathymetry and partition. **AZS**: Azov Sea; **WBS**: western Black Sea; **EBS**: eastern Black Sea.

4.1 Western Black Sea Shelf

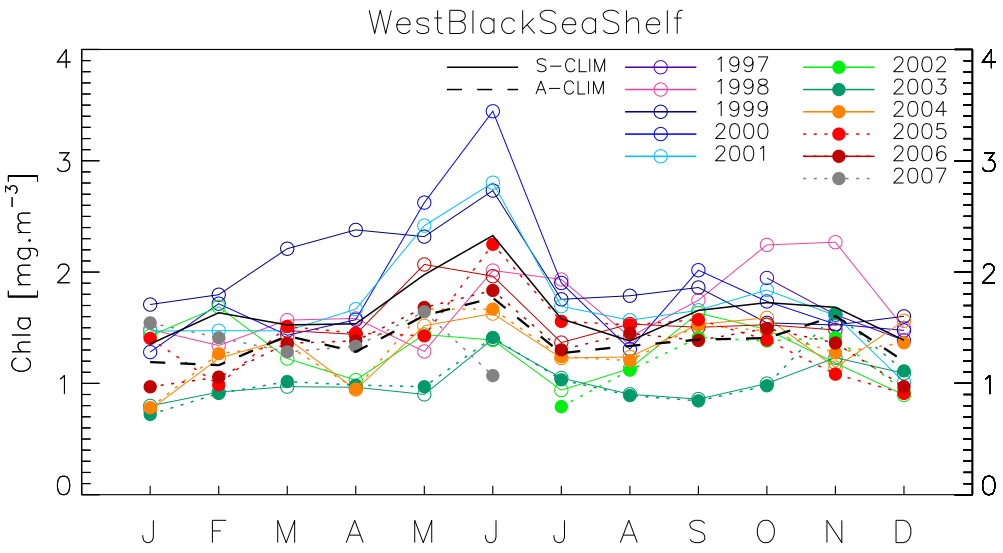

Figure 4.2: Chl*a* multi-annual time series for SeaWiFS (lines with open circles) and MODIS (filled circles with dotted line) and associated climatologies (black line and dashed line, respectively).

The time series over the western Black Sea Shelf (depth < 200 m) shows only a slight seasonal variability. The climatological values indicate a maximum in late spring (May-June) and a minimum in late summer. A clear trend can be noticed: all SeaWiFS Chl*a* monthly averages are below climatological average after March 2002. Conversely, the spring 2002 had a very strong positive anomaly from January to April, and the June maximum was very high in 2000. This inter-annual signal is also observed in K_d record. The SeaWiFS and MODIS series appear very close on average, particularly for Chl*a*. The MODIS series continues with relatively low values with respect to the beginning of the SeaWiFS series, and the resulting climatology is logically below the SeaWiFS counterpart.

Table 4.1: Western Black Sea Shelf; SeaWiFS Chl*a* inter-annual anomalies, computed as ratio of area-averaged Chl*a* concentrations. The 2^{nd} column gives the SeaWiFS climatological Chl*a* (in mg m^{-3}). In bold, anomalies below 0.8 or above 1.2. A datum of 1 means a regional monthly value close to climatology.

Month	mg m^{-3}	1998	1999	2000	2001	2002	2003	2004
J	1.354	1.10	**1.26**	0.95	1.09	1.05	**0.59**	**0.56**
F	1.634	0.82	1.10	1.05	0.90	1.03	**0.56**	**0.75**
M	1.525	1.03	**1.45**	0.94	0.96	0.80	**0.64**	0.92
A	1.535	1.03	**1.55**	1.02	1.09	**0.67**	**0.63**	**0.62**
M	1.976	**0.65**	1.17	**1.33**	**1.22**	**0.73**	**0.46**	**0.77**
J	2.328	0.87	1.17	**1.48**	**1.20**	**0.60**	**0.60**	**0.70**
J	1.580	**1.22**	1.11	**1.20**	1.07	**0.59**	**0.66**	**0.78**
A	1.381	1.03	**1.29**	0.95	1.14	0.82	**0.65**	0.90
S	1.655	1.06	1.12	**1.22**	1.00	0.99	**0.52**	0.92
O	1.725	**1.30**	0.90	1.01	1.07	0.86	**0.58**	0.92
N	1.684	**1.35**	0.91	0.91	0.96	**0.70**	**0.73**	**0.68**
D	1.388	1.08	1.15	1.06	**0.73**	**0.65**	**0.79**	1.13

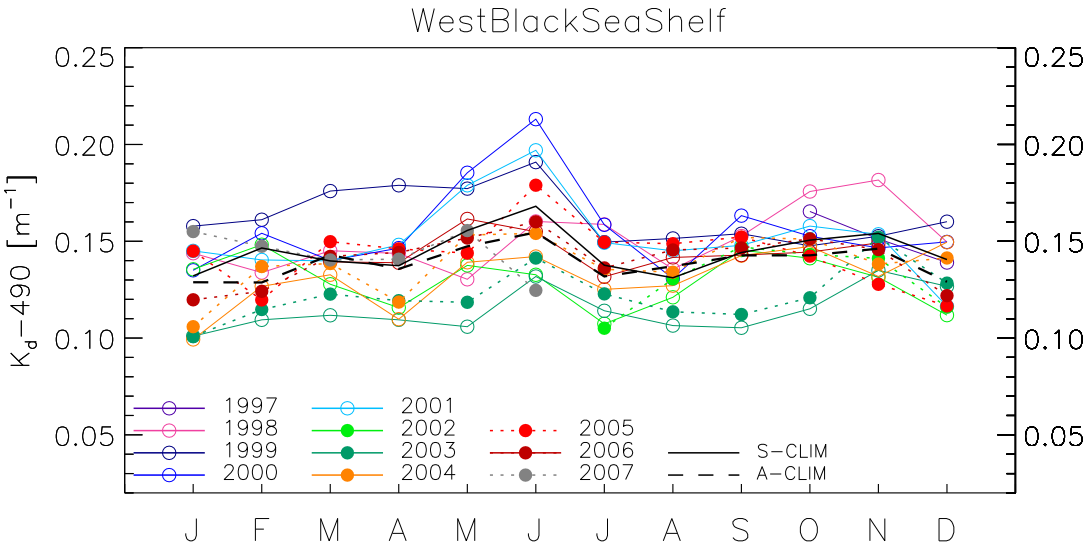

Figure 4.3: $K_d(490)$ multi-annual time series for SeaWiFS (lines with open circles) and MODIS (filled circles with dotted line) and associated climatologies (black line and dashed line, respectively).

4.2 Western Deep Black Sea

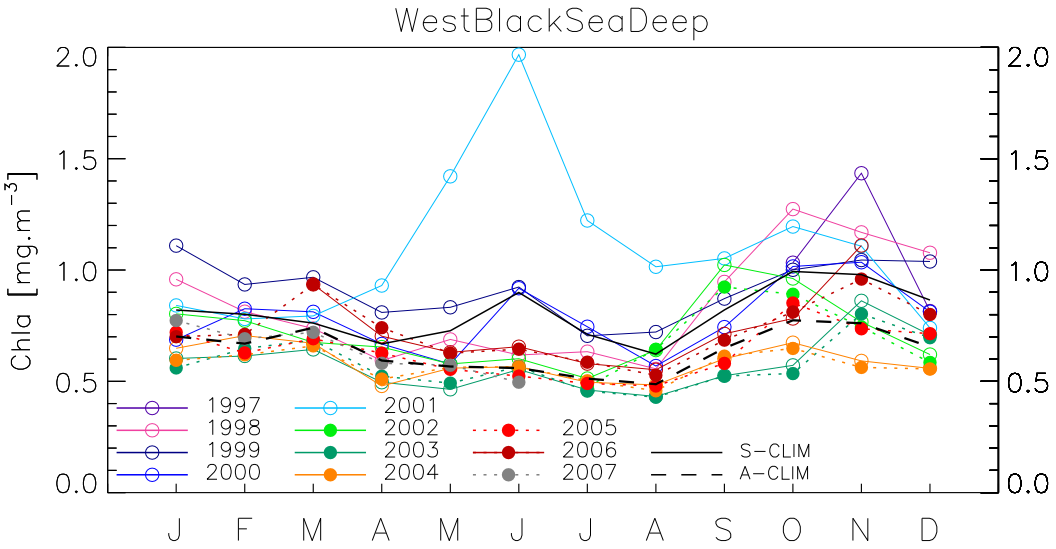

Figure 4.4: Chl*a* multi-annual time series for SeaWiFS (lines with open circles) and MODIS (filled circles with dotted line) and associated climatologies (black line and dashed line, respectively).

Not surprisingly, the time series over the western deep Black Sea (depth $>$ 200 m) shows reduced levels of Chl*a* with respect to the shelf region. Two slight climatological maxima are found in June and autumn. Again, two prominent features can be noticed: a spectacular Chl*a* peak in 2001 (with high Chl*a* values from April to August, a signal also seen for K_d), and lower values for the last 3 years (and continuously negative anomalies from October 2002 to December 2004). These lower levels are confirmed by the MODIS data, and the associated climatology shows higher values of Chl*a* and K_d in autumn-winter, and lower ones in spring-summer.

Table 4.2: Western Deep Black Sea; SeaWiFS Chl*a* interannual anomalies, computed as ratio of area-averaged Chl*a* concentrations. The 2^{nd} column gives the SeaWiFS climatological Chl*a* (in mg m^{-3}). In bold, anomalies below 0.8 or above 1.2. A datum of 1 means a regional monthly value close to climatology.

Month	mg m^{-3}	1998	1999	2000	2001	2002	2003	2004
J	0.820	1.17	**1.35**	0.84	1.03	0.98	**0.73**	**0.79**
F	0.801	1.01	1.17	1.03	0.97	0.96	**0.77**	0.88
M	0.761	0.97	**1.27**	1.07	1.04	0.89	0.84	0.88
A	0.668	0.89	**1.21**	1.00	**1.39**	0.98	**0.74**	**0.72**
M	0.727	0.95	1.15	**0.79**	**1.95**	**0.79**	**0.64**	**0.77**
J	0.899	**0.69**	1.03	1.02	**2.19**	**0.67**	**0.62**	**0.63**
J	0.711	0.89	0.99	1.05	**1.72**	**0.72**	**0.65**	**0.70**
A	0.622	0.89	1.16	0.91	**1.63**	1.03	**0.69**	**0.78**
S	0.821	1.15	1.06	0.91	**1.28**	**1.25**	**0.64**	**0.73**
O	0.994	**1.28**	1.01	1.02	**1.20**	0.97	**0.58**	**0.68**
N	0.979	1.19	1.07	1.06	1.13	**0.78**	0.88	**0.60**
D	0.865	**1.25**	**1.20**	0.94	0.86	**0.72**	0.82	**0.65**

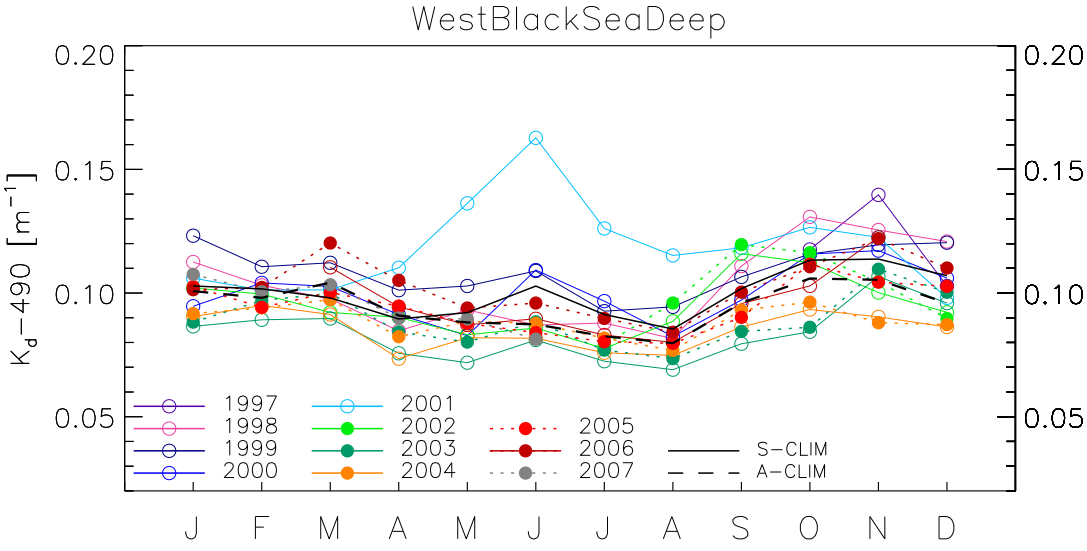

Figure 4.5: $K_d(490)$ multi-annual time series for SeaWiFS (lines with open circles) and MODIS (filled circles with dotted line) and associated climatologies (black line and dashed line, respectively).

4.3 Eastern Deep Black Sea

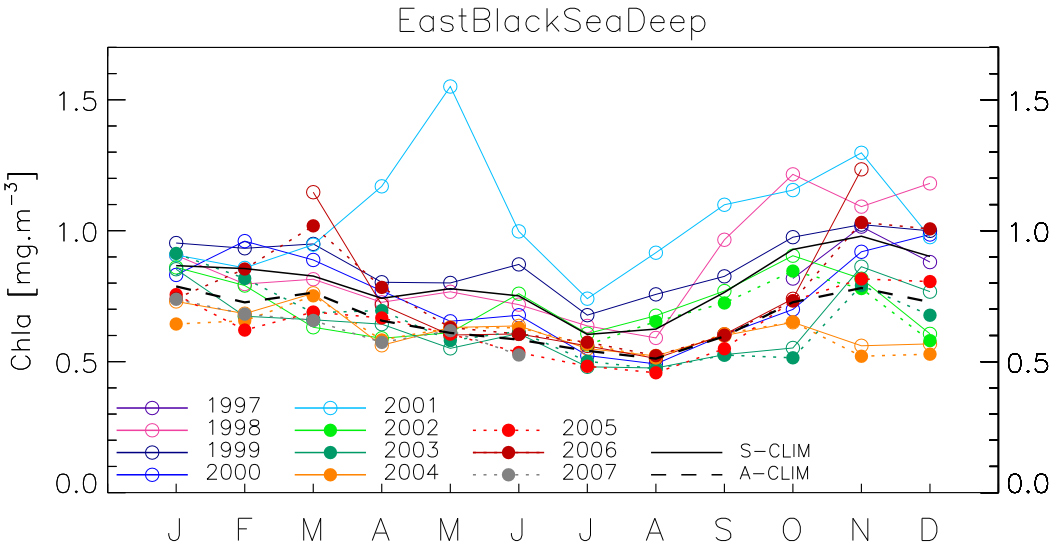

Figure 4.6: Chl*a* multi-annual time series for SeaWiFS (lines with open circles) and MODIS (filled circles with dotted line) and associated climatologies (black line and dashed line, respectively).

In the eastern part of the deep Black Sea, the seasonal cycle is similar to that of the western part, with a clearer minimum in July-August. Similarly, a large inter-annual event is clearly visible in 2001, but with an earlier peak (in May). SeaWiFS and MODIS Chl*a* are lower after autumn 2002 (and are consistent with one another).

Table 4.3: Eastern Deep Black Sea; SeaWiFS Chl*a* interannual anomalies, computed as ratio of area-averaged Chl*a* concentrations. The 2^{nd} column gives the SeaWiFS climatological Chl*a* (in mg m^{-3}). In bold, anomalies below 0.8 or above 1.2. A datum of 1 means a regional monthly value close to climatology.

Month	mg m^{-3}	1998	1999	2000	2001	2002	2003	2004
J	0.867	1.05	1.10	0.96	1.05	0.99	0.98	0.84
F	0.855	0.93	1.09	1.12	1.00	0.92	**0.79**	**0.80**
M	0.827	0.99	1.15	1.07	1.14	**0.76**	**0.80**	0.92
A	0.742	0.98	1.08	1.04	**1.58**	**0.79**	0.87	**0.76**
M	0.779	0.98	1.03	0.84	**1.99**	**0.78**	**0.71**	0.81
J	0.751	0.96	1.16	0.90	**1.33**	1.01	0.81	0.85
J	0.604	1.05	1.12	0.87	**1.23**	1.00	**0.80**	0.91
A	0.624	0.95	**1.21**	**0.79**	**1.47**	1.08	**0.76**	0.84
S	0.764	**1.26**	1.08	**0.79**	**1.44**	1.01	**0.69**	**0.78**
O	0.928	**1.31**	1.05	**0.75**	**1.24**	0.97	**0.59**	**0.70**
N	0.979	1.12	1.05	0.94	**1.33**	0.83	0.88	**0.57**
D	0.902	**1.31**	1.11	1.09	1.08	**0.67**	0.85	**0.63**

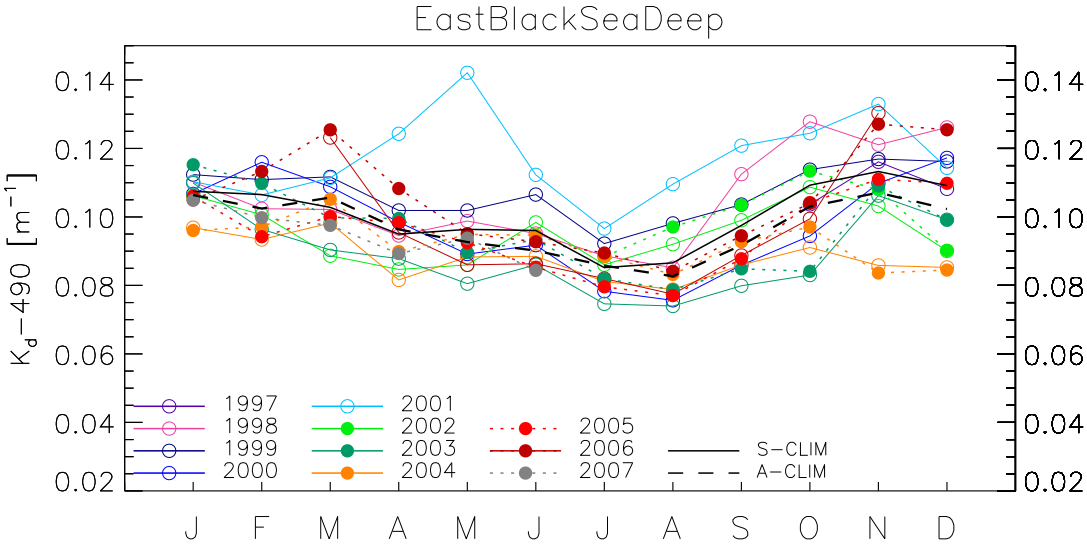

Figure 4.7: $K_d(490)$ multi-annual time series for SeaWiFS (lines with open circles) and MODIS (filled circles with dotted line) and associated climatologies (black line and dashed line, respectively).

4.4 Azov Sea

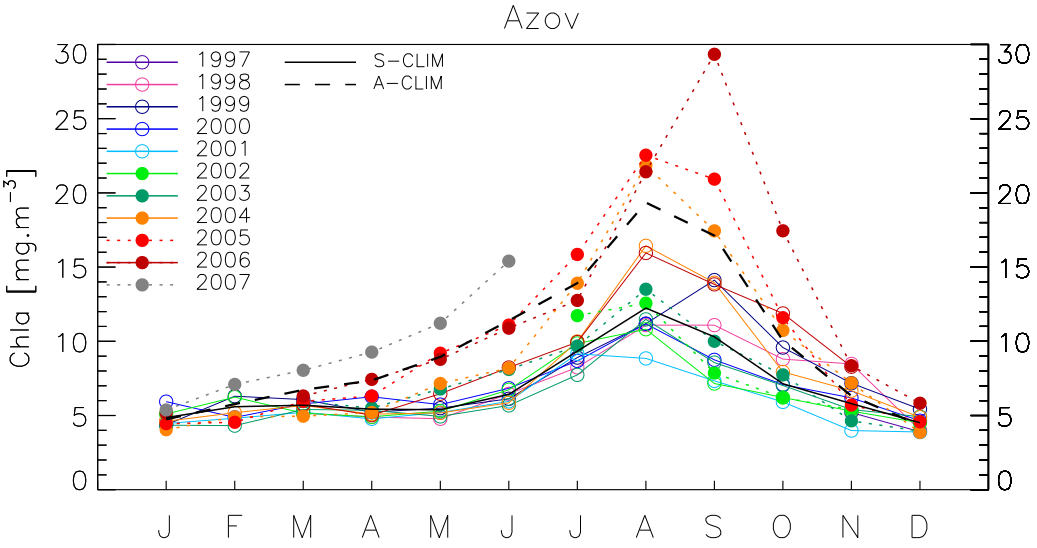

Figure 4.8: Chl*a* multi-annual time series for SeaWiFS (lines with open circles) and MODIS (filled circles with dotted line) and associated climatologies (black line and dashed line, respectively).

The time series for the Azov Sea is here added only for completeness. The basin is both shallow and very turbid, and information on its bio-optical properties is not known from the authors. Interestingly, the MODIS Chl*a* values of the last three years are much higher than the previous levels.

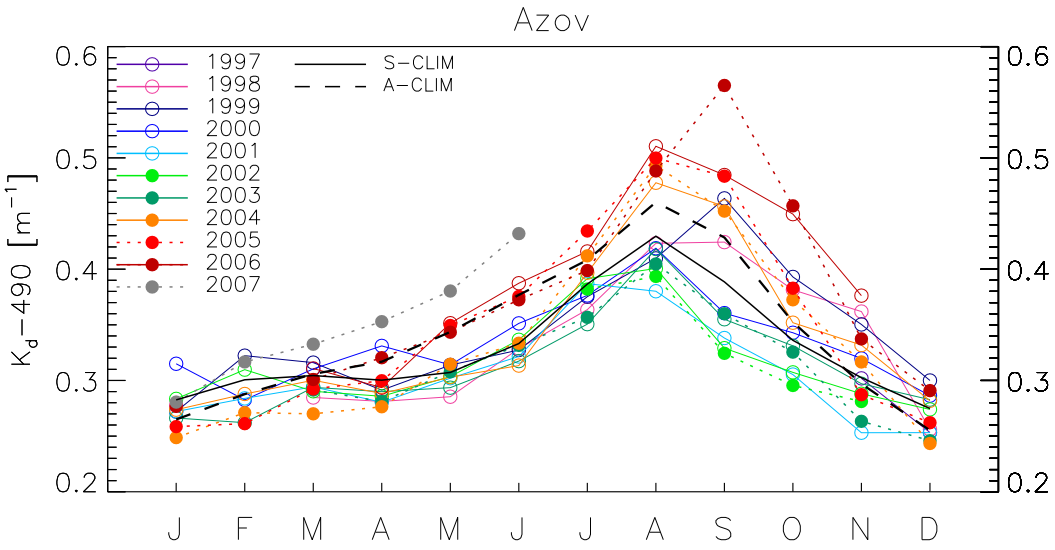

Figure 4.9: $K_d(490)$ multi-annual time series for SeaWiFS (lines with open circles) and MODIS (filled circles with dotted line) and associated climatologies (black line and dashed line, respectively).

Section 5

Northeast Atlantic Domain

The partition of the Northeast Atlantic is shown on Figures 5.1 and 5.2. The overall division relies on the partition by ICES region (or FAO region 27). The analysis has been performed on clusters of these regions, namely the Norwegian Sea (region IIa), the Faroe Plateau (region Vb), the Iceland Shelf (region Va), the North Sea (regions IVa to IVc), the northwestern British coasts (around the Hebrides Islands, regions VIa and VIIb), the Irish Sea (VIIa), the Celtic Sea (VIIf, g, h, j), the English Channel (VIId and VIIe), the Gulf of Biscaye (VIIIa and VIIIb, and VIIIc and VIIId), the Iberian Upwelling (IXa), the northeast Atlantic (regions VIb, VIIc, VIIk and XII), and the Azores basin (regions VIIIe, IXb and X).

For each domain, the time series of Chl$a$ and $K_d(490)$ are given for the years 1997 to 2004 using SeaWiFS (lines with open circles) and for years 2002 to 2007 for MODIS (filled circles with dotted line). The climatologies from SeaWiFS (Dec. 1997-Nov. 2004, continuous line) and MODIS (Jul. 2002-Jun. 2007, dashed line) are over-plotted for reference.

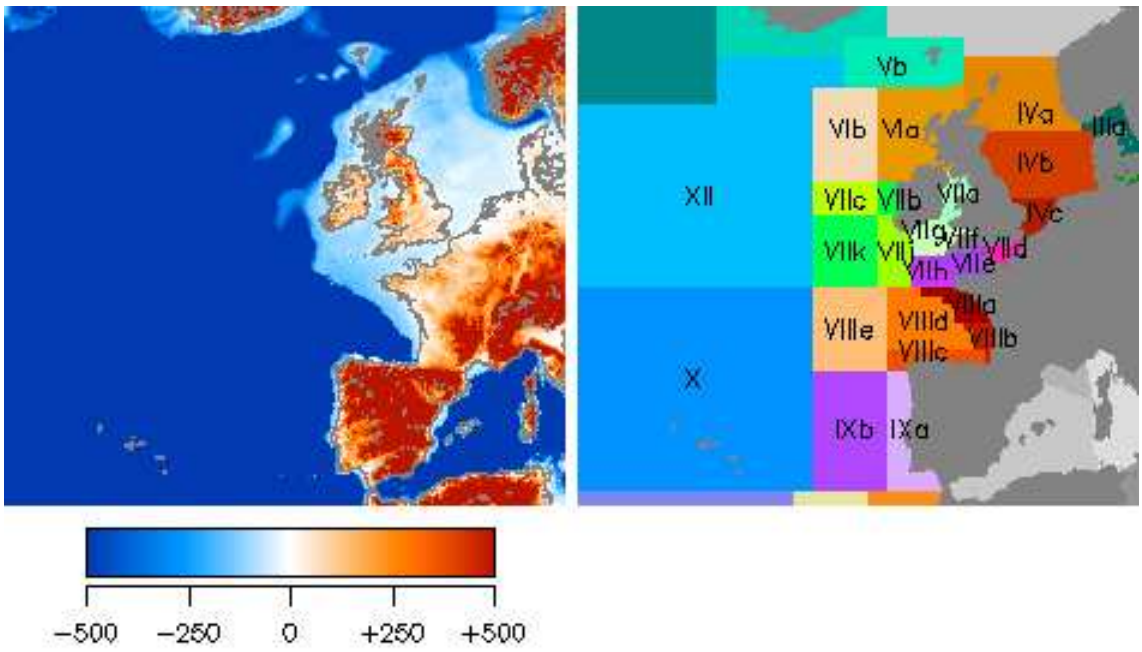

Figure 5.1: Distribution of the Northeast Atlantic Basin bathymetry and partition.

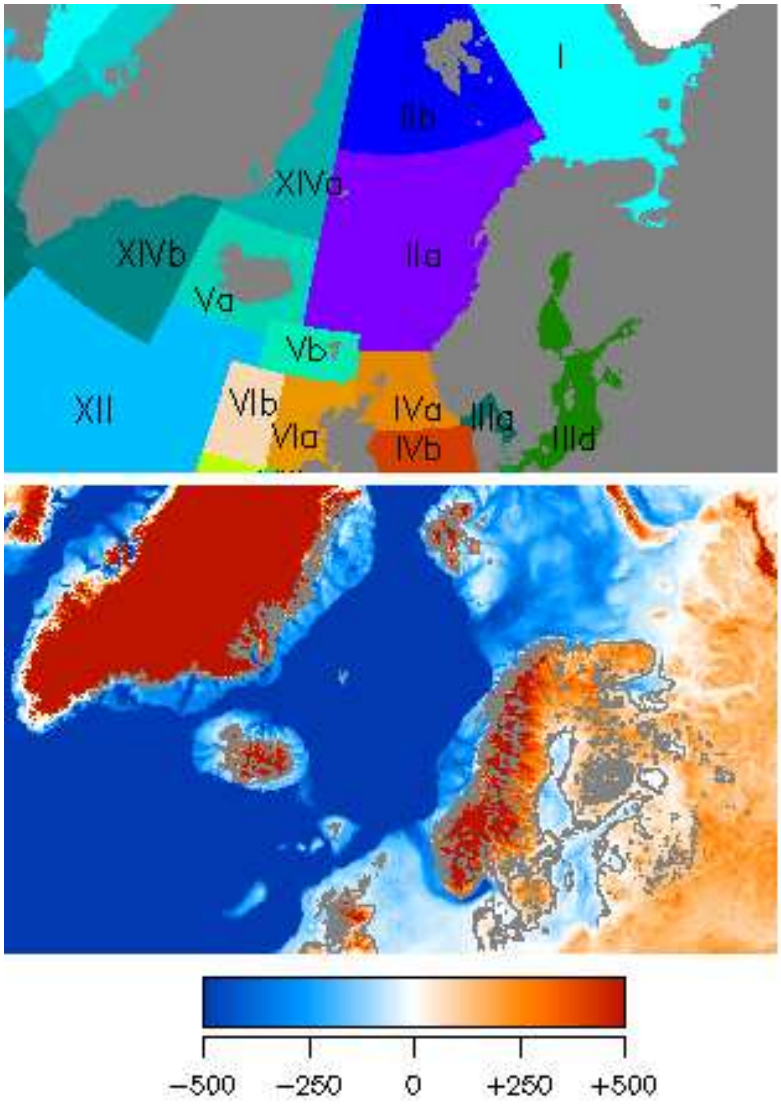

Figure 5.2: Distribution of the Northeast Atlantic Basin bathymetry and partition.

5.1 Norwegian Sea

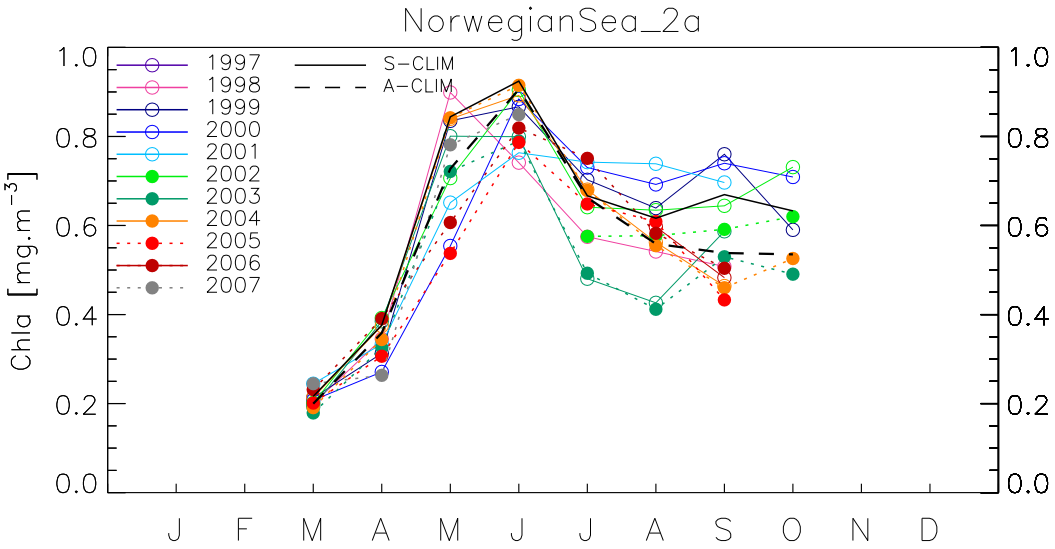

Figure 5.3: Chl*a* multi-annual time series for SeaWiFS (lines with open circles) and MODIS (filled circles with dotted line) and associated climatologies (black line and dashed line, respectively).

The inter-annual signals for the Norwegian Sea pertain mainly to the rate of increase from the minima (in March) to the annual peak (May-June), and the subsequent summer Chl*a* and K_d levels. For instance in 2003, the Chl*a* values were quite low in July-August, but higher in 2000 and 2001. The SeaWiFS and MODIS series compare reasonably well.

Table 5.1: Norwegian Sea; ICES Region IIa; SeaWiFS Chl*a* inter-annual anomalies, computed as ratio of area-averaged Chl*a* concentrations. The 2^{nd} column gives the SeaWiFS climatological Chl*a* (in mg m^{-3}). In bold, anomalies below 0.8 or above 1.2. A datum of 1 means a regional monthly value close to climatology.

Month	mg m^{-3}	1998	1999	2000	2001	2002	2003	2004
J	-	-	-	-	-	-	-	-
F	-	-	-	-	-	-	-	-
M	0.216	0.92	0.98	0.96	1.13	0.93	0.89	0.99
A	0.376	0.92	0.83	**0.72**	0.89	1.04	1.02	1.00
M	0.844	1.06	0.99	**0.66**	**0.77**	0.84	0.95	0.99
J	0.924	0.80	0.94	0.96	0.83	0.98	0.86	0.97
J	0.667	0.86	1.05	1.10	1.11	0.96	**0.72**	1.02
A	0.616	0.88	1.04	1.12	1.20	1.03	**0.69**	0.91
S	0.669	**0.76**	1.14	1.11	1.04	0.96	0.88	**0.69**
O	0.633	-	0.93	1.12	-	1.16	-	-
N	-	-	-	-	-	-	-	-
D	-	-	-	-	-	-	-	-

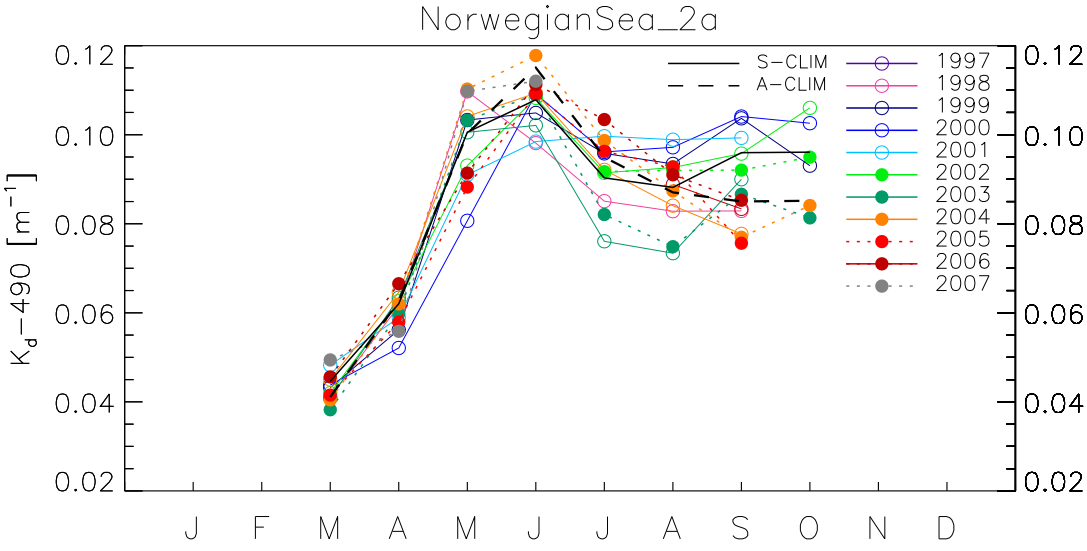

Figure 5.4: $K_d(490)$ multi-annual time series for SeaWiFS (lines with open circles) and MODIS (filled circles with dotted line) and associated climatologies (black line and dashed line, respectively).

5.2 Faroe Plateau

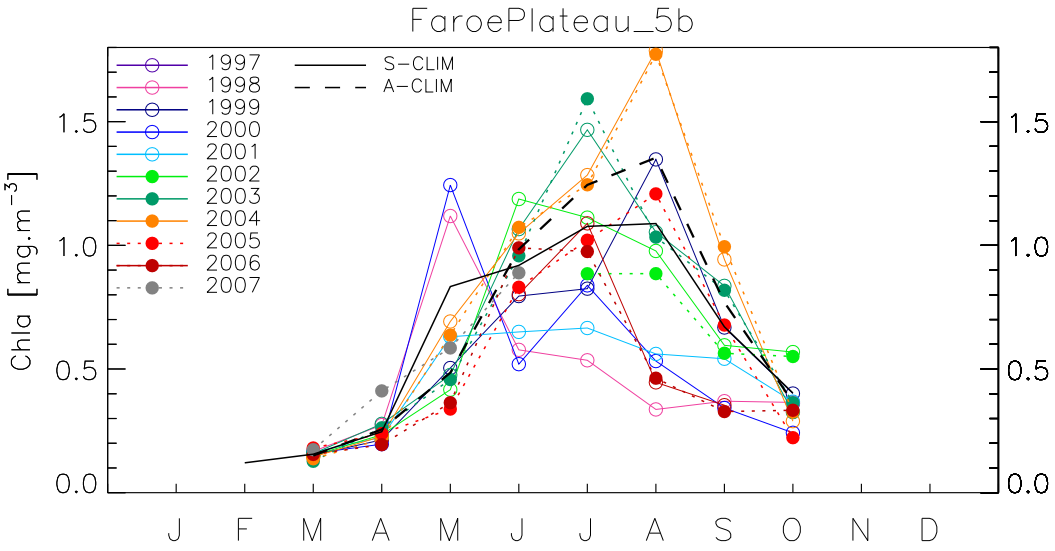

Figure 5.5: Chl*a* multi-annual time series for SeaWiFS (lines with open circles) and MODIS (filled circles with dotted line) and associated climatologies (black line and dashed line, respectively).

The SeaWiFS climatology shows for the region a fairly extended seasonal maximum, but that results from averaging several yearly cycles with different timing. For instance, the years 1998 and 2000 had Chl*a* and K_d peaks in May and lower values the rest of the year, whereas in 1999, these peaks were observed late, in August. The whole year 2001 is characterized by negative anomalies. There was a broad seasonal maximum in 2002 (June to August), also observed in 2003 but with a sharp July peak. The year 2004 reproduces the evolution in 1999, with a much higher August maximum. Overall, the region is characterized by a very high level of inter-annual variations.

Table 5.2: Faroe Plateau; ICES Region Vb; SeaWiFS Chl*a* inter-annual anomalies, computed as ratio of area-averaged Chl*a* concentrations. The 2^{nd} column gives the SeaWiFS climatological Chl*a* (in mg m^{-3}). In bold, anomalies below 0.8 or above 1.2. A datum of 1 means a regional monthly value close to climatology.

Month	mg m^{-3}	1998	1999	2000	2001	2002	2003	2004
J	-	-	-	-	-	-	-	-
F	0.121	-	-	-	-	-	-	-
M	0.155	1.07	0.97	1.02	1.05	0.97	1.02	0.93
A	0.246	1.11	0.87	**0.80**	0.91	0.95	1.13	0.92
M	0.833	**1.34**	**0.60**	**1.49**	**0.76**	**0.50**	**0.57**	0.83
J	0.919	**0.63**	0.87	**0.57**	**0.71**	**1.29**	1.16	1.14
J	1.077	**0.50**	**0.77**	**0.78**	**0.62**	1.03	**1.36**	1.19
A	1.088	**0.31**	**1.24**	**0.49**	**0.52**	0.90	0.97	**1.64**
S	0.671	**0.55**	1.00	**0.51**	0.81	0.89	**1.25**	**1.41**
O	0.403	0.91	0.99	**0.60**	0.91	**1.41**	0.81	**0.72**
N	-	-	-	-	-	-	-	-
D	-	-	-	-	-	-	-	-

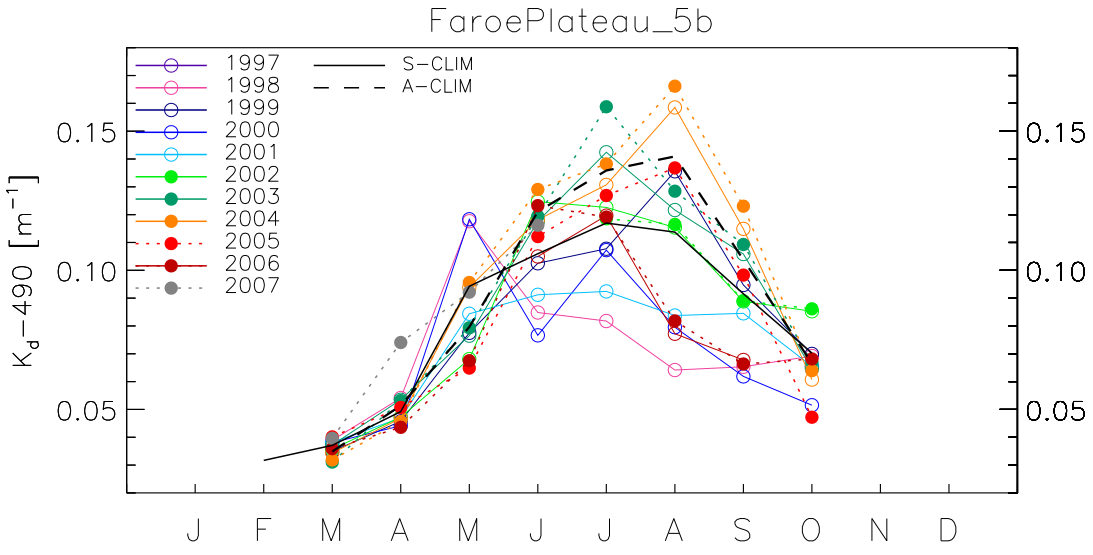

Figure 5.6: $K_d(490)$ multi-annual time series for SeaWiFS (lines with open circles) and MODIS (filled circles with dotted line) and associated climatologies (black line and dashed line, respectively).

5.3 Iceland Shelf

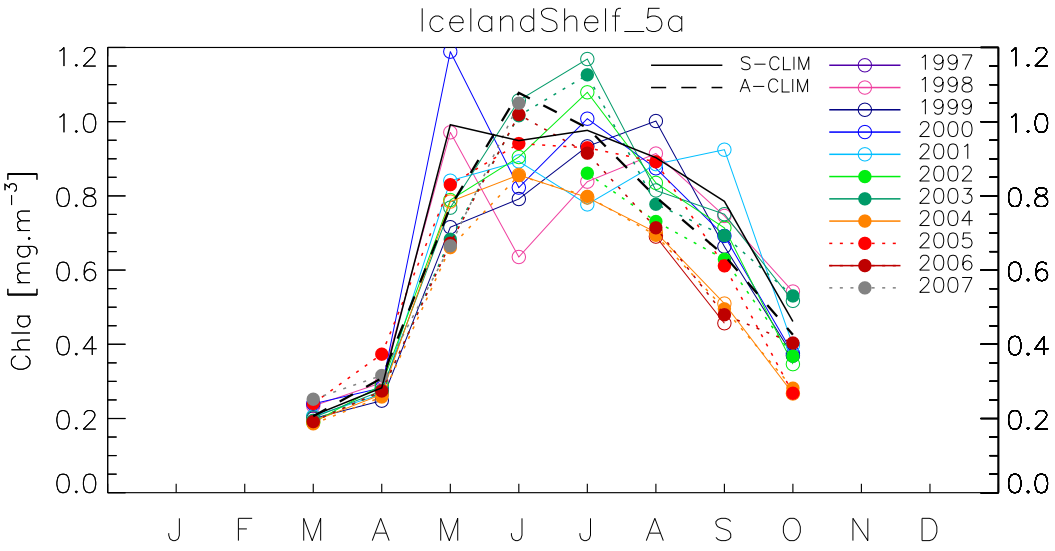

Figure 5.7: Chl*a* multi-annual time series for SeaWiFS (lines with open circles) and MODIS (filled circles with dotted line) and associated climatologies (black line and dashed line, respectively).

The seasonal cycle on the Iceland Shelf is somewhat similar to that on the Faroe Plateau but the inter-annual variations are much more constrained. 1998 and 2000 had a similar evolution, with a strong initial Chl*a* and K_d peak (in May) followed by a low in June. In 2001, there was a second seasonal peak in September.

Table 5.3: Iceland Shelf; ICES Region Va; SeaWiFS Chl*a* inter-annual anomalies, computed as ratio of area-averaged Chl*a* concentrations. The 2^{nd} column gives the SeaWiFS climatological Chl*a* (in mg m^{-3}). In bold, anomalies below 0.8 or above 1.2. A datum of 1 means a regional monthly value close to climatology.

Month	mg m^{-3}	1998	1999	2000	2001	2002	2003	2004
J	-	-	-	-	-	-	-	-
F	-	-	-	-	-	-	-	-
M	0.208	1.12	0.96	1.15	0.99	0.91	0.97	0.93
A	0.283	1.05	0.88	1.00	0.94	1.03	0.97	0.94
M	0.992	0.98	**0.72**	1.20	0.85	**0.80**	**0.77**	**0.79**
J	0.949	**0.67**	0.83	0.87	0.94	0.95	1.11	0.90
J	0.977	0.86	0.96	1.03	**0.80**	1.10	1.20	0.81
A	0.903	1.01	1.11	0.97	0.98	0.92	0.90	**0.78**
S	0.785	0.95	0.84	0.88	1.18	0.91	0.96	**0.65**
O	0.461	1.18	0.80	0.81	0.86	**0.75**	1.12	**0.58**
N	-	-	-	-	-	-	-	-
D	-	-	-	-	-	-	-	-

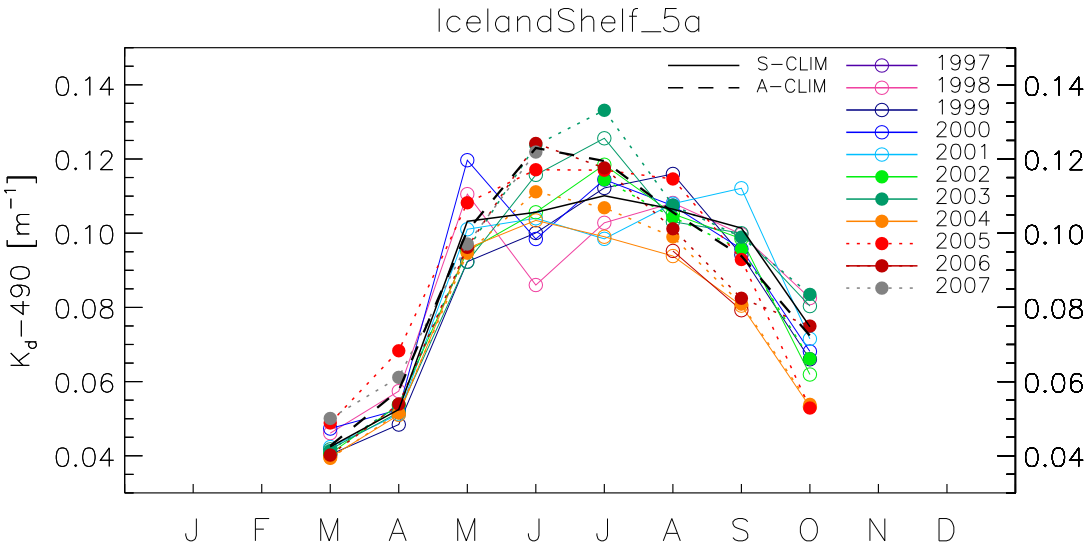

Figure 5.8: $K_d(490)$ multi-annual time series for SeaWiFS (lines with open circles) and MODIS (filled circles with dotted line) and associated climatologies (black line and dashed line, respectively).

5.4 North Sea

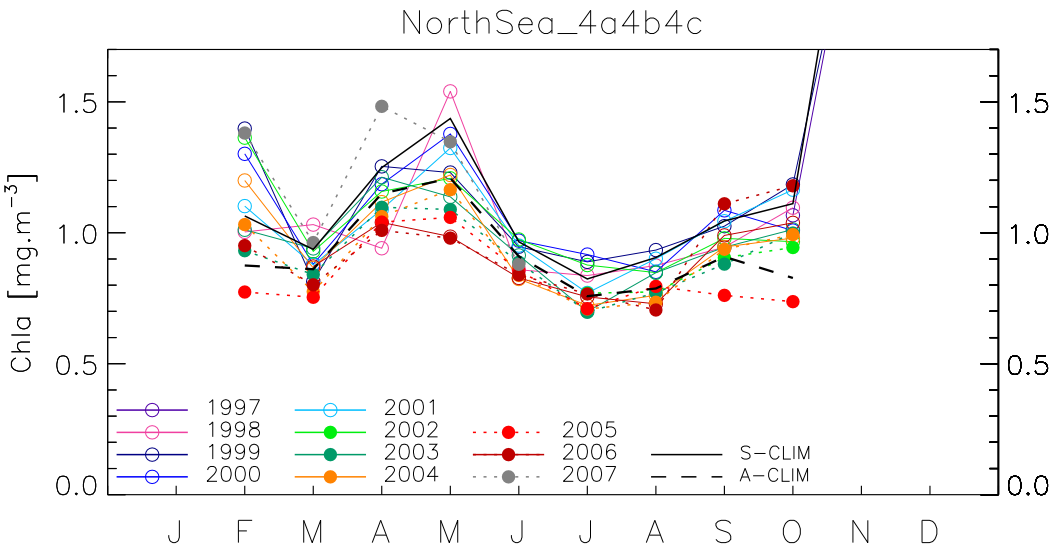

Figure 5.9: Chl*a* multi-annual time series for SeaWiFS (lines with open circles) and MODIS (filled circles with dotted line) and associated climatologies (black line and dashed line, respectively).

The annual maximum in the North Sea is found in April-May, with high values also displayed in February (a month when only the southernmost part is covered by the satellite data). Considering the biophysical complexity of the North Sea, the level of inter-annual variability is fairly low. Interestingly, most of the years 2003 to 2006 appear with Chl*a* averages below the climatology. MODIS derived Chl*a* and K_d monthly averages are high for the spring 2007.

Table 5.4: North Sea; ICES Regions IVa, b, c; SeaWiFS Chl*a* inter-annual anomalies, computed as ratio of area-averaged Chl*a* concentrations. The 2^{nd} column gives the SeaWiFS climatological Chl*a* (in mg m^{-3}). In bold, anomalies below 0.8 or above 1.2. A datum of 1 means a regional monthly value close to climatology.

Month	mg m^{-3}	1998	1999	2000	2001	2002	2003	2004
J	-	-	-	-	-	-	-	-
F	1.064	0.94	**1.31**	**1.22**	1.04	**1.28**	0.95	1.13
M	0.936	1.10	0.87	0.94	0.94	0.99	1.00	0.92
A	1.249	**0.75**	1.00	0.95	0.87	0.93	0.97	0.89
M	1.436	1.07	0.86	0.96	0.92	0.84	**0.79**	0.85
J	0.965	0.89	0.98	1.00	0.99	1.01	0.95	0.85
J	0.824	1.02	1.08	1.11	0.94	1.06	0.85	0.88
A	0.905	0.97	1.03	0.94	1.00	0.94	0.94	0.84
S	1.045	0.90	0.98	1.04	1.00	0.94	0.90	0.90
O	1.111	0.99	1.07	0.91	1.05	0.87	0.91	0.88
N	2.676	-	0.89	-	-	-	-	-
D	-	-	-	-	-	-	-	-

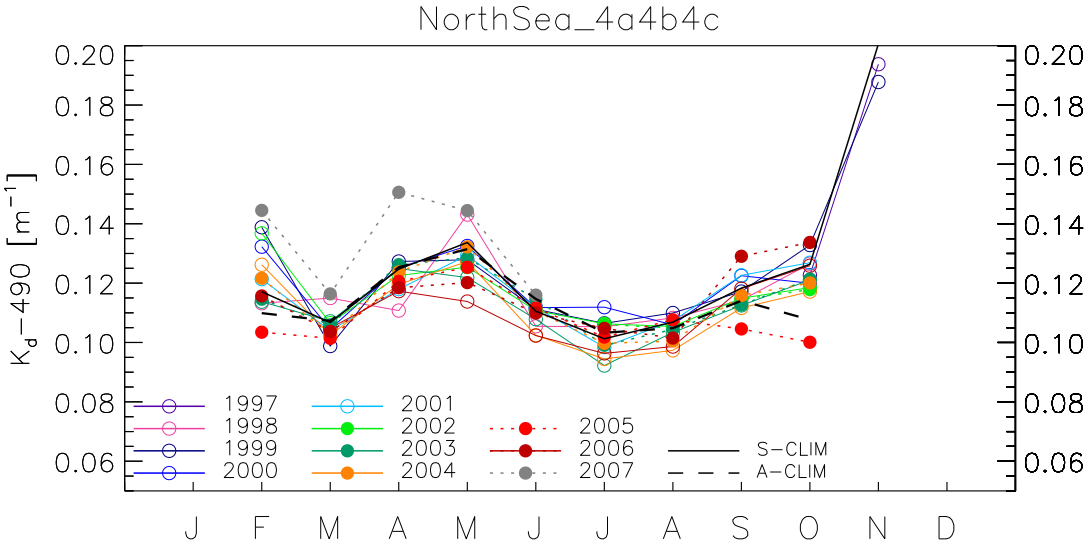

Figure 5.10: $K_d(490)$ multi-annual time series for SeaWiFS (lines with open circles) and MODIS (filled circles with dotted line) and associated climatologies (black line and dashed line, respectively).

5.5 Northwestern British coasts

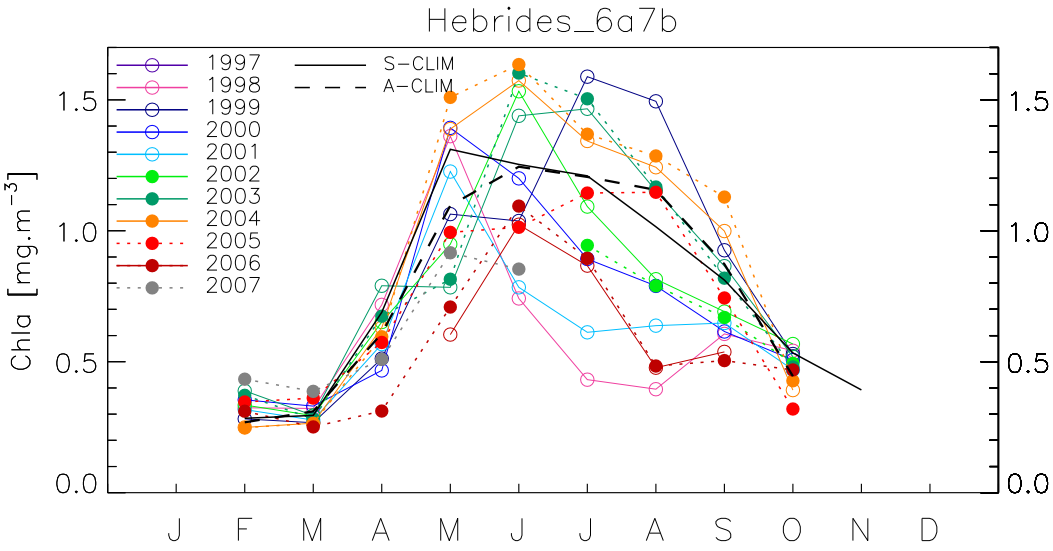

Figure 5.11: Chl*a* multi-annual time series for SeaWiFS (lines with open circles) and MODIS (filled circles with dotted line) and associated climatologies (black line and dashed line, respectively).

Most of the inter-annual variations are found in the timing, duration and strength of the seasonal maximum of Chl*a* and K_d. For instance, there is a clear seasonal peak in May 1998 and 2001 followed by a sharp decline, leading to monthly Chl*a* averages as low as half the climatological value. In 2002, the seasonal Chl*a* and K_d peaks were in June. Conversely, in 1999, there was a first increase in May and a maximum in July-August. A somewhat similar pattern happened in 2003 with a peak in June-July. The seasonal maximum was particularly long-lived in 2004 (from May to September). In 2005 to 2007, the MODIS Chl*a* record indicates rather low seasonal maxima. The agreement with SeaWiFS seems satisfactory for the previous years of common coverage.

Table 5.5: Northwestern British coasts; ICES Regions VIa and VIIb; SeaWiFS Chl$a$ inter-annual anomalies, computed as ratio of area-averaged Chl$a$ concentrations. The 2^{nd} column gives the SeaWiFS climatological Chl$a$ (in mg m^{-3}). In bold, anomalies below 0.8 or above 1.2. A datum of 1 means a regional monthly value close to climatology.

Month	mg m^{-3}	1998	1999	2000	2001	2002	2003	2004
J	-	-	-	-	-	-	-	-
F	0.284	1.14	0.99	**1.25**	1.12	1.18	**1.37**	0.88
M	0.295	1.09	0.91	1.12	0.94	1.00	1.00	0.90
A	0.689	1.04	**0.74**	**0.68**	0.82	0.95	1.15	0.91
M	1.311	1.04	0.81	1.06	0.94	**0.72**	**0.60**	1.06
J	1.253	**0.59**	0.83	0.96	**0.63**	**1.22**	1.15	**1.26**
J	1.210	**0.36**	**1.31**	**0.74**	**0.51**	0.90	**1.21**	1.11
A	1.015	**0.39**	**1.47**	**0.78**	**0.63**	0.80	1.14	**1.22**
S	0.812	**0.75**	1.14	**0.76**	**0.80**	0.85	1.07	**1.23**
O	0.534	1.02	0.99	0.95	0.88	1.06	0.97	**0.73**
N	0.392	-	-	-	-	-	-	-
D	-	-	-	-	-	-	-	-

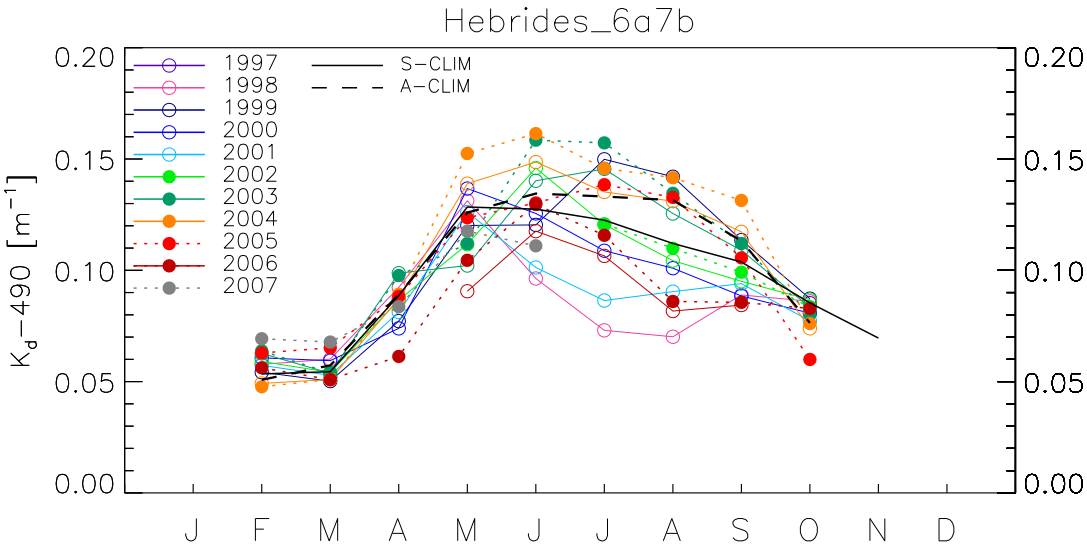

Figure 5.12: K$_d$(490) multi-annual time series for SeaWiFS (lines with open circles) and MODIS (filled circles with dotted line) and associated climatologies (black line and dashed line, respectively).

5.6 Irish Sea

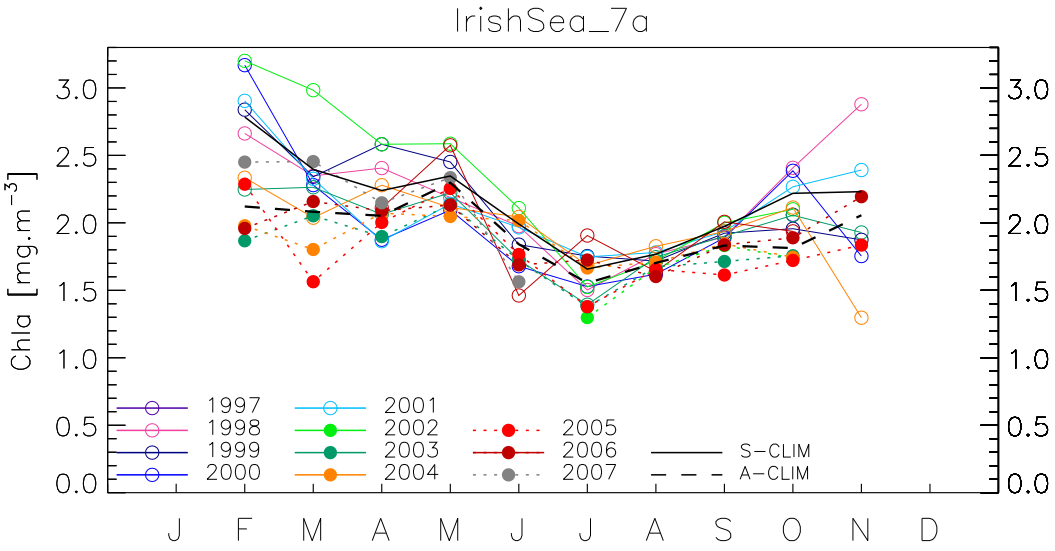

Figure 5.13: Chl*a* multi-annual time series for SeaWiFS (lines with open circles) and MODIS (filled circles with dotted line) and associated climatologies (black line and dashed line, respectively).

In terms of regional average, the Chl*a* and K_d series show little variation from year to year. Only worth mentioning are the relatively high and low values observed in 2002 and 2003, respectively.

Table 5.6: Irish Sea; ICES Region VIIa; SeaWiFS Chl*a* inter-annual anomalies, computed as ratio of area-averaged Chl*a* concentrations. The 2^{nd} column gives the SeaWiFS climatological Chl*a* (in mg m^{-3}). In bold, anomalies below 0.8 or above 1.2. A datum of 1 means a regional monthly value close to climatology.

Month	mg m^{-3}	1998	1999	2000	2001	2002	2003	2004
J	-	-	-	-	-	-	-	-
F	2.785	0.96	1.02	1.14	1.04	1.15	0.81	0.84
M	2.396	0.98	0.98	0.95	0.97	**1.24**	0.94	0.85
A	2.240	1.07	1.15	0.84	0.83	1.15	0.92	1.02
M	2.347	0.93	1.04	0.89	0.91	1.10	0.95	0.90
J	1.991	0.99	0.92	0.84	0.99	1.06	0.87	1.03
J	1.657	0.91	1.06	0.92	1.05	0.92	0.84	1.02
A	1.768	1.00	0.97	0.92	1.01	0.97	0.99	1.03
S	1.973	0.96	0.97	0.96	0.98	1.01	0.96	0.98
O	2.219	1.09	0.88	1.08	1.02	0.95	0.93	0.95
N	2.231	**1.29**	0.84	**0.79**	1.07	-	0.86	**0.58**
D	-	-	-	-	-	-	-	-

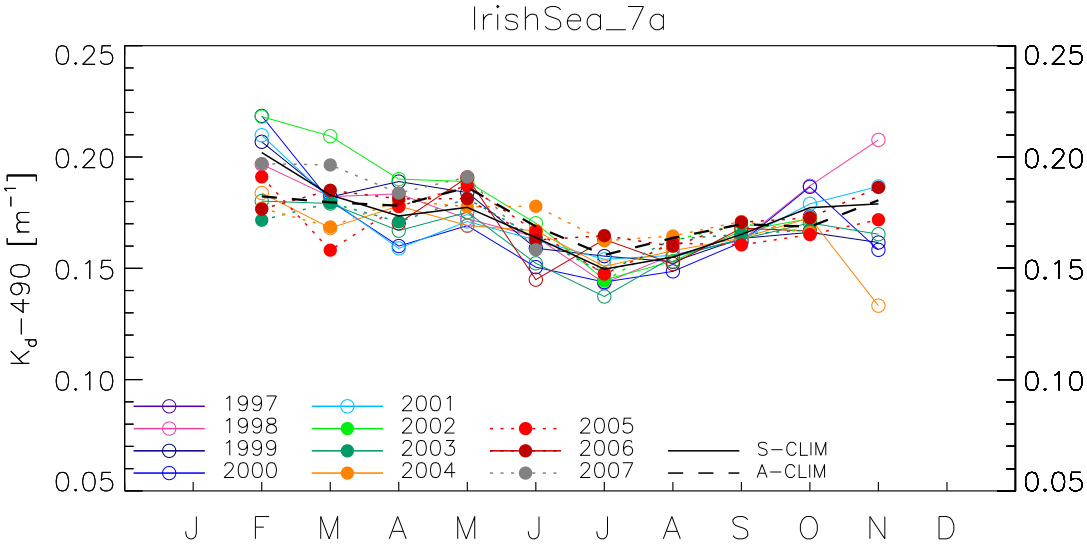

Figure 5.14: $K_d(490)$ multi-annual time series for SeaWiFS (lines with open circles) and MODIS (filled circles with dotted line) and associated climatologies (black line and dashed line, respectively).

5.7 Celtic Sea

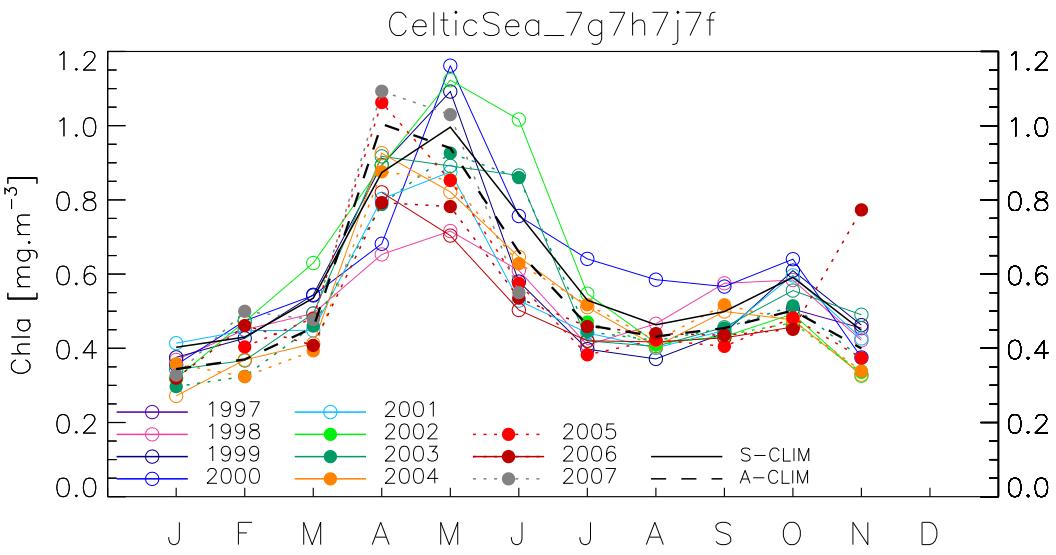

Figure 5.15: Chl*a* multi-annual time series for SeaWiFS (lines with open circles) and MODIS (filled circles with dotted line) and associated climatologies (black line and dashed line, respectively).

In the Celtic Sea, there are clear spring Chl*a* and K_d peaks, with a secondary maximum in October. The spring bloom has shown varying intensity and timing during the SeaWiFS record. It was low in 1998 and to a lesser extent in 2001, and relatively high in May 1999, 2000 and 2002. In 2000, the Chl*a* levels remained fairly high after May up to October. As for the recent MODIS record, it shows an early and strong maximum in April 2005 and 2007, and rather low values in 2006.

Table 5.7: Celtic Sea; ICES Regions VIIf, g, h, j; SeaWiFS Chl*a* inter-annual anomalies, computed as ratio of area-averaged Chl*a* concentrations. The 2^{nd} column gives the SeaWiFS climatological Chl*a* (in mg m^{-3}). In bold, anomalies below 0.8 or above 1.2. A datum of 1 means a regional monthly value close to climatology.

Month	mg m^{-3}	1998	1999	2000	2001	2002	2003	2004
J	0.403	0.92	0.93	0.88	1.03	**0.79**	0.85	**0.67**
F	0.430	1.05	0.99	1.10	1.04	1.10	0.85	0.86
M	0.535	0.92	1.02	1.01	0.84	1.18	0.92	**0.77**
A	0.874	**0.75**	1.02	**0.78**	0.92	1.02	1.05	1.06
M	0.996	**0.72**	1.10	1.17	0.88	1.13	0.90	0.82
J	0.762	0.80	**0.76**	0.99	**0.69**	**1.33**	1.14	0.85
J	0.530	**0.77**	**0.75**	**1.21**	0.83	1.03	**0.79**	0.96
A	0.463	1.01	0.80	**1.26**	0.87	0.90	0.87	0.87
S	0.499	1.15	0.88	1.14	0.90	0.86	0.92	1.00
O	0.591	0.99	1.03	1.08	1.01	0.83	0.94	0.81
N	0.449	0.94	1.03	0.84	0.95	**0.73**	1.09	**0.73**
D	-	-	-	-	-	-	-	-

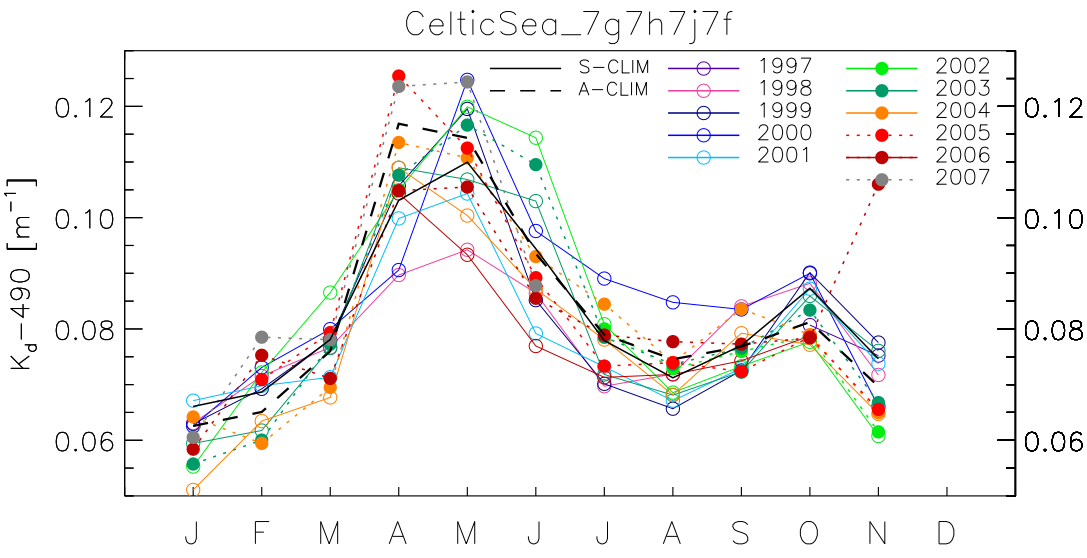

Figure 5.16: $K_d(490)$ multi-annual time series for SeaWiFS (lines with open circles) and MODIS (filled circles with dotted line) and associated climatologies (black line and dashed line, respectively).

5.8 English Channel

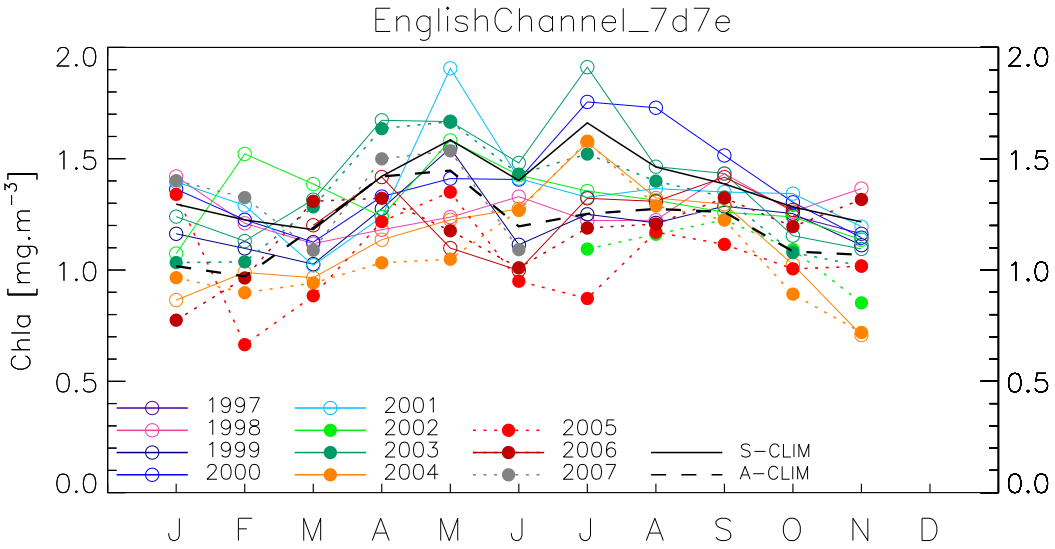

Figure 5.17: Chl*a* multi-annual time series for SeaWiFS (lines with open circles) and MODIS (filled circles with dotted line) and associated climatologies (black line and dashed line, respectively).

The optically complex waters of the English Channel do not show a marked seasonal cycle (on the basis of the standard ocean color record). Interestingly, the average SeaWiFS Chl*a* concentrations appear rather low in 2004, as are the MODIS derived series for the last couple of years. The SeaWiFS values were also relatively low in 1999. A period of sustained positive anomalies was observed in the middle part of 2003. The K_d climatologies from SeaWiFS and MODIS compare very well.

Table 5.8: English Channel; ICES Regions VIId, e; SeaWiFS Chl*a* inter-annual anomalies, computed as ratio of area-averaged Chl*a* concentrations. The 2^{nd} column gives the SeaWiFS climatological Chl*a* (in mg m^{-3}). In bold, anomalies below 0.8 or above 1.2. A datum of 1 means a regional monthly value close to climatology.

Month	mg m^{-3}	1998	1999	2000	2001	2002	2003	2004
J	1.296	1.10	0.90	1.05	1.08	0.83	0.96	**0.67**
F	1.225	0.99	0.90	1.00	1.05	**1.24**	0.92	0.81
M	1.181	0.95	0.87	0.95	0.86	1.17	1.11	0.82
A	1.421	0.83	0.90	0.94	0.87	0.87	1.18	**0.80**
M	1.585	**0.78**	0.98	0.89	**1.20**	1.00	1.05	**0.77**
J	1.402	0.95	**0.79**	1.00	1.01	1.02	1.06	0.91
J	1.661	**0.74**	**0.75**	1.06	**0.80**	0.82	1.15	0.95
A	1.463	0.84	0.83	1.18	0.93	0.90	1.00	0.90
S	1.387	1.03	0.93	1.09	0.97	0.91	1.03	0.93
O	1.283	0.98	0.98	1.02	1.05	0.96	0.90	**0.80**
N	1.216	1.12	0.91	0.94	0.98	0.93	0.90	**0.58**
D	-	-	-	-	-	-	-	-

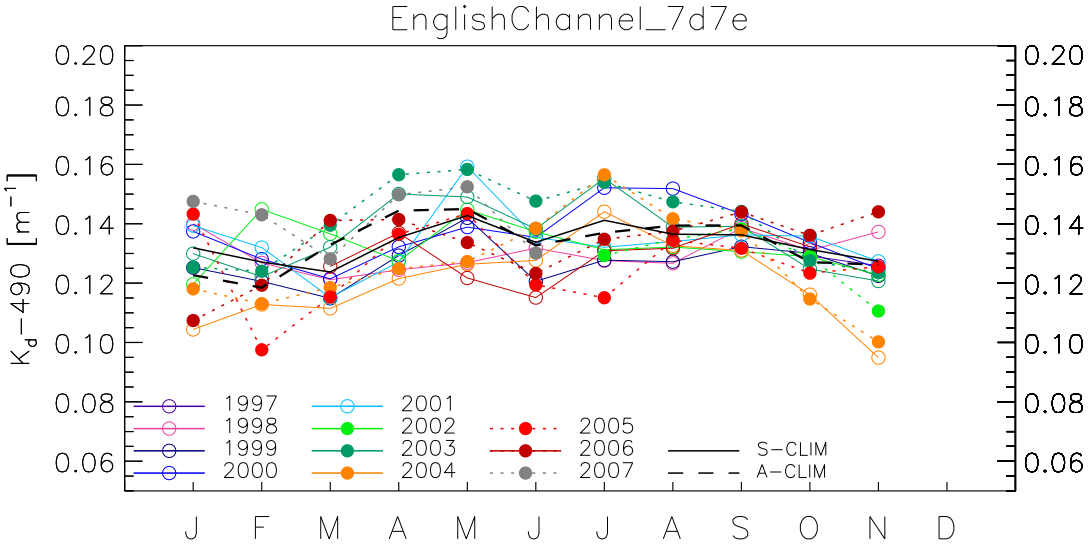

Figure 5.18: $K_d(490)$ multi-annual time series for SeaWiFS (lines with open circles) and MODIS (filled circles with dotted line) and associated climatologies (black line and dashed line, respectively).

5.9 Bay of Biscaye - Shelf

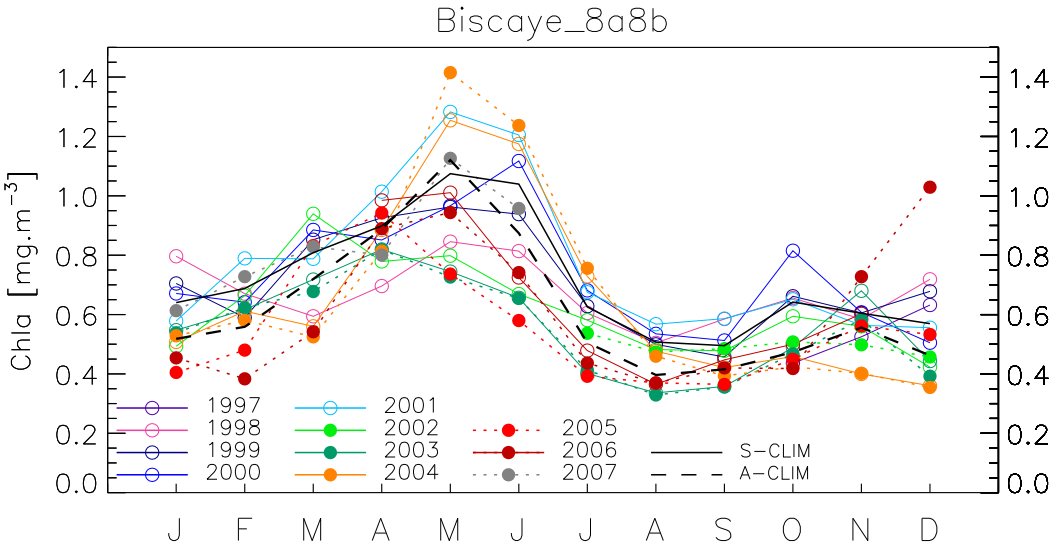

Figure 5.19: Chl*a* multi-annual time series for SeaWiFS (lines with open circles) and MODIS (filled circles with dotted line) and associated climatologies (black line and dashed line, respectively).

In the shelf and coastal parts of the Bay of Biscaye, the SeaWiFS cycle indicates a clear spring maximum in April to June. The years 1998 (with monthly values less than 0.8 times climatology for a four-month period), 2002 (after an early start) and 2003 had low values for the April-May peak. Actually, the Chl*a* anomaly was continuously negative from April 2002 to October 2003. Conversely, 2003 and 2004 had relatively high values. The MODIS derived Chl*a* values for 2005 and 2006 appear in the mid to low range. In general, the SeaWiFS and MODIS series appear rather coherent.

Table 5.9: Bay of Biscaye; ICES Regions VIIIa, b; SeaWiFS Chl*a* inter-annual anomalies, computed as ratio of area-averaged Chl*a* concentrations. The 2^{nd} column gives the SeaWiFS climatological Chl*a* (in mg m^{-3}). In bold, anomalies below 0.8 or above 1.2. A datum of 1 means a regional monthly value close to climatology.

Month	mg m^{-3}	1998	1999	2000	2001	2002	2003	2004
J	0.640	**1.24**	1.10	1.05	0.90	**0.77**	0.85	**0.79**
F	0.688	0.97	0.86	0.93	1.15	0.96	0.90	0.89
M	0.808	**0.73**	1.05	1.09	0.97	1.16	0.89	**0.69**
A	0.899	**0.77**	1.03	0.95	1.13	0.87	0.91	0.98
M	1.075	**0.79**	0.90	0.90	1.19	**0.74**	**0.69**	1.17
J	1.039	**0.78**	0.90	1.07	1.16	**0.64**	**0.63**	1.13
J	0.625	0.97	1.00	1.09	1.08	0.93	**0.64**	1.16
A	0.507	0.99	0.98	1.05	1.12	0.95	**0.66**	0.94
S	0.495	1.18	0.92	1.04	1.18	0.97	**0.72**	0.85
O	0.642	1.02	1.03	**1.27**	1.01	0.93	**0.76**	**0.71**
N	0.604	0.97	1.00	1.00	0.93	0.93	1.13	**0.66**
D	0.569	**1.26**	1.19	0.89	0.98	**0.74**	**0.78**	**0.63**

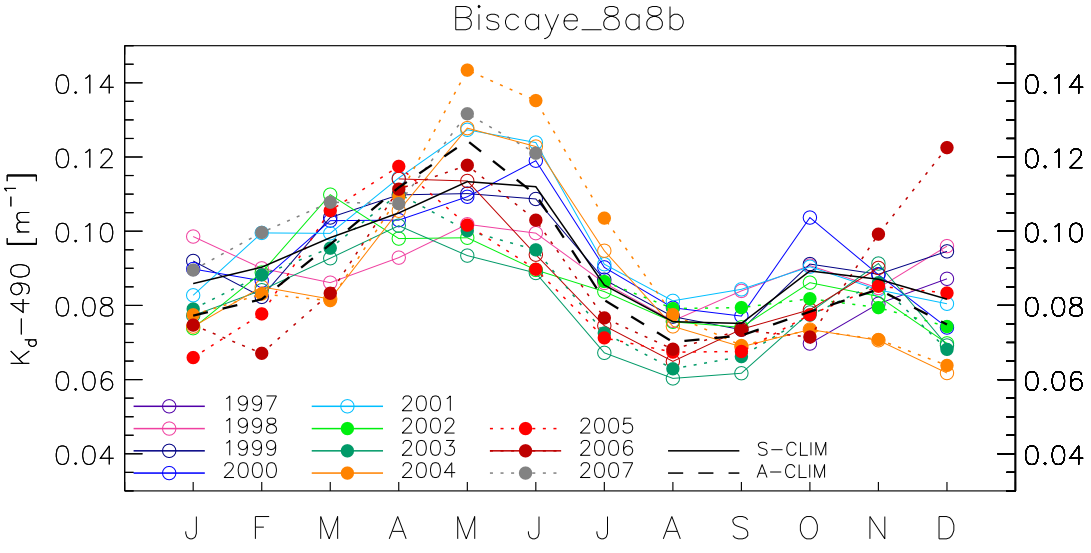

Figure 5.20: $K_d(490)$ multi-annual time series for SeaWiFS (lines with open circles) and MODIS (filled circles with dotted line) and associated climatologies (black line and dashed line, respectively).

5.10 Bay of Biscaye - Slope

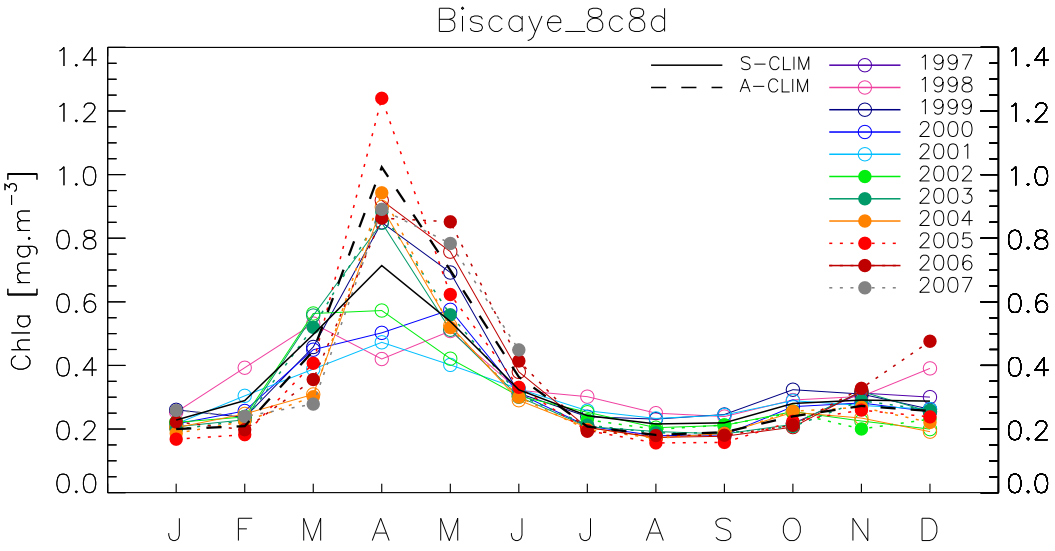

Figure 5.21: Chl*a* multi-annual time series for SeaWiFS (lines with open circles) and MODIS (filled circles with dotted line) and associated climatologies (black line and dashed line, respectively).

With respect to the shelf and coastal parts of the Bay of Biscaye, the open waters are characterized by a more distinct seasonal cycle with a sharper peak between March and May. This period is also that of the largest inter-annual signals. The years 1998, 2000, 2001 (with a strong negative anomaly for three months), and 2002 had low values for the April-May peak. Actually, the Chl*a* anomaly was continuously negative from April 2002 to October 2003. Conversely, 1999, 2003 and 2004 had relatively high values. The MODIS derived Chl*a* and K_d records display rather large values in spring, above the SeaWiFS climatology and logically the MODIS climatology for spring end up as noticeably higher. This is particularly interesting considering that the two satellite products agree reasonably well.

Table 5.10: Bay of Biscaye; ICES Regions VIIIc, d; SeaWiFS Chl*a* inter-annual anomalies, computed as ratio of area-averaged Chl*a* concentrations. The 2^{nd} column gives the SeaWiFS climatological Chl*a* (in mg m^{-3}). In bold, anomalies below 0.8 or above 1.2. A datum of 1 means a regional monthly value close to climatology.

Month	mg m^{-3}	1998	1999	2000	2001	2002	2003	2004
J	0.228	1.11	1.14	0.95	0.95	0.97	0.91	0.89
F	0.289	**1.36**	0.82	0.89	1.05	0.82	**0.79**	0.86
M	0.497	1.07	0.92	0.90	**0.78**	1.13	1.12	**0.62**
A	0.714	**0.59**	1.19	**0.70**	**0.66**	0.80	1.19	**1.26**
M	0.538	0.94	**1.29**	1.07	**0.75**	**0.78**	0.95	0.97
J	0.323	1.00	0.97	0.96	1.01	0.94	0.93	0.90
J	0.242	**1.25**	0.99	0.86	1.06	1.04	0.86	0.85
A	0.216	1.16	1.07	0.83	1.08	0.95	0.89	**0.80**
S	0.219	1.09	1.12	0.83	1.11	0.96	0.84	0.85
O	0.280	1.04	1.15	0.96	1.03	0.91	**0.77**	0.90
N	0.291	1.04	1.07	0.97	0.94	**0.77**	1.09	0.81
D	0.288	**1.36**	0.91	0.89	0.91	**0.69**	0.88	**0.67**

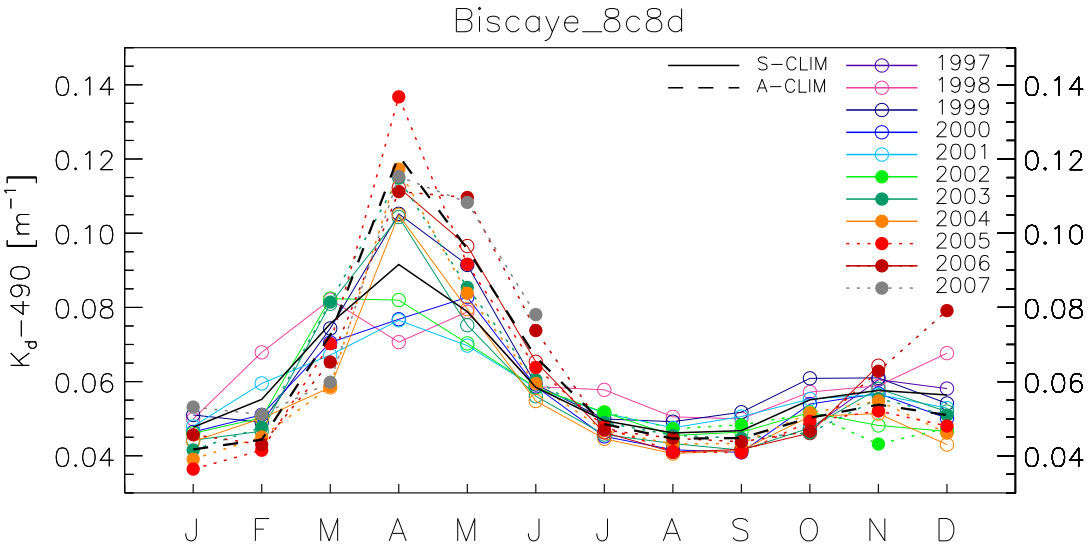

Figure 5.22: $K_d(490)$ multi-annual time series for SeaWiFS (lines with open circles) and MODIS (filled circles with dotted line) and associated climatologies (black line and dashed line, respectively).

5.11 Iberian Upwelling

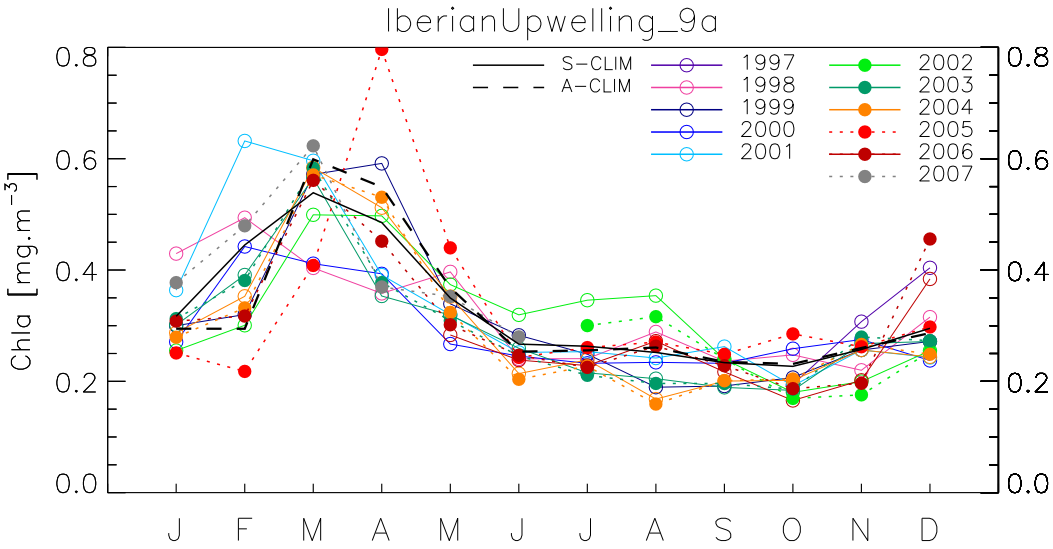

Figure 5.23: Chl*a* multi-annual time series for SeaWiFS (lines with open circles) and MODIS (filled circles with dotted line) and associated climatologies (black line and dashed line, respectively).

As for the Bay of Biscaye, most of the inter-annual signal is found in spring, even though the variations during the summer minimum are much higher. The spring peak for Chl*a* and K_d is centered on March. The years 1998 and 2000 had low values for the spring peak, whereas 2002 and 2004 had relatively higher values. The spring maximum was large and early in 2001, but with a fast demise; similarly, the peak in 2003 decreased rapidly. Conversely, it was strong and late in 1999. A large positive anomaly can be noticed in summer 2002, whereas these values were lower than climatology in 2003 and 2004. There was a large April maximum displayed by the MODIS Chl*a* and K_d in April 2005 (but not in 2006). The spring maximum in 2007 seems to have been short-lived.

Table 5.11: Iberian Upwelling; ICES Regions IXa; SeaWiFS Chl*a* inter-annual anomalies, computed as ratio of area-averaged Chl*a* concentrations. The 2^{nd} column gives the SeaWiFS climatological Chl*a* (in mg m^{-3}). In bold, anomalies below 0.8 or above 1.2. A datum of 1 means a regional monthly value close to climatology.

Month	mg m^{-3}	1998	1999	2000	2001	2002	2003	2004
J	0.317	**1.36**	0.95	0.85	1.15	0.81	0.95	0.91
F	0.445	1.11	**0.72**	0.99	**1.42**	**0.68**	0.88	**0.79**
M	0.539	**0.75**	1.06	**0.76**	1.11	0.93	1.05	1.08
A	0.485	**0.74**	**1.22**	0.81	0.81	1.02	**0.73**	1.05
M	0.350	1.13	0.97	**0.76**	0.91	1.07	0.91	1.01
J	0.267	0.90	1.06	0.92	0.94	1.20	0.97	0.80
J	0.263	0.91	0.95	0.88	0.96	**1.31**	0.82	0.91
A	0.252	1.15	**0.75**	0.93	0.96	**1.41**	0.81	**0.67**
S	0.234	1.01	0.82	0.99	1.12	1.03	0.81	0.86
O	0.227	1.09	0.91	1.14	0.85	**0.79**	0.81	0.89
N	0.257	0.85	1.00	1.07	1.00	**0.78**	1.04	1.00
D	0.295	1.07	0.92	0.80	0.82	0.86	0.92	0.83

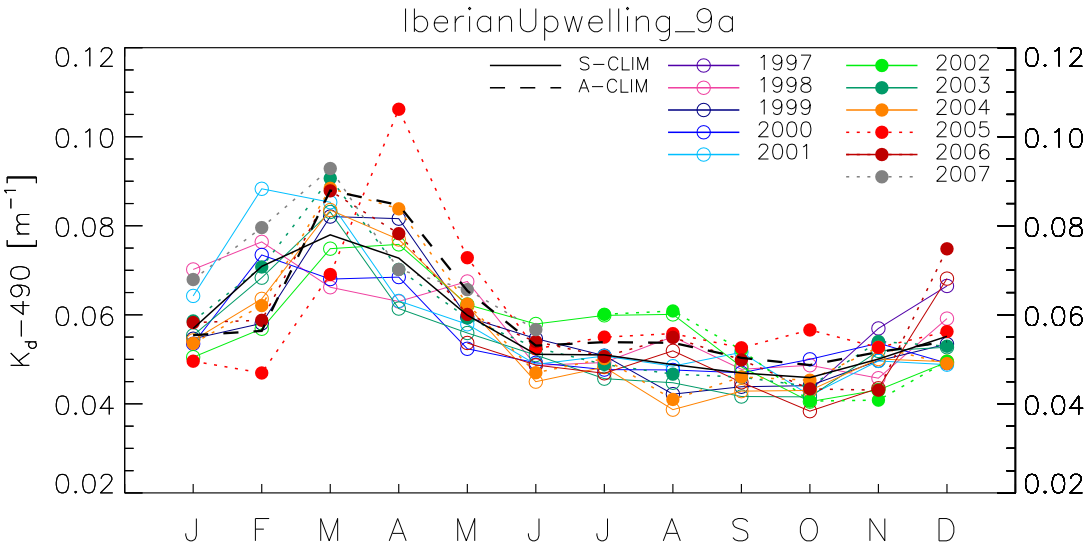

Figure 5.24: $K_d(490)$ multi-annual time series for SeaWiFS (lines with open circles) and MODIS (filled circles with dotted line) and associated climatologies (black line and dashed line, respectively).

5.12 Northeast Atlantic

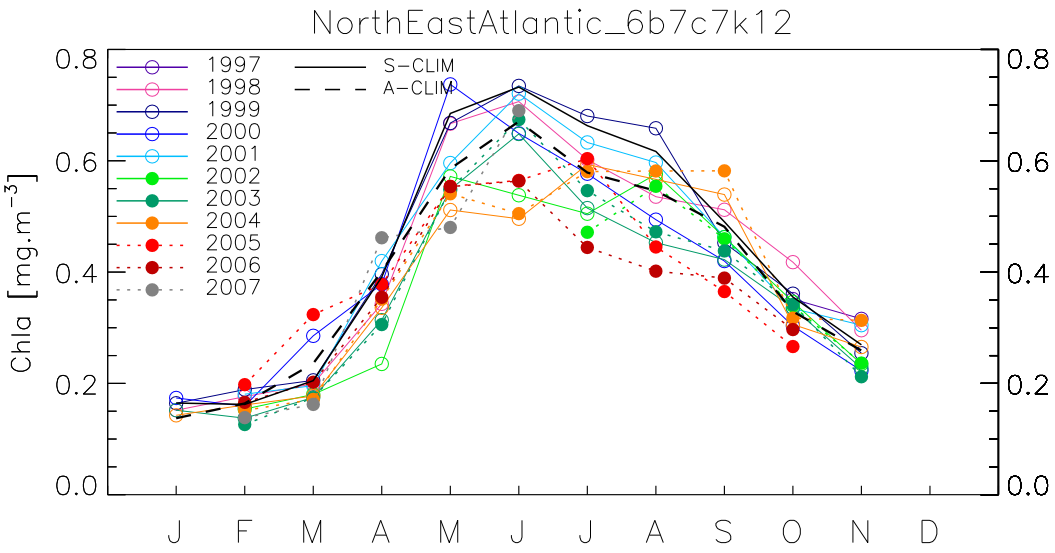

Figure 5.25: Chl*a* multi-annual time series for SeaWiFS (lines with open circles) and MODIS (filled circles with dotted line) and associated climatologies (black line and dashed line, respectively).

After March, the Chl*a* and K_d values in the Northeast Atlantic start to increase, then show a broad annual maximum. Part of the temporal width of the maximum represented here is due to the sequential shift in seasonal maximum towards higher latitudes as time goes. Both SeaWiFS and MODIS seasonal cycles appear as robust features. Interestingly, the SeaWiFS Chl*a* levels appear rather low on average for 2002-2004 (in fact, the monthly anomaly is almost continuously negative for that period).

Table 5.12: North East Atlantic; ICES Regions VIb, VIIc, VIIk, XII; SeaWiFS Chl*a* inter-annual anomalies, computed as ratio of area-averaged Chl*a* concentrations. The 2^{nd} column gives the SeaWiFS climatological Chl*a* (in mg m^{-3}). In bold, anomalies below 0.8 or above 1.2. A datum of 1 means a regional monthly value close to climatology.

Month	mg m^{-3}	1998	1999	2000	2001	2002	2003	2004
J	0.165	0.92	1.00	1.05	-	-	0.92	0.87
F	0.162	1.08	1.16	0.98	1.11	0.95	0.85	0.99
M	0.205	0.97	1.00	**1.39**	0.96	0.88	0.85	0.87
A	0.391	0.88	1.01	0.97	1.07	**0.60**	0.80	0.86
M	0.685	0.97	0.97	1.08	0.87	0.83	0.80	**0.75**
J	0.732	0.96	1.00	0.89	0.98	**0.73**	0.88	**0.68**
J	0.663	0.91	1.03	0.87	0.95	**0.76**	**0.78**	0.89
A	0.617	0.87	1.07	0.80	0.97	0.93	**0.73**	0.92
S	0.490	1.04	0.92	0.86	0.94	0.94	0.86	1.10
O	0.355	1.18	1.02	0.85	0.94	0.98	0.95	0.86
N	0.269	1.10	0.94	0.83	1.13	0.87	0.84	0.99
D	-	-	-	-	-	-	-	-

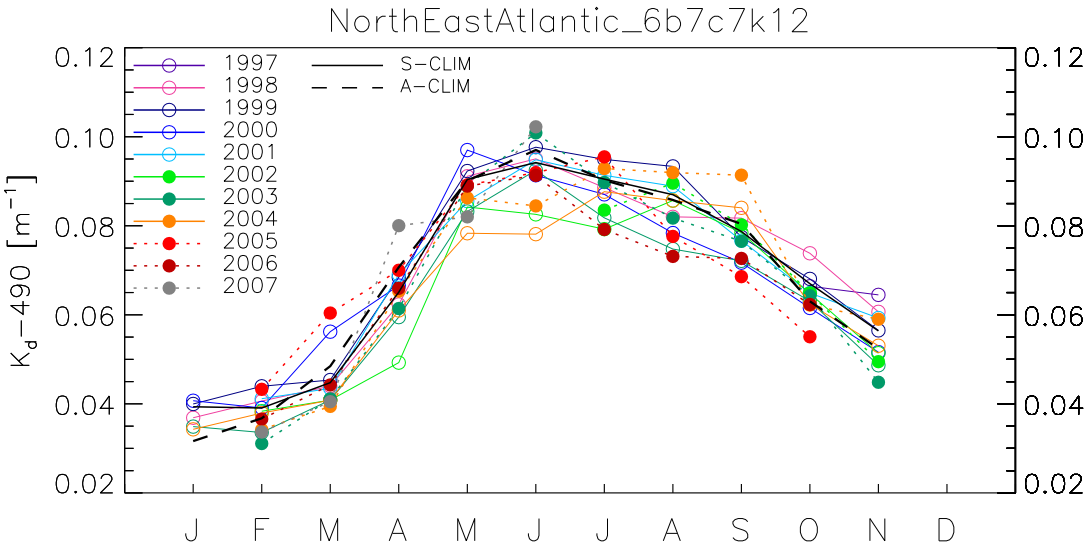

Figure 5.26: $K_d(490)$ multi-annual time series for SeaWiFS (lines with open circles) and MODIS (filled circles with dotted line) and associated climatologies (black line and dashed line, respectively).

5.13 Azores Basin

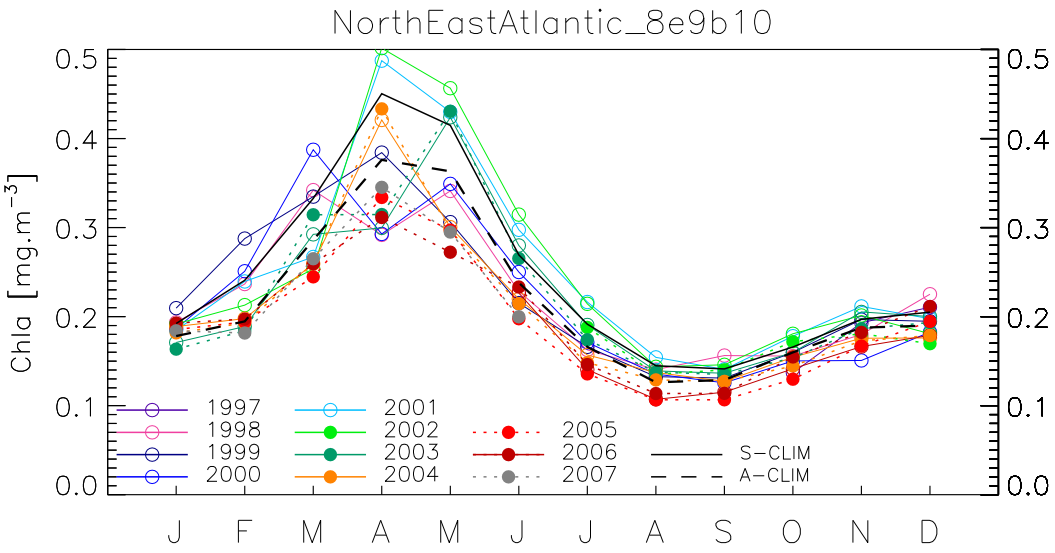

Figure 5.27: Chl*a* multi-annual time series for SeaWiFS (lines with open circles) and MODIS (filled circles with dotted line) and associated climatologies (black line and dashed line, respectively).

This region is the large ICES province offshore the Iberian upwelling. Not surprisingly, the spring bloom appear earlier than in the areas north of it, with peaks that vary from year to year. In 2001 and 2002, the spring maximum was in April, with large values; it was still in April but a lower intensity in 2004, whereas it was delayed to May in 2003. The peaks were smoother and of lower intensity in 1998-2000. This was also the case for the MODIS derived Chl*a* maxima in 2005-2007. The agreement between MODIS and SeaWiFS products is satisfactory for this region.

Table 5.13: North East Atlantic; ICES Regions VIIIe, IXb and X; SeaWiFS Chl*a* inter-annual anomalies, computed as ratio of area-averaged Chl*a* concentrations. The 2^{nd} column gives the SeaWiFS climatological Chl*a* (in mg m^{-3}). In bold, anomalies below 0.8 or above 1.2. A datum of 1 means a regional monthly value close to climatology.

Month	mg m^{-3}	1998	1999	2000	2001	2002	2003	2004
J	0.192	1.01	1.09	0.97	0.96	1.00	0.89	0.98
F	0.241	0.98	1.19	1.04	0.99	0.88	**0.78**	0.82
M	0.333	1.03	1.01	1.16	0.80	**0.76**	0.88	**0.78**
A	0.450	**0.65**	0.85	**0.65**	1.08	1.11	**0.67**	0.93
M	0.415	0.82	**0.74**	0.84	1.04	1.10	1.02	**0.72**
J	0.269	0.85	**0.80**	0.93	1.10	1.17	1.04	0.82
J	0.191	0.85	0.87	0.89	1.13	1.12	1.00	0.82
A	0.145	0.97	0.92	0.94	1.07	0.99	0.96	0.95
S	0.141	1.11	0.93	0.89	1.00	1.03	0.97	0.90
O	0.166	0.94	0.96	0.91	1.07	1.09	0.96	0.93
N	0.197	0.91	1.00	**0.77**	1.07	1.02	1.04	0.89
D	0.205	1.10	0.95	0.89	0.96	0.88	0.98	0.86

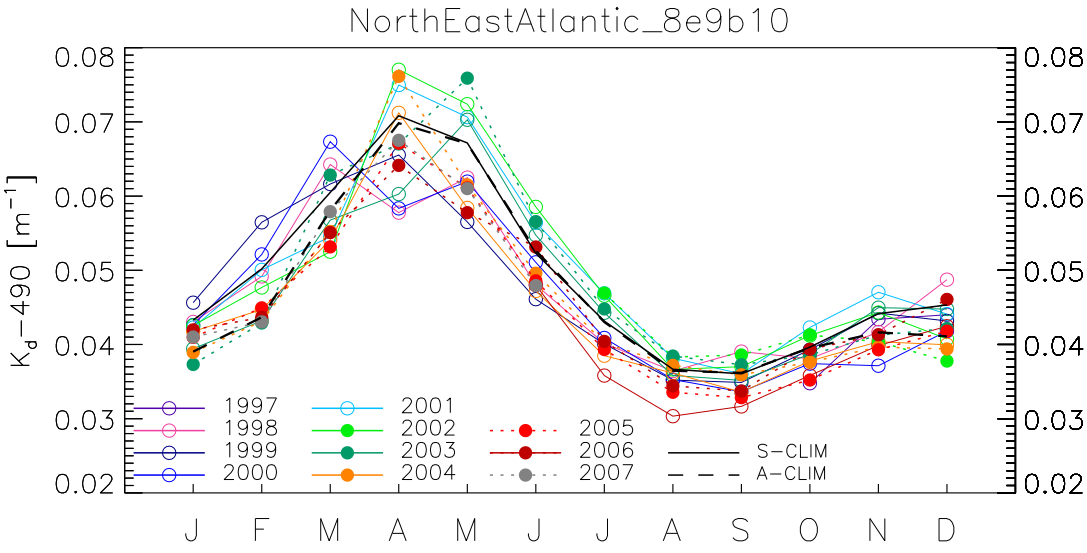

Figure 5.28: $K_d(490)$ multi-annual time series for SeaWiFS (lines with open circles) and MODIS (filled circles with dotted line) and associated climatologies (black line and dashed line, respectively).

Section 6

Statistical Analysis of Temporal Variability

This part is a brief synthesis of a statistical analysis aiming at describing the main features of the temporal variability characterizing the European marine regions that have been presented in the previous sections.

6.1 Statistical Approach

The original monthly time series (X_t) can be decomposed into three additive components:

$$X_t = S_t + T_t + Y_t \tag{6.1}$$

where S_t represents the seasonal component (assumed to be rigorously cyclical), T_t the trend component (assumed to be linear), and Y_t the irregular component (i.e., inter- and sub-annual terms which are not described by the trend and the seasonal cycle).

Before the time series decomposition, the potential outliers are identified and removed from the series. For a given month m, a record is identified as outlier in the monthly sub-series (X(i...m...t)) if it does not lie within the range $\bar{x} \pm 3\sigma$, where $\bar{x}$ and σ represent, respectively, the mean and standard deviation of the sub-series for the month m.

The procedure of time series decomposition does not allow the presence of gap in the data set. However, some months can be almost completely absent of the time series (typically during winter for high latitude regions). In this case, a synthetic time series is generated keeping only months with a valid record (i.e., with 10% of the surface area of the region associated with satellite values, see Section 1.4). The remaining missing values have been filled using the eigenvectors filtering (EVF) method (Ibanez and Conversi, 2002) which presents the advantage of preserving the temporal structure imbedded in the series.

The three components of the time series are derived as follows:

1. Seasonal Component

   A moving average of the series is computed in order to eliminate all the periodical (seasonal) variations. Classically, a 13-term moving average, MA_{2x12}, is used in order to eliminate the constant seasonality of order 12 while keeping the linear trends and minimizing the variance of the irregular component:

$$A_t = MA_{2\times12}(X_t) \tag{6.2}$$

where A_t is the smoothed time series. The moving average window width corresponds to the annual periodicity of the time series. In order to apply MA to any periodicity p, the classical filter $MA_{2\times12}$ has to be substituted by $MA_{2\times p}$ if p is even or by MA_p is the period is odd (Pezzulli et al., 2005). Moving averages cause some data at the extremities of the time series to be excluded from the analysis. Several methods have been suggested to overcome this problem (Findley et al., 1998). The simplest approach consists in replicating the first and last values until the gaps are filled (i.e., circular method, Pezzulli et al., 2005). The difference between the original X_t and the de-seasonalized time series A_t gives the seasonal component plus the irregular component. The seasonal component of the series, S_t, is eventually computed as the average for each month m of the year (a climatological value).

2. Trend Component

   The de-seasonalized time series A_t, redefined as X_t-S_t, represents the sum of the irregular Y_t and trend components T_t. The trend is estimated by linear regression (least square) on the seasonally adjusted time series:

$$T_t = a.[Y_t + T_t] + c \tag{6.3}$$

   The statistical significance of the linear trend has been tested by comparing the slope of the linear function to 0 (two tailed Student's-t statistics).

3. Irregular Component

   Finally, the irregular component Y_t is obtained by subtracting the linear trend from the de-seasonalized series A_t. Y_t is expected to be stationary (its autocorrelation should be non-significant) and of mean 0.

The relative contributions of S_t, T_t, and Y_t to the total variance of the original series are estimated considering the decomposition:

$$s_X^2 = s_S^2 + s_T^2 + s_Y^2 + 2\,cov(T_t, S_t, Y_t) \tag{6.4}$$

In practice, the three variance terms account for most of the total variance and are reported for each region in the following section as percentage of their sum, with the dominant term written in italic. Furthermore, the percentage difference between the final and initial values of a series due to the linear trend is also given, in bold characters if significant at a 95% level of confidence. The number N in the tables is the number of months considered for statistical analysis as the length of the annual cycle on the basis of the available satellite data.

6.2 Baltic Sea

Chl*a*	N	Var S (%)	Var T (%)	Var Y (%)	Diff. T (%)
Skagerrak	9	24.1	19.6	*56.3*	**-37.3**
Kattegat	9	24.5	5.2	*70.2*	**-15.9**
Belt Sea	9	29.1	0.3	*70.6*	-4.3
Arkona Sea	9	*68.6*	1.7	29.7	-12.5
Gulf of Gdansk	9	*62.9*	0.0	37.1	+1.8
S. Baltic Proper (west)	9	*69.7*	3.1	27.2	**-20.6**
S. Baltic Proper (east)	9	*74.5*	0.2	25.3	-6.6
Gotland Basin (west)	9	*79.2*	0.0	20.8	-0.3
Gotland Basin (east)	9	*71.3*	0.4	28.3	+12.0
N. Baltic Proper	9	*73.6*	0.0	26.4	+2.4
Gulf of Riga	8	47.6	0.0	*52.4*	+0.1
Gulf of Finland	8	*76.0*	0.4	23.6	+8.7
Aland Sea	9	*54.9*	0.0	45.1	+0.6
Archipelago	8	*55.1*	0.2	44.7	-3.2
Bothnian Sea	8	*64.3*	8.8	26.9	**-17.0**
Bothnian Bay	7	*73.4*	1.0	25.6	-11.3

Table 6.1: Summary table for Chl*a* in the Baltic Sea provinces. N: number of months in 1 year, Var S, T, Y: percentage of variance explained by the Seasonal, Trend and Irregular components respectively (italic: dominant component). Diff. T represents the relative variation of the original series due to the trend component (bold: significative trend).

In general, the variance due to the seasonal component is dominant in the Baltic Sea, even though a specific characteristic of this basin is the high level of variance explained by the irregular term Y. Contrary to the specifically Baltic regions, the variability for the Skagerrak and Kattegat areas is found dominantly in the irregular term. The coastal regions of the Belt Sea, the Gulfs of Riga and Gdansk, the Aland Sea and the Archipelago region are associated with a high Y variance term. A significant decreasing trend is detected in the Skagerrak, Kattegat, the southwest Baltic Proper and the Bothnian Sea for both Chl*a* and $K_d(490)$. The trend in the Arkona Sea is found significant for $K_d(490)$ only.

$K_d(490)$	N	Var S (%)	Var T (%)	Var Y (%)	Diff. T (%)
Skagerrak	9	23.8	24.9	*51.3*	**-22.0**
Kattegat	9	30.6	7.4	*62.0*	**-11.3**
Belt Sea	9	22.0	0.5	*77.5*	-2.8
Arkona Sea	9	*61.1*	3.9	35.1	**-9.4**
Gulf of Gdansk	9	*64.3*	0.0	35.7	0.0
S. Baltic Proper (west)	9	*67.6*	5.3	27.1	**-12.7**
S. Baltic Proper (east)	9	*75.0*	0.4	24.6	-4.3
Gotland Basin (west)	9	*80.2*	0.2	19.5	-3.5
Gotland Basin (east)	9	*77.4*	0.1	22.5	+2.7
N. Baltic Proper	9	*71.8*	0.0	28.2	0.4
Gulf of Riga	8	38.8	0.2	*61.0*	-1.8
Gulf of Finland	8	*71.9*	0.0	28.1	-0.6
Aland Sea	9	36.6	0.1	*63.2*	1.3
Archipelago	8	38.7	0.9	*60.4*	-2.9
Bothnian Sea	8	41.2	14.7	*44.1*	**-10.4**
Bothnian Bay	7	*56.5*	2.8	40.7	-7.7

Table 6.2: Summary table for $K_d(490)$ in the Baltic Sea provinces.

6.3 Mediterranean Sea

Chl*a*	N	Var S (%)	Var T (%)	Var Y (%)	Diff. T (%)
N. Adriatic Sea	12	37.8	5.6	*56.6*	**-28.6**
C. Adriatic Sea	12	*60.3*	4.7	35.1	**-16.4**
S. Adriatic Sea	12	*65.0*	4.5	30.5	**-16.5**
Alboran Sea	12	*69.7*	0.5	29.8	-7.1
Gulf of Lions	12	*73.1*	0.2	26.7	-6.6
Ligurian Sea	12	*74.9*	2.0	23.1	**-18.9**
Balearic Sea	12	*80.7*	0.1	19.2	+4.7
Provencal Basin	12	*82.9*	1.4	15.7	**-15.8**
Algerian Basin	12	*83.8*	0.2	16.1	-5.4
Tyrrhenian Sea	12	*82.0*	0.4	17.6	-7.1
N. Ionian Sea	12	*83.7*	0.7	15.6	-7.1
S. Ionian Sea	12	*84.3*	0.0	15.7	-1.1
Aegean Sea	12	*76.2*	1.7	22.1	**-9.3**
N. Levantine Basin	12	*83.8*	0.1	16.1	-3.0
S. Levantine Basin	12	*84.3*	0.5	15.2	-6.5

Table 6.3: Summary table for Chl*a* in the Mediterranean Sea provinces. N: number of months in 1 year, Var S, T, Y: percentage of variance explained by the Seasonal, Trend and Irregular components respectively (italic: dominant component). Diff. T represents the relative variation of the original series due to the trend component (bold: significative trend).

The Mediterranean Sea is characterized as expected by the importance of the seasonal component, with an associated variance exceeding 75% over a large part of the basin. An exception to that is the Adriatic Sea, where the irregular component has a larger weight, and is actually the dominant term in its northern part. The irregular term reaches 30% of the variance in the Alboran Sea, a figure likely resulting from the year-to-year variations of the gyres in that area. The trend component is rather low for most of the provinces, but it reaches 4-5% for Chl*a* and 6-7% for $K_d(490)$ in the three Adriatic zones. The negative trend found there is significant at the 95% level. Interestingly the trend is negative for all provinces (except the Balearic Sea for Chl*a*). Other provinces for which this trend is significant are the Ligurian Sea and Provencal Basin in the northwest part of the Mediterranean Sea, and the Aegean Sea for both Chl*a* and K_d, and the North Ionian Sea and South Levantine Basin for K_d only.

$K_d(490)$	N	Var S (%)	Var T (%)	Var Y (%)	Diff. T (%)
N. Adriatic Sea	12	*47.0*	7.5	45.6	**-18.2**
C. Adriatic Sea	12	*51.2*	7.4	41.4	**-11.7**
S. Adriatic Sea	12	*54.8*	5.9	39.3	**-11.2**
Alboran Sea	12	*72.3*	0.4	27.3	-4.1
Gulf of Lions	12	*75.2*	0.6	24.2	-6.2
Ligurian Sea	12	*77.9*	3.0	19.1	**-13.9**
Balearic Sea	12	*80.4*	0.0	19.6	1.5
Provencal Basin	12	*84.3*	1.7	14.0	**-10.6**
Algerian Basin	12	*86.0*	0.3	13.8	-4.2
Tyrrhenian Sea	12	*80.7*	0.7	18.7	-5.5
N. Ionian Sea	12	*76.4*	1.1	22.5	**-5.2**
S. Ionian Sea	12	*72.6*	0.1	27.3	-1.4
Aegean Sea	12	*65.5*	3.6	30.9	**-7.7**
N. Levantine Basin	12	*75.7*	1.0	23.4	-4.5
S. Levantine Basin	12	*74.1*	1.9	23.9	**-6.1**

Table 6.4: Summary table for $K_d(490)$ in the Mediterranean Sea provinces.

6.4 Black Sea

Chl*a*	N	Var S (%)	Var T (%)	Var Y (%)	Diff. T (%)
W. Black Sea - Shelf	12	18.4	27.7	*53.9*	**-42.4**
W. Black Sea - Deep	12	17.2	18.9	*63.9*	**-38.8**
E. Black Sea - Deep	12	19.4	17.8	*62.8*	**-31.0**

Table 6.5: Summary table for Chl*a* in the Black Sea regions. N: number of months in 1 year, Var S, T, Y: percentage of variance explained by the Seasonal, Trend and Irregular components respectively (italic: dominant component). Diff. T represents the relative variation of the original series due to the trend component (bold: significative trend).

The Black Sea is characterized by the dominant part of the variance due to the irregular term Y (54% to 64%). The variance associated with the linear trend is also very high, with basin-scale downward trends all significant.

$K_d(490)$	N	Var S (%)	Var T (%)	Var Y (%)	Diff. T (%)
W. Black Sea - Shelf	12	13.6	32.7	*53.7*	**-26.2**
W. Black Sea - Deep	12	21.9	21.6	*56.5*	**-24.2**
E. Black Sea - Deep	12	24.5	19.4	*56.2*	**-19.1**

Table 6.6: Summary table for $K_d(490)$ in the Black Sea regions.

6.5 Northeast Atlantic Domain

Chl*a*	N	Var S (%)	Var T (%)	Var Y (%)	Diff. T (%)
Norwegian Sea (IIa)	7	*82.7*	0.0	17.3	-2.4
Faroe Plateau (Vb)	8	*47.7*	7.1	45.2	**+74.5**
Iceland Shelf (Va)	8	*82.5*	0.5	17.0	-9.2
North Sea (IVa,b,c,)	9	*74.2*	3.2	22.6	**-11.3**
N.W. British Coasts (VIa, VIIb)	9	*57.3*	3.6	39.2	**+40.6**
Irish Sea (VIIa)	9	*60.0*	1.3	38.6	-7.1
Celtic Sea (VIIg,h,j,f)	11	*72.1*	0.0	27.9	-0.6
English Channel (VIId,e)	11	40.1	0.1	*59.8*	-2.7
Bay of Biscaye - Shelf (VIIIa,b)	12	*55.2*	0.7	44.1	-8.0
Bay of Biscaye - Open (VIIIc,d)	12	*66.8*	1.0	32.2	-12.9
Iberian Upwelling (IXa)	12	*67.3*	0.8	31.9	-9.6
N.E. Atlantic (VIb, VIIc,k, XII)	10	*85.7*	2.4	11.9	**-17.7**
Azores Basin (VIIIe,IXb,X)	12	*73.7*	0.0	26.2	-1.4

Table 6.7: Summary table for Chl*a* in the Northeast Atlantic provinces. N: number of months in 1 year, Var S, T, Y: percentage of variance explained by the Seasonal, Trend and Irregular components respectively (italic: dominant component). Diff. T represents the relative variation of the original series due to the trend component (bold: significative trend).

Obviously the provinces regrouped in this section are very diverse and logically the distribution of the variance terms reflects these differences. Truly oceanic provinces like the Norwegian Sea, the Iceland Shelf, the northeast Atlantic region or the Azores Basin have a large seasonal variance, whereas the irregular term has a larger weight for coastal / shelf provinces like the northwest British coasts, the Irish Sea, the Englidh Channel (dominant term), the Bay of Biscaye and the Iberian Upwelling. The two provinces northwest British coasts and Faroe Plateau exhibit large positive and significant trends. Conversely, there is a negative significant trend for both Chl$a$ and K_d in the North Sea and northeast Atlantic region. Caution is required for a province like the latter: the process of averaging the signal over such a large area could hide patterns of change more contrasted than the present results. Negative trends are also found for the two sub-divisions of the Bay of Biscaye but only those for K_d are found significant.

K_d(490)	N	Var S (%)	Var T (%)	Var Y (%)	Diff. T (%)
Norwegian Sea (IIa)	7	*86.0*	0.0	14.0	-1.3
Faroe Plateau (Vb)	8	*60.2*	5.9	33.9	**+33.7**
Iceland Shelf (Va)	8	*87.0*	0.6	12.4	-6.8
North Sea (IVa,b,c,)	9	*70.6*	4.2	25.2	**-7.2**
N.W. British Coasts (VIa, VIIb)	9	*65.3*	3.2	31.6	**+20.4**
Irish Sea (VIIa)	9	*61.7*	1.6	36.7	-4.2
Celtic Sea (VIIg,h,j,f)	11	*73.7*	0.2	26.1	-2.4
English Channel (VIId,e)	11	41.4	1.0	*57.6*	-3.8
Bay of Biscaye - Shelf (VIIIa,b)	12	*53.6*	2.2	44.2	**-7.9**
Bay of Biscaye - Open (VIIIc,d)	12	*70.3*	2.9	26.8	**-12.1**
Iberian Upwelling (IXa)	12	*69.3*	1.3	29.5	-7.2
N.E. Atlantic (VIb, VIIc,k, XII)	10	*87.3*	2.6	10.1	**-12.0**
Azores Basin (VIIIe,IXb,X)	12	*78.8*	0.0	21.2	-1.4

Table 6.8: Summary table for K_d(490) in the Northeast Atlantic provinces.

Section 7

Conclusions

Obviously, from the Norwegian Sea or the Baltic Sea to the subtropical Atlantic and the oligotrophic eastern Mediterranean, the bio-optical variability in European waters is enormous, and the seasonal cycles and inter-annual signals are very diverse. The focus of the work, as a first review of the Chl*a* and $K_d(490)$ records over European seas with 10 year of ocean color data, has been placed simultaneously on the seasonal and inter-annual variability and on a synthesis at a European scale (rather than a detailed study of particular regions). Not surprisingly, no clear basin-scale evolution is emerging over the time period considered, even though strong departures from climatology were noticed. It was not in the scope of this work (nor realistic) to provide an explanation for all the events that have appeared; the temporal evolution for selected areas should be thoroughly investigated with the support of literature results, in situ data, and/or other environmental variables. In any case, the uncertainty associated with the satellite products for the various regions has a strong bearing on the significance of the detected patterns. Notwithstanding this, some basin-scale features can be noticed. For instance, it is the case of the increase in satellite Chl*a* over the Baltic Sea associated with the spectacular cyanobacteria bloom of July 2005 (e.g., Zibordi et al., 2006d). Other examples are the strong event of 2001 in the Black Sea, and the lower Chl*a* levels in this basin after 2002. The case of the former could actually be misleading and much overestimated (Oguz and Ediger, 2006). For the latter, the Black Sea has known clear ecosystem shifts in the past decades (Oguz, 2005a, b). More investigations are needed on these topics and other patterns of variability. To go a step further, a simple statistical analysis has been performed on the SeaWiFS record that has highlighted significant trends for some regions, like the Adriatic Sea, the waters between Scotland and the Faroe Plateau or the Black Sea. More complete studies on this are on-going.

As described in Section 1, the two satellite products considered here are very coherent in terms of modeling, and the derived products result from standard settings. Geographically speaking, the use of single processing chain and algorithms for the entire European domain has also the advantage of enabling a direct comparison between all regions. On the other hand, the use of standard algorithms developed for global applications, indiscriminately for all the European waters, is fraught with a varying degree for uncertainties. This has not been addressed in the present document, even though some of these uncertainties can emerge in the differences between the SeaWiFS and MODIS products. In regions with a strong bio-optical specificity, like the Baltic Sea, there is in fact no ground to expect that the standard Chl*a* algorithms for SeaWiFS or MODIS should function accurately (for this matter it is also true for the MERIS Algal I prod-

uct). Conversely, improvements can be achieved with recent developments of regional algorithms (among others, Darecki et al. 2005, for the Baltic Sea, D'Ortenzio et al. 2002 or Volpe et al., 2007, for the open Mediterranean Sea, D'Alimonte and Zibordi, 2003, for the north Adriatic Sea) or new approaches. One challenge for future determinations of satellite Chl*a* should be the integration at European scale of a set of regional algorithms developed in a coherent manner (see for instance D'Alimonte et al., 2003).

Overall, one result of this report is the encouraging agreement between SeaWiFS and MODIS Chl*a* and $K_d(490)$, even though the comparison between these products has been here rather qualitative. This is however in line with large scale analyzes found in other studies (Franz et al., 2005; Djavidnia et al., 2006a, b). Obviously, the consistency of these satellite products is much favored by the use of similar vicarious calibration procedures (Eplee et al., 2001), atmospheric correction schemes (including the same family of aerosol models), and bio-optical algorithms for the calculation of Chl*a* and $K_d(490)$. This still does not prevent the existence of significant differences, the most obvious one being noticed for the Baltic Sea. We now add a few more comments on this province since it epitomizes some of the challenges lying ahead for the development of a high-quality long-term ocean color series for the European seas. This region can be placed in a global context by Figure 7.1 (reproduced from Djavidnia et al., 2006a). The two axis represent the root mean square differences (in ordinate) and the bias (abscissa) between SeaWiFS and MODIS (log-transformed) Chl*a* for the various global regions (Longhurst 1998). These statistics are computed using all grid points in each province using monthly mean maps and then averaged over 3 years of concurrent data. Typically, the areas termed Norwegian Sea, Northeast Atlantic or Azores Basin would be associated with the provinces SARC, NADR and NASE, respectively. MEDI and BCKS are for the entire Mediterranean and Black Seas, respectively. The province for the Baltic Sea, BALT, stands out as an outlier, for its high level of RMS differences and for its negative bias (i.e., MODIS Chl*a* higher than the SeaWiFS equivalent). This has resulted evident in the figures of Section 2, and poses the question of the creation of a consistent multi-sensor time series for the Baltic. Moreover, this is not specific to the Chl*a* product but is already apparent at the level of the water-leaving radiance spectra (not shown). This is a major challenge for Baltic Sea studies, that will require investigations upon the functioning of the atmospheric correction schemes as well as the bio-optical algorithms.

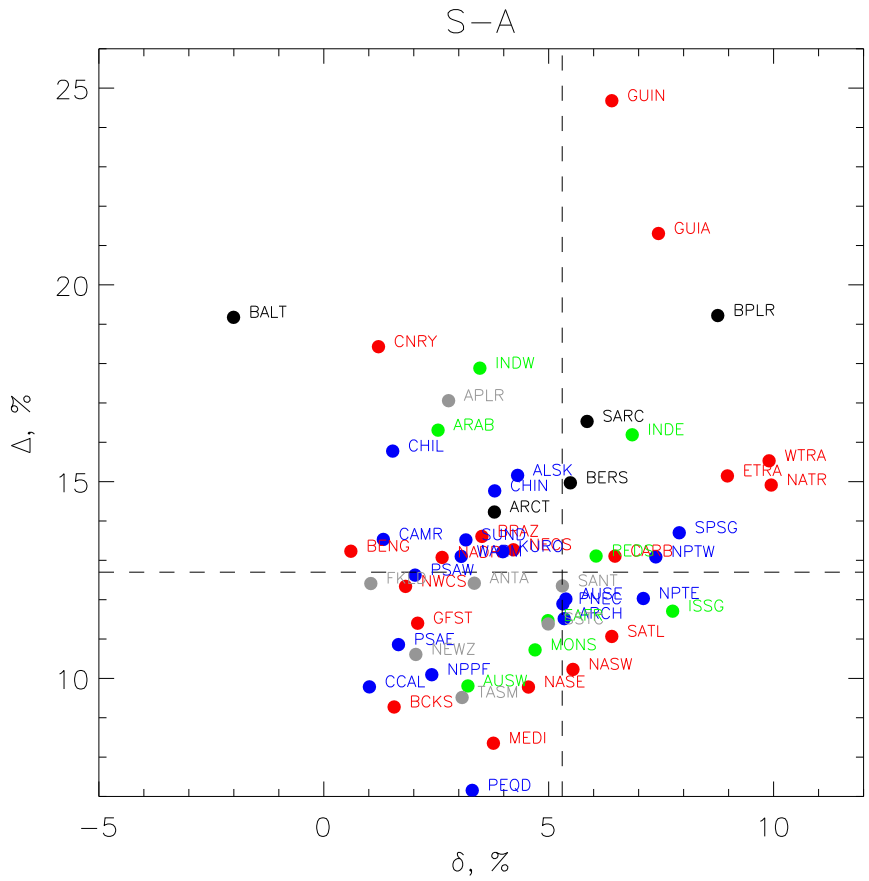

Figure 7.1: Root mean square difference versus bias of log-transformed Chl*a* for the biogeographical provinces of the global ocean. Reproduced from Djavidnia et al., (2006a). In red are Atlantic provinces, in black northern latitude provinces, in blue Pacific provinces, in green Indian Ocean provinces, in grey Southern Ocean provinces.

Acknowledgements

The author would especially like to thank the Ocean Biology Processing Group and the Distributed Active Archive Center (Code 902) at the Goddard Space Flight Center of the U.S. National Aeronautics and Space Administration for the production and the distribution of the SeaWiFS and MODIS-Aqua raw data, and all accompanying software and documentation.

Bibliography

[1] Berthon, J.-F., Zibordi, G., Doyle, J.-P., Grossi, S., van der Linde, D., & Targa, C. (2002). Coastal Atmosphere and Sea Time Series (CoASTS): Data analysis. *NASA Technical Memorandum, 2002-206892, vol. 20*, 1-25, Eds., S.B. Hooker, & E.R. Firestone, NASA-GSFC, Greenbelt, Maryland.

[2] Bricaud, A., Bosc, E., & Antoine, D. (2002). Algal biomass and sea surface temperature in the Mediterranean basin. Intercomparison of data from various satellite sensors, and implications for primary production estimates. *Remote Sensing of Environment, 81*, 163-178.

[3] Campbell, J.W. (1995). The lognormal distribution as a model for bio-optical variability in the sea. *Journal of Geophysical Research, 100*, 13237-1325.

[4] D'Alimonte, D., & Zibordi, G. (2003). Phytoplankton determination in an optically complex coastal region using a multilayer perceptron neural network. *IEEE Transactions on Geoscience and Remote Sensing, 41*, 2861-2868.

[5] D'Alimonte, D., Mélin, F., Zibordi, G., Berthon, J.-F. (2003). Use of the novelty detection technique to identify the range of applicability of the empirical ocean color algorithms. *IEEE Transactions on Geoscience and Remote Sensing, 41*, 2833-2843.

[6] Darecki, M., Kaczmarek, S., & Olszewski, J. (2005). SeaWiFS ocean colour chlorophyll algorithms for the southern Baltic Sea. *International Journal of Remote Sensing, 26*, 247-290.

[7] Djavidnia, S., Mélin, F., & Hoepffner, N. (2006). Analysis of multi-sensor global and regional ocean colour products. *JRC Publication*, EUR Report 22238EN, 218pp., Contribution MERSEA MERSEA-WP02-JRC

[8] Djavidnia, S., Mélin, F., & Hoepffner, N. (2006). Assessment of global and regional ocean sea surface chlorophyll *a*. In *European Operational Oceanography: Present and Future*, Proc. 4th Conference on EuroGOOS, pp. 122-127, 2006.

[9] D'Ortenzio, F., Marullo, S., Ragni, M., Ribera d'Alcalà, M., & Santoleri, R. (2002). Validation of empirical SeaWiFS algorithms for chlorophyll-a retrieval in the Mediterranean Sea. A case study for oligotrophic seas. *Remote Sensing of Environment, 82*, 79-94.

[10] Eplee, R.E., Robinson, W.D., Bailey, S.W., Clark, D.K., Werdell, P.J., Wang, M., Barnes, R.A., & McClain, C.R. (2001). Calibration of SeaWiFS. II. Vicarious techniques. *Applied Optics, 40*, 6701-6718.

[11] Feldman, G.C., Kuring, N.A., Ng, C., Esaias, W.E., McClain, C.R., Elrod, J.A., Maynard, N., Endres, D., Evans, R., Brown, J., Walsh, S., Carle, M., & Podesta, G. (1989). Ocean color: Availability of the global data set. *EOS Transactions of the American Geophysical Union, 70*, 634-641.

[12] Findley, D. F., Monsell, B. C., Bell, W. R., Otto, M. C. and Chen, B.-C. (1998). New capabilities and methods of the X-12-ARIMA seasonal adjustment program (with discussion). *Journal of Business and Economic Statistics, 16*, 127-177.

[13] Franz, B.A., Werdell, P.J., Meister, G., Bailey, S.W., Eplee, R.E., Feldman, G.E., Kwiatkowska, E., McClain, C.R., Patt, F.S., & Thomas, D. (2005). The continuity of ocean color measurements from SeaWiFS to MODIS. *SPIE Proceedings, 5882-34*, San Diego, U.S., 31^{st} Jul.-2^{nd} Aug., 2005.

[14] Frouin, R., Franz, B.A., Werdell, P.J. (2003). The SeaWiFS PAR product. *NASA Technical Memorandum, 2000-206892, vol. 22*, "Algorithm updates for the fourth SeaWiFS data reprocessing", Chap. 8, 46-50, Eds., S.B. Hooker, & E.R. Firestone, NASA-GSFC, Greenbelt, Maryland.

[15] Fu, G., Baith, K.S., & McClain, C.R. (1998). SeaDAS: The SeaWiFS Data Analysis System. *Proceedings of The 4^{th} Pacific Ocean Remote Sensing Conference*, 73-79, Qingdao, China, July 28-31, 1998.

[16] Gordon H.R., & Wang, M. (1994). Retrieval of water-leaving radiance and aerosol optical thickness over the oceans with seaWiFS: a preliminary algorithm. *Applied Optics, 33*, 443-452.

[17] Hooker, S.B., Esaias, W.E., Feldman, G.C., Gregg, W.W., & McClain, C.R. (1992). An overview of SeaWiFS and ocean color. *NASA Technical Memorandum, 1992-104566, vol. 1*, 1–24, Eds., S.B. Hooker, & E.R. Firestone, NASA-GSFC, Greenbelt, Maryland.

[18] Hovis, W.A., Clark, D.K., Anderson, F., Austin, R.W., Wilson, W.H., Baker, E.T., Ball, D., Gordon, H.R., Mueller, J.L., El-Sayed, S.Z., Sturm, B., Wrigley, R.C., & Yentsch, C.S. (1980). Nimbus-7 coastal zone color scanner: system description and initial imagery. *Science, 210*, 60-63.

[19] Ibanez F., Conversi, A. (2002). Prediction of missing values and detection of 'exceptional events' in a chronological planktonic series: A single algorithm. *Ecological Modelling, 154*, 9-23.

[20] IOCCG Report Number 4 (2004). Guide to the creation and use of ocean colour, Level-3, binned data products. Ed. D. Antoine, 88 pp.

[21] Lee, Z.P., Carder, K.L., & Arnone, R.A. (2002). Deriving inherent optical properties from water color: a multiband quasi-analytical algorithm for optically deep waters. *Applied Optics, 41*, 5755–5772.

[22] Lee, Z.P., Darecki, M., Carder, K.L., Davis, C.O., Stramski, D., & Rhea, W.J. (2005). Diffuse attenuation coefficient of downwelling irradiance: An evaluation of remote sensing methods. *Journal of Geophysical Research, 110*, C02017, doi:10.1029/2004JC002573.

[23] Longhurst, A.R. (1998). Ecological Geography of the Sea. *Academic Press*, San Diego, 398pp.

[24] McClain, C.R., Feldman, G.C., & Hooker, S.B. (2004). An overview of the SeaWiFS project and strategies for producing a climate research quality global ocean bio-optical time series, *Deep-Sea Res., II, 51*, 5-42.

[25] Mélin, F., Berthon, J.-F., & Zibordi, G. (2005). Assessment of apparent and inherent optical properties derived from SeaWiFS with field data. *Remote Sensing Environment, 97*, 540–553.

[26] Mélin, F., Zibordi, G., & Djavidnia, S. (2007a). Development and validation of a technique for merging satellite derived aerosol optical depth from SeaWiFS and MODIS. *Remote Sensing Environment, 108*, 436-450.

[27] Mélin, F., Zibordi, G., & Berthon, J.-F. (2007b). Assessment of satellite ocean color products at a coastal site. *Remote Sensing Environment, 110*, 192-215.

[28] Mélin, F., & Zibordi, G. (2007). An optically-based technique for producing merged spectra of water leaving radiances from ocean color remote sensing. *Applied Optics, 46*, 3856-3869.

[29] Oguz, T. (2005a). Long-term impacts of anthropogenic forcing on the Black Sea ecosystem. *Oceanography, 18*, 112-121.

[30] Oguz, T. (2005b). Black Sea ecosystem response to climatic teleconnections. *Oceanography, 18*, 122-133.

[31] Oguz, T., & Ediger, D. (2006). Comparison of in situ and satellite-derived chlorophyll pigment concentrations, and impact of phytoplankton bloom on the suboxic layer structure in the western Black Sea during May-June 2001. *Deep-Sea Research, II, 53*, 1923-1933.

[32] O'Reilly, J.E., Maritorena, S., Siegel, D.A., O'Brien, M.C., Toole, D.A., Mitchell, B.G., Kahru, M., Chavez, F.P., Strutton, P., Cota, G.F., Hooker, S.B., McClain, C.R., Carder, K.L., Mueller-Karger, F.E., Harding, L., Magnusson, A., Phinney, D., Moore, G.F., Aiken, J., Arrigo, K.R., Letelier, R., & Culver, M. (2000). Ocean color chlorophyll *a* algorithms for SeaWiFS, OC2, and OC4: Version 4. *NASA Technical Memorandum, 2000-206892, vol. 11*, Chap. 2, 9-23, Eds., S.B. Hooker, & E.R. Firestone, NASA-GSFC, Greenbelt, Maryland.

[33] Patt, F.S., Barnes, R.A., Eplee, R.E., Franz, B.A., Robinson, W.D., Feldman, G.C., Bailey, S.W., Gales, J., Werdell, P.J., Wang, M., Frouin, R., Stumpf, R.P., Arnone, R.A., Gould, R.W., Martinolich, P.M., Ransibrahmanakul, V., O'Reilly., J.E., & Yoder, J.A. (2003). Algorithm updates for the fourth SeaWiFS data reprocessing. *NASA Technical Memorandum, 2003-206892, vol. 22*, 1-74, Eds., S.B. Hooker, & E.R. Firestone, NASA-GSFC, Greenbelt, Maryland.

[34] Pezzulli, S., Stephenson, D.B., Hannachi, A. (2005). The variability of seasonality. *Journal of Climate, 18*, 71-88.

[35] Salomonson V.V., Barnes, W.L., Maymon, P.W., Montgomery, H.E., & Ostrow, H. (1989). MODIS: Advanced facility instrument for studies of the Earth as a system. *IEEE Transactions on Geoscience and Remote Sensing, 27*, 145-152.

[36] Volpe, G., Santoleri, R., Vellucci, V., Ribera d'Acalá, M., Marullo, S., D'Ortenzio, F.: The colour of the Mediterranean Sea: Global versus regional bio-optical algorithms evaluation and implication for satellite chlorophyll estimates. *Remote Sensing of Environment, 107*, 625-638.

[37] Wang, M., Knobelspiesse, K.D., & McClain, C.R. (2005). Study of the Sea-viewing Wide Field-of-View Sensor (SeaWiFS) aerosol optical property data over ocean in combination with the ocean color products. *Journal of Geophysical Research, 110*, D10S06, doi:10.1029/2004JD004950.

[38] Werdell, P.J. (2005). Ocean color K490 algorithm evaluation. http://oceancolor.gsfc.nasa.gov/REPROCESSING/SeaWiFS/R5.1/k490_update.html

[39] Yoder, J.A., McClain, C.R., Feldman, G.C., Esaias, W.E. (1993). Annual cycles of phytoplankton chlorophyll concentrations in the global ocean: A satellite view. *Global Biogeochemical Cycles, 7*, 181-193.

[40] Zibordi, G., Berthon, J.-F., Doyle, J.-P., Grossi, S., van der Linde, D., Targa, C., & Alberotanza, L. (2002). Coastal Atmosphere and Sea Time Series (CoASTS): A long-term measurement program. *NASA Technical Memorandum, 2002-206892, vol. 19*, 1-29, Eds., S.B. Hooker, & E.R. Firestone, NASA-GSFC, Greenbelt, Maryland.

[41] Zibordi, G., Berthon, J.-F., Bulgarelli, B., D'Alimonte, D., van der Linde, D., Mélin, F., & Targa, C. (2004a). Ocean colour validation activities at the Acqua Alta Oceanographic Tower in the Northern Adriatic Sea. *International Journal of Remote Sensing, 25*, 1533–1537.

[42] Zibordi, G., Mélin, F., Hooker, S.B., & Holben, B.N. (2004b). An autonomous above-water system for the validation of ocean color radiance data. *IEEE Transactions on Geoscience and Remote Sensing, 42*, 401–415.

[43] Zibordi, G., Mélin, F., & Berthon, J.-F. (2006a). Comparison of SeaWiFS, MODIS and MERIS radiometric products at a coastal site. *Geophysical Research Letters, 33*, L06617, doi:10.1029/2006GL025778.

[44] Zibordi, G., Mélin, F., & Berthon, J.-F. (2006b). A time series of above-water radiometric measurements for coastal water monitoring and remote sensing product validation. *IEEE Transactions on Geoscience and Remote Sensing Letters, 3*, 120-124.

[45] Zibordi, G., Holben, B.N., Hooker, S.B., Mélin, F., Berthon, J.-F., Slutsker, I., Giles, D., Vandemark, D., Feng, H., Rutledge, K., Schuster, G., & Al Mandoos, A. (2006c). A network for standardized ocean color validation measurements. *EOS Transactions of the American Geophysical Union, 87*, 30, 293,297.

[46] Zibordi, G., Strömbeck, N., Mélin, F., Berthon, J.-F. (2006d). Tower-based radiometric observations at a coastal site in the Baltic Proper. *Estuarine, Coastal and Shelf Science, 69*, 649-654.

European Commission

EUR 22916 EN – Joint Research Centre – Institute for Environment and Sustainability
Title: Multi-Year Analysis of Standard Ocean Colour Products for the European Seas
Author(s): F. Mélin, V. Vantrepotte
Luxembourg: Office for Official Publications of the European Communities
2007-09-17 – 124 pp. – 21 x 29.7 cm
EUR – Scientific and Technical Research series – ISSN 1018-5593

Abstract
A 10-year time series of ocean colour products has been assembled for the European Seas from the SeaWiFS and MODIS full resolution satellite imagery. The JRC ocean colour archive is first briefly described. Then the study focuses on the analysis of the spatial and temporal variability of standard products such as the chlorophyll *a* pigment concentration and the diffuse attenuation coefficient. The European seas are partitioned into a set of specific regions for which average time series are derived and analysed in terms of seasonal and inter-annual variability. Finally, a statistical analysis yields a decomposition of the series into seasonal, irregular and linear trend components, thus providing a classification of the European waters on the basis of their temporal variations.

The mission of the JRC is to provide customer-driven scientific and technical support for the conception, development, implementation and monitoring of EU policies. As a service of the European Commission, the JRC functions as a reference centre of science and technology for the Union. Close to the policy-making process, it serves the common interest of the Member States, while being independent of special interests, whether private or national.